EXAMINING THE IMPACT OF SPATIAL DEVELOPMENT PATTERNS ON REGIONAL HEAT ISLAND EFFECT IN METROPOLITAN REGIONS OF THE UNITED STATES

A Dissertation

by

HEEJU KIM

Submitted to the Office of Graduate Studies of
Texas A&M University
in partial fulfillment of the requirements for the degree of

DOCTOR OF PHILOSOPHY

Chair of Committee,	Samuel D. Brody
Committee Members,	Walter G. Peacock
	Chanam Lee
	Wesley E. Highfield
Head of Department,	Forster Ndubisi

August 2013

Major Subject: Urban and Regional Sciences

ABSTRACT

The urban heat island effect is considered one of the main causes of global warming and is contributing to increasing temperatures in the urban United States. This phenomenon enhances the intensity of summer heat waves and the risk to public health due to increased exposure to extreme thermal conditions.

Characteristics of spatial development patterns can significantly affect urban temperature because they are related to the arrangement of development and land surface materials, which are crucial elements needed to determine land surface temperature. While previous studies revealed that the effect of the urban heat island varies depending on different land use types and surface characteristics, few have considered the overall development patterns of urban form. I address this under-studied aspect of heat hazards by analyzing the relationship between spatial development pattern and urban heat island effect across a sample of 353 metropolitan regions of the U.S. Specifically, I employ a series of landscape metrics to measure urban development patterns using a national land cover dataset from the U.S. Geological Survey. Linear regression models are used to statistically isolate the effect of different spatial development patterns on increasing the urban heat island effect while controlling for multiple contextual variables including built-environment, environmental, and demographic characteristics.

The result of this study showed that the daytime mean surface urban heat island effect (4.04˚F) is higher than that of nighttime (2.41˚F). Ecological context (i.e.

Ecoregions) has proved to be a statistically significant modulator that helps to explain the spatial distribution of the urban heat island effect.

Regarding the main research question of this study, the results indicate that specific categories of urban development pattern including density, continuity, and clustering are statistically associated with increasing the urban heat island effect. This initial evidence suggests that the overall development patterns are an important issue to consider when mitigating the adverse impacts related to the urban heat island effect. In addition, when contextual heat contributors are held constant, the intensity of the urban heat island effect can differ depending on the configuration of development in urban areas.

This study can be used as a starting point for a comprehensive approach to both spatial land development and hazard-resistant planning by providing alternative ways of measuring and modeling spatial development patterns.

DEDICATION

To my husband, Taeho

ACKNOWLEDGEMENTS

I would like to thank my committee chair, Dr. Brody for his constant guidance and support. He is an amazing mentor and teacher. He always encourages and supports me, which helped me to get this point. Since moving to the U.S. for graduate school, I have felt very lucky and blessed to have him in my life. I would also like to thank my committee members, Dr. Peacock, Dr. Lee, and Dr. Highfield for their constant and thoughtful advice.

My gratitude also extends to my wonderful friends and colleagues for making my time at Texas A&M University a great experience. Boah, you have been my best friend since the start of graduate school, and I am so happy that we were able to share all of our experiences while in the United States. I would also like to thank to my friends at the Hazard Reduction and Recovery Center and the Master of Urban Planning and Urban and Regional Science program. I hope and believe that we can work together as a researchers and urban planners in the near future.

I am very grateful to my parents, my sister and her family, and my brother. My gratitude also goes to my in-laws. They have always encouraged me to move forward in my life with their constant support, understanding and patience. I believe my achievement was sincerely rooted in their love.

Most importantly, thanks from the bottom of my heart to my husband Taeho. You always stand by my side, whatever I do and wherever I am. Without your endless love, support, and trust, I would have never completed this dissertation. I promise to support everything you do for the rest of our lives. Thank you for being a good friend, thoughtful listener and wonderful husband. I love you.

NOMENCLATURE

UHIE	Urban Heat Island Effect
USGS	U.S. Geological Survey
NLCD	National Land Cover Dataset
AVHRR	Advanced Very High Resolution Radiometer
MODIS	Moderate Resolution Imaging Spectroradiometer
MWCF	Marine West Coast Forest
NFM	Northwestern Forested Mountain
MC	Mediterranean California
NAD	North American Desert
GP	Great Plain
NF	Northern Forest
ETF	Eastern Temperate Forest
TWF	Tropical Wet Forest

TABLE OF CONTENTS

Page

LIST OF FIGURES

Page

LIST OF TABLES

Page

CHAPTER I

INTRODUCTION

1.1. Research Background

Extreme heat waves (EHW) are the leading cause of weather-related deaths across the U.S. (NCDC, 2004). Although EHWs do not often appear to be as serious as other weather-related hazards, the number of deaths caused by EHWs in the U.S. in the past 20 years (1991-2010) is higher than those by any other hazard (Weather Fatalities by NWS, NOAA).

The summer of 1995 was the most severe heat wave disaster in U.S history, and is described in detail in *Heat Wave: A Social Autopsy of Disaster in Chicago* by Eric Klinenberg (2002). The book stated that over 700 people died due to extended periods of high temperatures. Also, extreme heat waves are associated with other natural hazards such as drought, wildfire, and flooding, which are also very harmful to both the environment and humans. There are two major expected causes that increase the frequency and intensity of heat waves: climate change (i.e. global warming) and urban heat island effects (Guest et al., 1999; Kalkstein and Greene, 1997; Smoyer et al., 2000). While climate change is a global phenomenon, urban heat island effect is a regional or local phenomenon limited to metropolitan and urban areas.

In the U.S., over 80% (80.7%) of the population live in urban areas (U.S. Census 2010). Urban areas not only contribute to the creation of heat through increased development, but are also locations at risk for heat hazards. Thus, researchers in various

fields have attempted to examine the relationship between urban heat island effect and urban physical and social characteristics including city size, populations, and land cover/uses (Clarke, 1972; Oke, 1973; Landsberg, 1981; Quattrochi et al., 2000; Streutker, 2002; Rosenziweig et al., 2005; Stone et al., 2006; Chen et al. 2006; Jenerette et al., 2007; Hu and Jia, 2010).

Characteristics of spatial development patterns can be some of the most significant factors to affect urban temperature because they are related to the arrangement and land surface materials, which are crucial elements needed to determine land surface temperature. Because of this indissoluble relationship between spatial development patterns and temperature, smart and sustainable spatial planning strategies play key roles in attempting to reduce and prevent extreme heat waves, including urban heat island effect. However, there are very few empirical studies that have explored spatial development patterns to better understand the urban heat island effect on a regional scale.

1.2. Research Purpose and Objectives

The goal of this study is to better understand the impacts of spatial development patterns on urban heat island effect, which are major contributors to the intensity of summer heat waves. This study will analyze in detail the composition and configuration of development patterns in urbanized areas using landscape metrics. Then, it will examine the relationship between measured development patterns and urban heat island effect (UHIE). The main research question for this study is "***What characteristics of spatial***

development patterns influence the UHIE?"

The specific objectives of this study are to:

1. Investigate UHIE at a regional scale in a metropolitan region in the U.S. by comparing the temperature difference between urbanized and non-urbanized areas utilizing thermal remote sensing data;
2. Measure spatial patterns of development on a regional scale in urbanized areas of the metropolitan region in the U.S. based on the concepts of landscape metrics;
3. Examine the relationship between spatial development patterns and UHIE by employing statistical models; and
4. Suggest the policy implications and design guidelines for reducing UHIE considering spatial development patterns.

CHAPTER II

LITERATURE REVIEW

This section provides an understanding of the main concepts of this study, including the UHIE, spatial development patterns, and landscape metrics. The first part of this section explains UHIE and reviews previous studies on UHIE. The second part of this section outlines the spatial patterns of development and reviews previous research on measuring spatial development patterns. Also, this section explains the basic concepts of landscape metrics and its implications in measuring spatial development patterns. The third part of this section lists previous research on urban heat island effect and development patterns. A summary of research findings and gaps in the literature concludes this section.

2.1. Understanding Urban Heat Island Effect

Urban heat island effect (UHIE) is a well-known phenomenon that is one of the most prevailing consequences of increasing temperatures due to urban development (Landsberg, 1981). The urban heat island (UHI) was first documented by Luke Howard in his climate research in London in 1833. Based on "Recent Advances and Issues in Meteorology," the UHIE is detailed as "an area of higher temperatures in an urban setting compared to the temperature of the suburban and rural surroundings. It appears as an "island" in the pattern of isotherms on a surface map" (p.264). This effect can be measured as both surface and atmospheric phenomena. Figure 2.1 shows the temperature profile illustrating surface temperature and near-surface (measured 1-2 meters from the ground)

air temperature across varying intensities of urbanized land uses (Stone & Rodgers, 2001).

UHIE has also been a rising issue in various study fields including climatology, geography, and public health because UHIE exacerbates existing environmental threats to human health through thermal stress (Oke, 1973; Katsoulis, 1985; Lee, 1992). This phenomenon contributes to the rising intensity of summer heat waves and the risk of death due to increased exposure to extreme thermal conditions. As a result, those who live in a city center have a higher heat-related mortality rate than those living in suburban or rural areas (Lo and Quattrochi, 2003; Conti et al., 2005; Tan et al., 2010). Another concern of UHIE is air pollution. Higher temperatures increase ozone pollution (Lo and Quattrochi, 2003) because it can trigger the chemical reactions that form ozone (Cardelino and Chameides, 2000).

Numerous researchers have studied UHIE. These efforts began in the early 1970s and the research of Clarke (1972) is one of the starting points. In his study entitled "Some Effects of the Urban Structure on Heat Morality," he argued that higher death rates in cities are due to climate modification (temperature, wind speed, radiant heat, and microclimatic effect) accompanied by urbanization. Based on case studies of historic heat waves in U.S., he concluded that:

> The urban thermal environment can be partially controlled through appropriate urban land use. The adequate provision of green areas judiciously spaced over the metropolitan region is one example. The effect of green areas on the nocturnal thermal climate of cities is substantial. Siting of urban activities with respect to

micro- and mesoclimates is another avenue open to the planner; the heat stress on occupants of housing units without air conditioning would be considerably less in suburban areas or on the fringe of a large park than if they are located in the heat of the urban complex. (p.103)

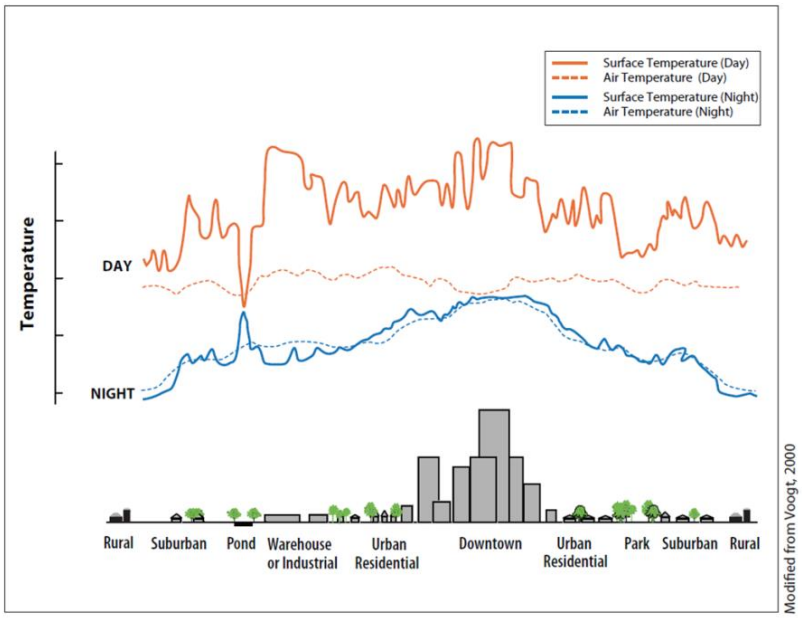

Figure 2.1. Profiles of Urban Heat Island (EPA, 2008b)

Another early researcher, Oke (1973), asserted that city size (measured by population) and UHIE are related. In his study, results indicated that the intensity of UHIE under calm and clear weather conditions is related to the inverse of regional wind speed and the logarithm of the population. He concluded that restricted land use in large cities can reduce climate change. He also explained in his book, *Boundary Layer Climate* (1987), that urban construction and deforestation are sufficient to raise the average temperature of a city by several degrees over that of peripheral non-urbanized areas.

Heat islands develop in areas that have a high percentage of non-reflective, water-resistant surfaces and a low percentage of vegetated and moisture-trapping surfaces. In particular, materials such as stone, concrete, and asphalt can trap heat at the surface (Landsberg, 1981; Quattrochi et al., 2000). Thus, some studies on UHIE emphasize the importance of land use planning to control urban temperature. For instance, Kalnay and Cai (2003) examined the impact of urbanization and land use change on climate. Their study revealed that the estimated surface warming per century because of changes in land use is at least twice as high as previous estimates based on urbanization alone. Hu and Jia (2010) showed that each land use category contributes different amount of heat on urban temperature. They also argued in same study that the fraction of vegetation cover is negatively correlated with land surface temperature.

Further research has continued to uncover relationships between temperature and urban natural and built environment in various study areas utilizing different methods. For example, Streutker (2002) argued that increasing amounts of dark and impervious surfaces that absorb relatively more sunlight can be one significant cause of UHIE. Yoshida et al. (2004) pointed out that diminished green areas, low wind velocity due to a high density of buildings, and changes in street surface coating materials are the main factors that increase air temperature. Rosenziweig et al. (2005) explained that population shifts, urban and suburban growth, land-use change, and production and dispersal of anthropogenic emissions and pollutants interact with regional climates as well as influence the frequency and intensity of specific weather events. Additional recent research on physical structure and UHIE, conducted in metropolitan Phoenix, Arizona, analyzed the relationship between

mean surface temperatures, vegetation density, and socioeconomic characteristics across census tracts. They include socioeconomic variables since residential segregation of neighborhoods is strongly influenced by vegetation and surface temperature. This research established a statistically significant link between vegetation density and daytime surface temperature based on various determinants of neighborhood surface temperature (Jenerette et al., 2007).

Sometimes, a study area has been narrowed down to the parcel-level. Stone et al. (2006), for example, studied residential parcel design and surface heat island formation in a major metropolitan region of the southeastern U.S. They argued that parcel-based research about surface warming can lead to parcel-specific land use policies such as zoning regulations, subdivision regulations, and building codes.

Urban heat island-related studies are rapidly expanding due to remote sensing technologies, which is able to detect surface temperature. The surface temperature is the most important element in the study of urban climatology (Voogt and Oke, 2003). To overcome the limitations of ground-based temperature measurement, satellite-derived surface temperature data have been utilized for urban climate analysis. The first satellite-based surface temperature observation in urban areas was reported by Rao (1972) in his surface urban heat island study. Since then, a variety of sensor-platform combinations (satellite, aircraft, ground-based) have been used to generate remote observations of the surface urban heat island in many studies (Voogt and Oke, 2003).

Voogt and Oke (2003) explained that there are three main research themes in

thermal remote sensing for urban climate. The first theme is the examination of the relationship between urban thermal patterns and urban surface characteristics. This type of research has utilized AVHRR (Advanced Very High Resolution Radiometer) or Landsat thermal imagery combined with land uses or land cover maps to examine the spatial patterns of surface temperature. The second theme is the application of thermal remote sensing to analyze the urban surface energy balance. This type of study is accomplished by pairing urban climate models of the urban atmosphere with remotely sensed observations. The third major research theme of thermal remote sensing is the study of the relation between atmospheric urban heat islands and surface urban heat islands. Traditionally, urban heat island effect was analyzed based on ground-based observation, which represents atmospheric urban heat islands. After developing various satellite sensors for thermal data, several studies have analyzed surface-air temperature relations. Also, satellite observations have been used to detect and correct for air temperature if there is contamination from any urban influence (Voogt and Oke, 2003).

There are three major sensors on the satellite platform to analyze surface temperature: AVHRR, Landsat TM/ETM+, and MODIS Terra/Aqua. Although all three sensors detect surface temperature, each of the sensors has different temporal and spatial resolution as well as different temperature calibration methods. AVHRR (Advanced Very High Resolution Radiometer) has 1.1km of spatial resolution and the repeat cycle is twice a day. Thermal band of Landsat TM/ETM+ have 120m and 60m respectively with a 16-day repeat cycle. Both AVHRR and Landsat TM/ETM+ need atmospheric correction and thermal calibration to estimate surface temperature. Land surface temperature calculated

from MODIS Terra and Aqua have 1km spatial resolution and the repeat cycle is twice a day. MODIS datasets provide atmospheric corrected and calibrated temperature readings (Kelvin). Thus, AVHRR and MODIS Terra/Aqua are suitable for large study areas with frequent observation and Landsat TM/ETM are better suited to small study areas and detail analysis.

2.2. Spatial Development Patterns and Landscape Metrics

Spatial development patterns in urban areas are one of the most important elements used to determine the urban form of a built environment. The forms and footprints of urban built environments ultimately shape the environmental and social conditions within which we live (Brody et al., 2012). Spatial development pattern can describe various aspects of built environment and its characteristics are determined depending on research fields or subjects. In this study, spatial development pattern refers to spatial arrangement of physical development on land surface.

Urbanization is fundamentally a spatial process (Wu et al., 2011). Thus, the importance of urban and suburban development patterns have been documented by previous studies. Development patterns are responsible for the environmental, social, and economic conditions of local communities (Porter, 2000; Squires, 2002; Ewing, 2008; Freilich et al. 2010; Brody et al. 2012).

The development patterns based on densities in the U.S can be characterized by two ends of the spectrum: sprawl and compact. Sprawling development patterns currently

dominate much of the American landscape, yet there is no universally accepted definition of sprawl (Brody et al. 2012). Despite this limitation, there are widely referred literatures that defined conceptual characteristics of sprawl (Burchell et al, 1998; Galster et al. 2001; Ewing et al. 2003). Burchell et al. (1998) listed characteristics of sprawl in terms of three distinct types: spatial patterns, root causes, and main consequences of sprawl. Characteristics of spatial patterns include low density, unlimited outward expansion, land uses spatially segregated, leapfrog development, and widespread commercial strip development. Two causes of sprawl listed in his book are no central ownership or planning and highly fragmented land-use governance. Finally, the three consequences of sprawl are explained as transport dominance by motor vehicles, great variance in local fiscal capability, and reliance on filtering for low-income housing.

While the study of Burchell et al. (1998) considers various aspects of sprawl, the studies of Galster et al. (2001) and Ewing et al. (2003) are more focused on the spatial characteristics of sprawl. Galster et al. (2001) argued in their research that sprawl is identified as eight distinct dimensions of land use patterns: density, continuity, concentration, clustering, centrality, nuclearity, mixed uses, and proximity. They tested thirteen large urbanized areas from different regions of the U.S. based on six out of eight indicators (except continuity and diversity) to analyze housing sprawl and then ranked them to see if these indexes can explain sprawl development patterns correctly. Ewing et al. (2003), in their research about the relationship between urban sprawl and physical activity, obesity, and morbidity, suggested four dimensions of large scale (i.e. metropolitan region) urban form extracted from several observed variables via principal components

analysis: residential density, mix of land uses, degree of centering, and street accessibility. Otherwise, they employed six additional sprawl index variables for the county level that reflect residential density and street accessibility: (1) gross population density; (2) percentage of the county population living at low suburban densities; (3) percentage of the county population living at moderate to high urban densities; (4) the net density in urban areas; (5) average block size; and (6) percentage of blocks with areas less than 1/100 square mile, the size of a typical traditional urban block bordered by sides just over 500 feet in length.

Techniques of Geographic Information System (GIS) and Remote Sensing (RS) have allowed researchers to measure spatial development patterns more quantitatively. For example, Song and Knaap (2004) measured urban form to analyze the spatial pattern of urban sprawl in the metropolitan regions of Portland, Oregon. They used GIS to analyze various physical characteristics representing urban form, including the number of street intersections, median perimeter of blocks, lot size, acres of mixed-use land, median distance to commercial sites/ bus stops/parks, and so on. Additional research at the micro-urban level was conducted by Emily (2005). This research examined good urban form for an inner-city neighborhood. She used layering, which is a basic concept of GIS with eight measurements that represent urban form, including the enclosure, lost space, sidewalks, public space, incompatible streets, lot width, proximity and mixed-use.

On the other hand, some studies that use up-to-date measuring development patterns utilized the public domain statistical package FRAGSTATS (McGarigal et al., 2002), which measures landscape or development patterns with various landscape indices

based on raster (e.g. remote sensing data) and vector datasets (Herold et al., 2003; Wu et al., 2011). These measurements have been widely used by ecologists and conservation biologists as well as geographers (Brody et al., 2012; Wei Ji et al., 2006).

Landscape metrics are numeric measurements that quantify the spatial patterning of land cover patches, land cover classes, or entire landscape mosaics within a geographic area (McGarigal & Marks, 1995; See Fig 2.2). A patch refers to a relatively homogeneous area that differs from its surroundings. Patch-level metrics calculate characteristics of individual patches including size, shape, and distance from the nearest neighbor. In many applications, patch-level measures are not directly interpreted. Class-level metrics quantify characteristics of an entire class including total extent, average patch size and degree of aggregation or clumping, and return a unique value for each class. Thus, class-level indices provide spatial characteristics for a particular class. For example, this study is interested in knowing the total area of developed patches (i.e. impervious areas), average distance between high intensity developed patches, and aggregation of developed patches. On the other hand, landscape-level indices are a set of all patches within the area of interest. In raster data, a landscape is the entire collection of cells, regardless of class value. Landscape-level indices are is useful to quantify the overall composition and configuration of the patch mosaic and thus it can be interpreted as broad landscape pattern.

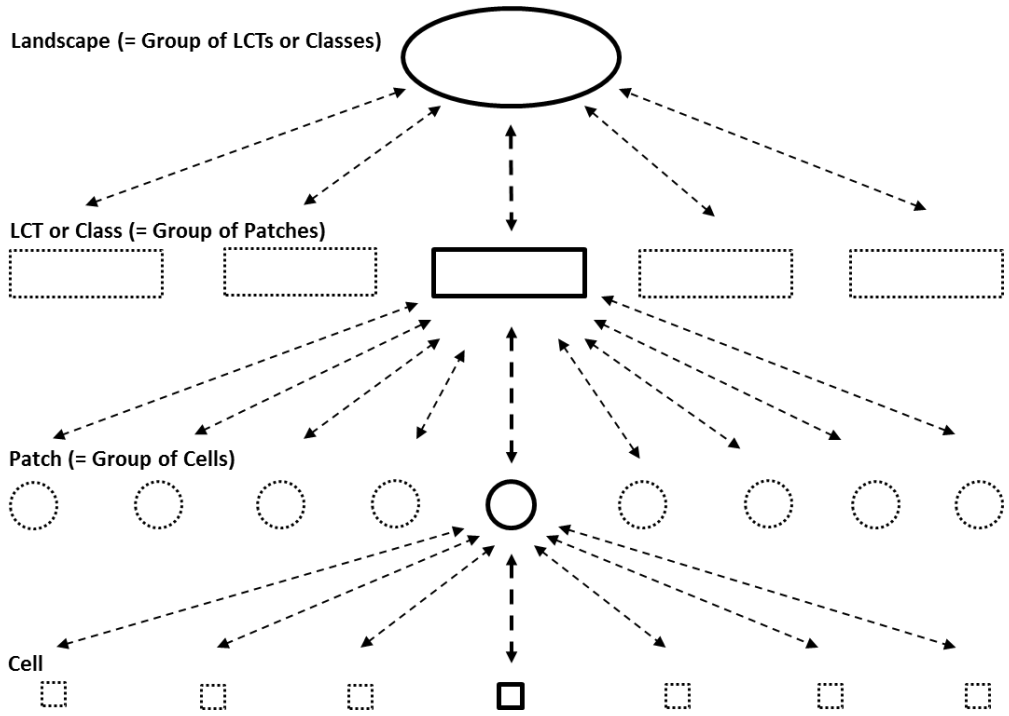

Figure 2.2. Conceptual diagram of the four levels of analysis provided in the metrics: cell, patch, class/land cover type (LCT), and landscape (Adopted from Leitão, 2006)

Landscape structure represents the composition and spatial distribution patterns of landscape elements. While composition refers to the number, type and extent of landscape elements, configuration refers to the spatial character arrangement, position, or orientation of landscape elements (Leitão, A., et al., 2006). In planning, the number and proportion of each land cover type can be measures of composition while the placement and distribution of each land cover type can be measures of configuration.

When considering a city as a large social organism, landscape metrics, which measure ecological landscape patterns, can definitely be used to measure forms of urban structure. However, only recent planning studies have attempted to analyze the dynamics

of an urban setting (i.e. development patterns) using landscape metrics to explain heterogeneous urban areas effectively (Herold et al., 2003; Ji et al., 2006; Schneider and Woodcock, 2008; Thapa and Murayama, 2009; Brody et al. 2012). The use of spatial metrics has provided a new platform for describing the spatial land use and land cover heterogeneity and morphological characteristics within the urban environment (Thapa and Murayama, 2009). Moreover, landscape metrics have found important applications in quantifying urban growth, sprawl, and fragmentation (Hardin et al. 2007).

Also, since GIS and RS techniques are being employed by a rapidly increasing number of users, landscape metrics have become a useful tool to measure urban form and development patterns. There have been efforts to employ concepts of landscape metrics in urban planning studies to analyze and quantify spatiotemporal change in terms of urban development patterns, built environment, and land use change (See Table 2.1).

Although every study analyzes different research areas and in various scales (e.g. spatial resolution or unit of analysis), a large portion of research is focused on a time series analysis for the same study area in order to see temporal changes. For example, Herold et al. (2002) considered landscape metrics pertinent information on image spatial form and utilized it to analyze urban land use structure and land cover changes that account for urban growth. They applied several landscape metrics to two test sites in California across three different land uses in order to detect changes and growth processes. Seto and Fragkias (2005) quantified the annual rate of land-use change using remote sensing imageries (i.e. Landsat TM) for four cities in southern China. This study also calculated landscape metrics scores spatiotemporally across three buffer zones to understand and compare the shapes

and trajectories of urban expansion. The result showed that the four cities exhibited common patterns in their shape, size, and growth rates despite their different economic development and policy histories. Thapa and Murayama (2009) analyzed spatiotemporal urbanization patterns in Kathmandu Valley, Nepal. They also utilized remote sensing data and selected spatial metrics to quantify and monitor landscape fragmentation, land-use complexity, proximity, dominancy, and diversity in both landscape and class levels. These five measurements of landscapes (composition and configuration of landscape pattern changes) are calculated by selected spatial metrics including patch density (PD), the largest patch index (LPI), edge density (ED), area weighted mean patch fractal dimension (AWMPFD), Euclidian nearest neighbor distance mean (ENNMN), cohesion (COHESION), contagion (CONTAG), and Shannon's diversity index (SHDI).

Unlike the above studies, Huang et al. (2007) applied landscape metrics to cross sectional analysis for seventy-seven large metropolitan regions in Asia, the U.S., Europe, Latin America and Australia. They calculated five spatial metrics for distinct dimensions of urban form. The result of this study clearly indicated that urban form of metropolitan regions differs across regions. Particularly, urban forms of metropolitan regions in the developing world are more compact and dense than their counterparts in either Europe or North America.

Some studies examined scale issues including grain size and unit of analysis in calculating landscape metrics with remote sensing imageries. Ji et al. (2006) examined trends and patterns of urban land-use change at the metropolitan, county, and city levels using remote sensing imageries and landscape metrics as spatial analytical methods. They

employed three landscape metrics, including patch density (PD), the largest patch index (LPI), and the aggregation index (AI) to understand and examine urban sprawl dynamics by calculating the built-up patch density and forest aggregation indices across jurisdictional levels. The result of this study revealed a scale effect in which the landscape response of urbanization can be better detected within a larger spatial unit (e.g. a metropolitan region or county as compared to a city). Wu et al. (2011) also mentioned scale issues in their research which quantified the spatiotemporal patterns of urbanization for two of the fastest growing metropolitan regions to understand the process of urbanization. This study analyzed landscape metrics in four different grain sizes (i.e. spatial resolution of remote sensing images) for two cities—Phoenix and Las Vegas— to figure out the scale issue. The result indicated that general patterns of urbanization are not be significantly affected by changing grain size.

Very recent research by Brody et al. (2012) utilized the landscape metrics concept from different angle. They employed flood loss as dependent variable to examine the impact of development patterns on flooding. Five landscape metrics are measured—total class area (CA), number of patches (NP), patch density (PD), proximity (PROX), and connectivity (CONNECT)— as indicators of urban development patterns across three development intensities (high, medium and low) to examine the effect of urban form on flood risk along the coast of the Gulf of Mexico. They found that a greater overall area of compact, high-intensity impervious surface reduces flood losses (i.e. insured property damage) except in the case of dense urban development that is situated in flood-prone areas. Also, areas with medium-intensity development (50-79 percent impervious surface

cover which is typical of dense suburban setting) showed more significant impact on property damage from floods than other development intensities. Specifically, an increase in the number and density of medium-intensity patches is the most influential combination in terms of significantly increasing insured property damage from flooding events. Finally, they concluded that regional planners should promote high-intensity, clustered development rather than low-density sprawling development patterns to foster flood-resilient communities.

Table 2.1 shows the summary of literatures that measure built environment and urban growth patterns using landscape metrics.

Table 2.1. Measuring urban form and growth patterns using landscape metrics

Authors	Year	Subject	Study Area	Landscape Metrics
Herold et al.	2002	Spatial Urban Growth Pattern	Santa Barbara/ Goleta, CA	FRACT (Fractal Dimension), %LAND (Percent of Landscape), PD (Patch Density), PSSD (Patch size standard deviation), ED (Edge Density), AWMPFD (Area weighted mean patch Fractal Dimension), CONTAG (Contagion Index)
Seto and Fragkias	2005	Spatiotemporal patterns of urban land use change	Four cities in China	ED, AWMPFD, NP (Number of Patches), MPS (Mean Patch Size), PSCOV (Patch size coefficient of variation)
Ji et al.	2006	Trends and Patterns of urban sprawl	Kansas Metropolitan region, County, City	PD, LPI (Largest Patch Index), AI (Aggregation Index)
Yu and Ng	2007	Spatial and Temporal dynamics of urban sprawl	Guangzhou City, China	NP, MPS, LPI, AWMSI (Area weighted mean shape index), AWMPFD, SHDI, CONTAG, COHISION
Haung et al.	2007	Comprehensive Urban form	77 metropolitan regions in the world	AWMSI (Area Weighted Mean Shape Index), AWMPFD, Centrality, CI (Compactness Index), CILP (Compactness index of the largest patch)
Thapa and Murayama	2009	Spatiotemporal patterns of urbanization	Kathmandu Valley	PD, LPI, ED, AWMPFD, ENNMN (Euclidian nearest neighbor distance mean), COHESION, CONTAG, SHDI (Shannon's Diversity Index)
Wu et al.	2011	Spatiotemporal patterns of urbanization	Phoenix and Las Vegas metropolitan regions	AWMFD, CONT, ED, LSI (Landscape Shape Index), MPS, PD, %Class, SHDI, Sqp (Square Pixel)
Brody et al.	2013	Impact of development patterns on flooding	Coastal Counties along Gulf Coast	CA (Class Area), NP, PD, PROX (Proximity), CONNECT (Connectance)

2.3. Urban Heat Island Effect (UHIE) and Urban Development Patterns

Urban growth and sprawl development pattern have significantly altered the biophysical environment. The replacement of soil and vegetation with impervious surfaces such as concrete, asphalt, and buildings is a major change in urban areas (Lo and Quattrochi, 2003). A most notable phenomenon that has arisen as a result of the expansion of development is that urban climates are warmer and more polluted than their rural counterparts (Lo and Quattrochi, 2003). Hence, temperature patterns of urban areas appear as an "island," which is known as an Urban Heat Island (UHI) (Sailor, 1995; Stevermer, 2002). As mentioned in the previous section, many preceding researchers have suggested that the UHI distribution is linked with complex urban components and is dependent on a number of factors (Jenerette et al., 2007; Weng, Lu, & Liang, 2006). Surface characteristics of urban areas appear to be the main contributor to the increased temperature (Jenerette al., 2007; Voogt&Oke, 2003). For example, UHIE is strongly related to a lack of vegetation, the materials used in the built environment, and urban canyon geometry (Oke, 1981; Rosenzweig et al., 2005).

Recently, there have been attempts to find relationships between urban form and temperature. Most of these attempts are focused on measuring land use or land cover patterns using GIS and RS datasets to discover their relationships with temperature. The following three studies explained how they measured the urban form regarding UHIE for the same study area, a metropolitan region of Atlanta, GA. In their study, "Urban Form and Thermal Efficiency," Stone and Rodgers (2001) analyzed the relationship between a single family residential urban form and thermal conditions in Atlanta, GA. They

constructed a database that included urban design elements that are related to the surface heat island—tree canopy cover, year of construction, number of bedrooms, impervious surface area, pervious surface area, and street intersection density— and measured them. They utilized GIS to build various datasets on a parcel-based map. Also, they described how they used an overlay function to measure the percentage of tree canopy cover in each single family parcel (which was a unit of analysis).

Lo and Quattrochi (2003) analyzed land use and land cover change in order to examine their relationships with temperature change. They calculated the amount and percentage of each land use category extracted from Landsat images over a period of twenty-five years (1973-1998). Also, they calculated the NDVI (Normalized Difference Vegetation Index), which measures the greenness of the environment as well as the amount of vegetation or biomass. The variations in the percentage of land use and the NDVI demonstrated how the urban form has changed throughout time.

More recently, empirical research on UHIE and impervious surfaces was conducted in the Atlanta metropolitan region by Lee and French (2009). They predicted the Atlanta metropolitan region's future amount of reduced impervious surface as a mitigation measure for UHIE in a metropolitan region. They utilized high-resolution aerial photography to divide impervious surfaces into different land use categories. Then, each land use category was multiplied by the land cover coefficient to estimate the current impervious surface area. Based on the estimated current impervious surface area, population, and employment rate, they predicted a future amount of impervious surfaces using regression models. Although this research is simply focused on impervious surfaces

in terms of urban form, it is meaningful because the amount of impervious surfaces is one of the critical factors that exacerbate the UHIE.

Another study of Stone et al. (2010) analyzed the relationship between the urban form of a metropolitan area and the mean annual rate of change for extreme heat events between 1956 and 2005. They employed the sprawl index created by Ewing et al. (2003), which includes centeredness, connectivity, density and land-use mix. They utilized GIS to measure each attribute. For example, connectivity was measured by average block size and the percentage of blocks less than approximately 500 feet on one side. In other words, as block size increased, the number of street intersections per unit of area decreased, which indicated street network density. Their results showed that "the most sprawling cities in top quartile experienced a rate of increases in extreme heat events that was more than double that of the most compact cities in the bottom quartile (Ewing, 2003)"

Most recently, Junxiang Li et al. (2011) conducted a case study of Shanghai, China that examined the impacts of landscape structure on surface UHIs using the NDVI, vegetation fraction, and the percentage of impervious surface area. They found that surface temperature had a large range of variations at a given level of NDVI, percent vegetation, and impervious surface area. Thus, they employed landscape metrics and analyzed correlations between landscape metrics and surface temperature to find the reason behind the temperature variations. They showed that the urban land surface temperature (LST) is not only influenced by land cover composition but also by its spatial configuration. Five metrics were measured at the class-level across land use categories: percent of land use (PLAND), edge density (ED), patch density (PD), landscape shape index (LSI), and

clumpiness. The following three metrics were measured at the landscape level: Shannon's evenness index (SHEI), Shannon's diversity index (SHDI), and contagion (Contagion). LST is generally negatively correlated with clumpiness on the pixel-by-pixel scale and Shannon's diversity index on the landscape scale, indicating that a mixture of impervious surfaces with other land cover types reduces surface UHIE.

2.4. Summary of and Gaps in the Literature

The literature above shows that urban built environments driven by development have clear impacts on UHIE. A large portion of the literature made efforts to examine the relationship between urban components and UHIE in order to find the factors that increase temperature. As a result, previous research suggested various factors that increase urban temperature in terms of land use, land cover, and surface characteristics. Although every study employs different variables and analytical methods, their results share the general consensus that increasing impervious surface area has a positive effect on urban temperature and the presence of vegetation and water in urban built environments reduces urban temperature. One gap in the research is that most of studies have analyzed one specific study area (ranging from a neighborhood to a metropolitan region) to examine the relationship between development characteristics and UHIE. This research is limited to the given conditions of that particular UHIE study area. The findings of one particular study are thus difficult to apply to other places. In contrast, my study covers multiple metropolitan regions in the continuous U.S. to provide a more comprehensive and

externalizable understanding of the relationship between UHIE and development patterns.

In recent years, some researchers have begun to pay more attention to urban development patterns as one of the factors that affect urban temperature. They attempted to analyze spatial development pattern by employing various indicators such as the sprawl index and landscape matrix. Both the sprawl index and landscape matrix provide an understanding of spatial characteristics of development patterns. Especially, landscape metrics are considered by researchers as a useful way to describe urban landscapes in terms of composition and configuration. Another research gap is that landscape metrics are traditional measurements in ecological studies, but only recently have planning studies discussed and utilized landscape metrics to quantify physical urban development patterns. Moreover, the spatial analysis of development patterns in relation to UHIE has been surprisingly limited, with some exceptions, including Stone et al. (2010) and Junxiang Li et al. (2011).

CHAPTER III

RESEARCH FRAMEWORK AND HYPOTHESES

Based on the literature review in the previous chapter, this study proposes the conceptual framework in Figure 3.1. In order to develop this framework, I extracted three potential factors that affect the UHIE: the built environment, natural environment, and demographic characteristics.

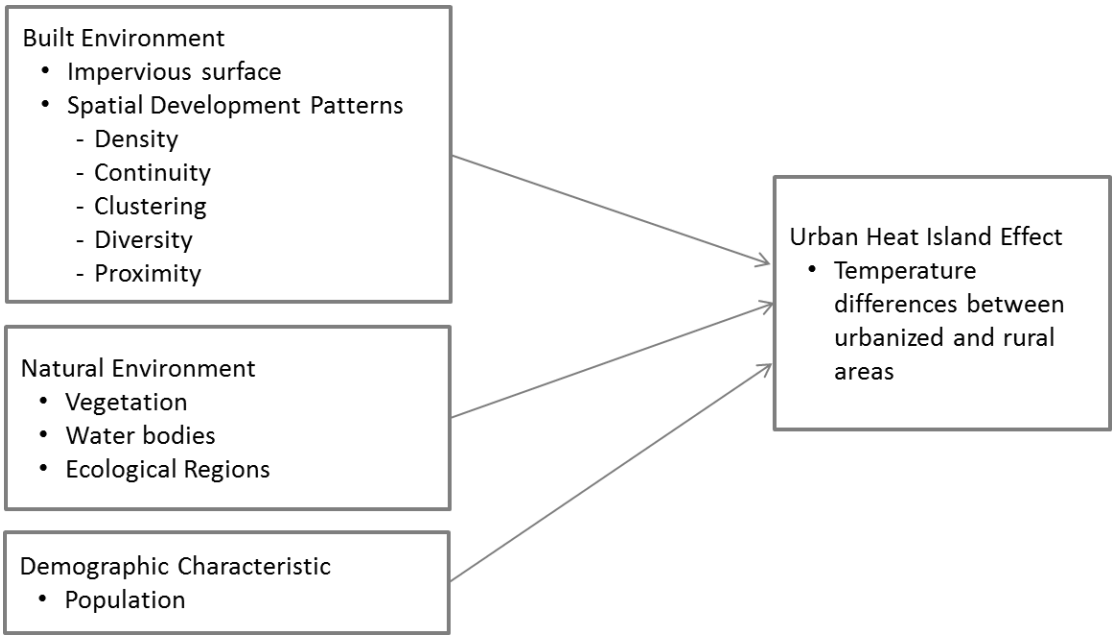

Figure 3.1. Research Framework

The main set of independent variables is associated with spatial development patterns based on five criteria: density, continuity, clustering, diversity and proximity. Control variables include the percentage of vegetation cover, percentage of water surface

cover, regional climate and population characteristics. The following sub-sections provide an understanding of key variables including UHIE and urban development patterns leading to specific research hypotheses to test the effect of development patterns on the UHIE.

3.1. Dependent Variable: Urban Heat Island Effect

The dependent variable for this study is UHIE, specifically the difference in surface temperature between urbanized and rural areas. Many previous studies on the topic of UHIE have used temperature differences (e.g. mean, daily maximum, and daily minimum) between urban and surrounding rural areas or between the inside and outside of a city to examine the degree and magnitude of UHIE. Since this study focuses on the regional UHIE, UHIE can be captured at the metropolitan level by comparing the temperatures of an urbanized area and a rural area in the same metropolitan regions.

There are two types of UHIEs: surface UHIE and atmospheric UHIE. It is known that atmospheric UHIE is observed to be larger at night while surface UHIE is observed to be larger during the day (Roth et al, 1989). While atmospheric UHIE is measured by the air temperature provided by weather station networks, the surface UHIE is obtained through surface temperature gathered by airborne or satellite thermal infrared remote sensing, which allows researchers to study surface UHIE on a regional scale (Yuan and Bauer, 2007). As a result, this study employs surface UHIE in the summer season as a dependent variable and uses both day and night temperatures to observe diurnal and nocturnal UHIE patterns (Detailed in Section 4.2.1).

3.2. Independent Variable: Urban Development Patterns

As discussed in the literature review of Section 2, previous studies have attempted to investigate the relationship between urban components and temperature. Although they used various methods for different study areas, there is a general consensus that the temperature or thermal efficiency level vary depending on the characteristics of the land surface, including imperviousness, vegetation, and surface of water on land. In considering the characteristics of land surface as components, the spatial development pattern is how these components are arranged. In other words, spatial development pattern refers to a configuration of various components and is an important concept used to describe urban land surface. Thus, this study employs spatial patterns of development as independent variables to examine the effect of spatial configuration of development on UHIE.

As mentioned earlier, there are two typical types of spatial development patterns in the U.S.: sprawl and compact. Using concepts (sprawl and compact) and characteristics to separate these two major development patterns, this study sets a main hypothesis and several sub-hypotheses to answer the research question posed above.

➔ ***Main Hypothesis: Metropolitan regions with a sprawling development pattern in urbanized area will have a higher Urban Heat Island Effect than the metropolitan regions with a compact development pattern in urbanized area.***

3.2.1. Density of Development

Density is the most cited indicator of sprawl in previous studies (Burchell et al.,

1998; Gordon and Richardson, 1997a, b; Sierra Club, 1998; Galster et al., 2001). It is usually measured by the relationship between population or residential units and land area. Alternatively, density, in terms of development patterns, is computed using the ratio of developed area to the total land size of urbanized area, which could provide relative degrees of development for each metropolitan region.

The density of development could be interpreted in various ways. In this study, the density of development is equal to the density of impervious surface since the "developed" category in land cover dataset refers to impervious surfaces. As mentioned in literature review section, increasing the amount of impervious surfaces has a positive relationship with urban temperature. Thus, the first sub-hypothesis is:

➔ ***Sub-Hypothesis 1: Metropolitan regions with a higher ratio of development in urbanized area will have a larger Urban Heat Island Effect than metropolitan regions with a lower ratio of development in urbanized areas.***

3.2.2. Continuity of Development

Continuity refers to the degree to which development has occurred in an unbroken fashion (Galseter et al. 2001). Continuity is also frequently cited as a controvertible dimension of development. There are two major forms of sprawl that are related to continuity: low-density continuous development and ribbon development (Harvey and Clark, 1965). Low density sprawl is less offensive and the lowest order of sprawl but the most ubiquitous type of development pattern. It displays a land consumptive development

pattern as opposed to one that is more planned and concentrated. Ribbon development usually refers a continuous development pattern coupled with high ways. This type of sprawl is composed of compact segments within development, but is extended in a line shape. Connected and wide-spreading development patterns create a large amount of impervious surfaces which produce heat in various ways: increasing automobile use increases air pollution and losing vegetation cover. Thus, this study measures the connectivity of developed areas to examine the degree of continuity of development which includes both concepts of low-density continuous development and ribbon development patterns.

➔ ***Sub-Hypothesis 2: Metropolitan regions with higher continuity of development in urbanized areas will have a larger Urban Heat Island Effect than metropolitan regions with a lower continuity of development in urbanized areas.***

3.2.3. Clustering of Development

Clustering is one of the compact development strategies in which land is developed in a tightly bunched area to minimize the amount of land consumed. This approach allows for compact developments while still protecting environmentally sensitive areas and agricultural lands. Moreover, clustering reduces the costs of site development involving the construction of roads and water/sewer infrastructure (Blaine and Schear, 1998). Clustering development can minimize the amount of impervious surface in urban areas. On the contrary, disaggregated development aggravates greater landscape heterogeneity

and fragmentation (Torrens and Alberti, 2000). Reducing overall impervious surface and protecting natural environment should therefore decrease urban temperature.

➔ ***Sub-Hypothesis 3: Metropolitan regions that contain a more clustered development pattern in urbanized areas will have a smaller Urban Heat Island Effect than the metropolitan regions with a less-clustered development pattern in urbanized areas.***

3.2.4. Diversity of Land Covers

The diversity of urban development indicates a land use mix, which means that at least two different land uses exist within the same spatial planning unit. Another attribute of sprawl-oriented development is the separation of different kinds of land uses from each other (Vermont Forum on Sprawl, 1999). A mixture of land uses in urban areas, including residential, business, commercial, and open space, decreases travel time and distance for those who live or work there (Galster et al., 2001). When this concept is applied to land covers, diversity can be measured by the number of land cover types in an urbanized area. Coexistence of development and other natural land covers (e.g. vegetation, water) allows an urban area to better control temperature (thermal comfort). In this sense, diversity of land cover in urban areas could reduce the impact of the UHIE.

➔ ***Sub-Hypothesis 4: Metropolitan regions with a greater diversity of land cover types in urbanized areas will have a smaller Urban Heat Island Effect than the metropolitan regions that have less diverse land covers in urbanized areas.***

3.2.5. Proximity of Land Covers

The proximity of urban development refers to the degree to which different land uses are physically close to each other within an urbanized area. Conceptually, proximity is the average distance people must travel on daily basis (Galster et al., 2001). One of the most important indicators of reduced proximity is poor accessibility because it affects the efficiency of household travel patterns (Ewing, 1997). Residents may commute far from home for out-of-home activities (i.e. residential accessibility) or out-of-home activities may be far from each other (i.e. destination accessibility). Thus, the urban areas where people have to travel long distances have lower proximity between land uses, and therefore can be considered as a sprawling type of development. When applied to land cover, proximity refers to how well development and natural environments are interspersed.. Sharing the borders of development with natural environments could attenuate the heat generated from developed areas.

➔ ***Sub-Hypothesis 5: Metropolitan regions with a higher proximity between different land covers in urbanized areas will have a lower Urban Heat Island Effect than metropolitan regions that have a lower proximity between different land covers in urbanized areas.***

3.3. Control Variables

3.3.1. Impervious Surface

The percent (amount) of impervious surface is a primary indicator used to estimate surface UHIE since most of the heat created derives from it. Impervious surfaces are covered surfaces which water cannot infiltrate and are highly associated with transportation features (streets, highways, parking lots and sidewalks) and building rooftops (Yuan and Bauer, 2007). Also, the amount of impervious surface is related to population growth and urbanization (Stankowski, 1972) and is an important indicator of environmental quality (Arnold & Gibbons, 1996). Thus, the amount or percent of impervious surface is often employed as a major predictor of urban expansion and used to analyze the relationship between land surface urban temperature and urban development. Previous studies have shown that a higher urban development intensity or imperviousness will, generally have a higher land surface temperature (Oke, 1976; Weng, 2001; Yuan and Bauer, 2006). Therefore, this study hypothesizes that an area containing a higher percentage of impervious surfaces will experience significantly greater UHIE.

3.3.2. Percentage of Vegetation Cover

Vegetation cover has shown to be an important factor in influencing urban temperature (Landsberg, 1981; Quattrochi et al., 2000.; Yoshida et al., 2004). Vegetation reduces air temperature through the evapotranspiration process, in which plants release water to the surrounding air, dissipating ambient heat (EPA, 2008b). Thus, numerous

studies have included the amount of vegetative cover as an important variable that affects UHIE. Vegetation cover represents the percentage of vegetated areas including forest, shrubland, and herbaceous sections in an urbanized area. As urban areas expand, more vegetation is lost and more surfaces are paved or covered with human-made structures (EPA, 2008b). This study hypothesizes that an area containing a higher percentage of vegetation cover will experience a significantly smaller UHIE.

3.3.3. Percentage of Watered Surface

Watered surface is another important variable related to UHIE. Water has a relatively low temperature during the daytime; therefore it reduces the average urban temperature. Watered landscapes affect surface temperature (Gober et al., 2010) and were discovered to be one of the coolest features among land use types with vegetation (Weng et al., 2006). Also, proximity to large bodies of water and mountain terrain may influence local wind patterns and urban heat island formation (EPA, 2008b). Thus, this study hypothesizes that an area containing a higher percentage of watered surfaces will experience a significantly smaller UHIE.

3.3.4. Population

Although UHIE is generally related to the physical elements of urban areas, population is an exceptional consideration. Population can be an indicator of various activities in a particular place including business, transportation, and energy consumption.

Oke (1973) found evidence that UHIE increases with population. He suggested the formula "UHI = 0.73log10 (pop), where pop denotes population. An example of this would be that a place with a population of ten has a warm bias of 0.73 °C, a place with a population of one thousand has a warm bias of 2.2 °C, and a large place with one million people has a warm bias of 4.4 °C. Therefore, this study hypothesizes that an area with a large population will experience a significantly larger UHIE.

3.3.5. Ecoregions

Ecological regions (Ecoregions) were developed by commission for environmental cooperation (CEC) in 1997 to assess the nature, condition and trends of the major ecosystems in North America (ECE, 1997) (See Figure 3.2). Ecoregions are the area of general similarity in ecosystems and in the type, quality, and quantity of environmental resources. They are used as a spatial framework for the research, assessment, management, and monitoring of ecosystems and ecosystem components. Ecological regions can be applied to various research, such as national and regional state of the environment reports, environmental resource inventories and assessments, setting regional resource management goals, determining carrying capacity, as well as developing biological criteria and water quality standards. This classification is especially important for evaluating the ecological risk, sustainability, and health of regional and large continental ecosystems. Ecological land is classified using a process of delineation and classification in ecologically distinctive areas of the Earth's surface. Each area can be considered as a

discrete system which has resulted from the mesh and interplay of the geologic, landform, soil, vegetative, climatic, wildlife, water and human factors that may be present. The dominance of any one or a number of these factors varies with the given ecological land unit.

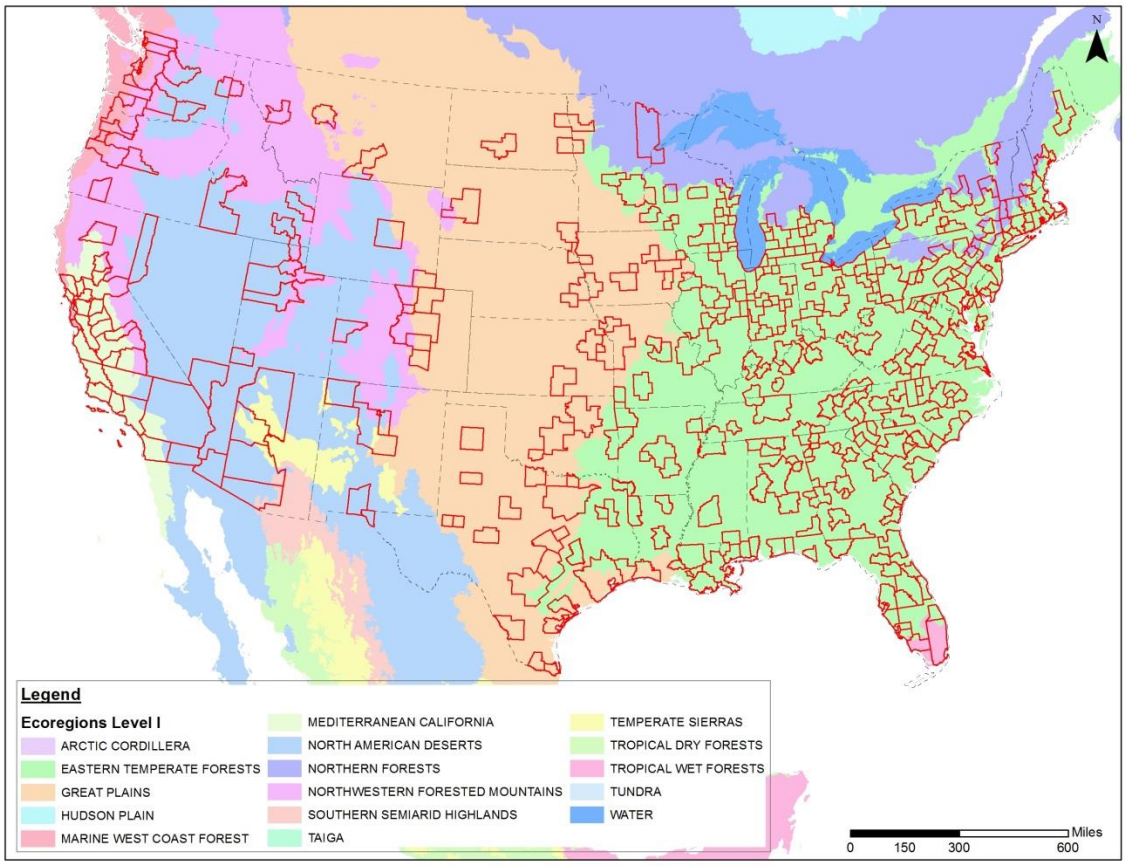

Figure 3.2. Ecoregions and Metropolitan regions in U.S.

Table 3.1. Variables, definitions, and expected impact

Variable Name		Variable Definitions	Source	Relationship Expected with UHIE
Dependent Variables				
UHIE	Day	Temperature difference between urban and rural at day time	MODIS dataset (MOD11A2 v.5) July 12, 2006	
	Night	Temperature difference between urban and rural at night time		
Independent Variables: Spatial Development Patterns				
Development Patterns	Density	Degree to which total land development ratio in urbanized area	Analysis Result by Fragstat 4.0 using USGS, NLCD (2006)	+
	Continuity	Degree to which development has been occurred in an unbroken fashion		+
	Clustering	Degree to which development has been clustered or aggregated		–
	Diversity	A number of land covers exists		–
	Proximity	Degree to which various land cover types has been close each other		–
Control Variables: Built, Natural Environments & Demographic Characteristic				
Impervious surface		Impervious surface area	USGS, NLCD(2006)	+
Vegetation		Vegetation covers	USGS, NLCD(2006)	–
Water surface		Watered surfaces	USGS, NLCD(2006)	–
Population		Population	U.S. Census (2010)	+
Ecoregions		Ecological regions	ECE, Ecological Regions Level I (1997)	Dummy

CHAPTER IV

RESEARCH METHODS

This section outlines and discusses the research methods used in this study. It includes three sub-sections. First, the study area chosen for this research is identified and described. Second, concept measurement is explained for employed dependent and independent variables. The third sub-section details data analysis methods used in this research. Finally, the last section discusses threats to the validity of this study.

4.1. Study Area (Spatial Sample Frame)

The spatial sample frame for this research comprises 353 metropolitan regions in the continuous U.S. (See Figure 4.1). Previous research suggests that metropolitan regions, containing two-thirds of the U.S. population and nearly three-quarters of its economic activities, need to be priority targets for climate change management action (Brown, Southworth & Sarzynski, 2008; Grover, 2010). Also, heat islands are more easily and clearly observed based in metropolitan regions than within any other cartographic boundaries such as counties or cities.

In the contiguous U.S., there are a total of 947 CBSAs (Core Based Statistical Areas) which are divided into two types of regions including metropolitan and micropolitan statistical areas (Census 2003). CBSAs are defined by the federal Office of Management and Budget (OMB) based on a set of official standards published in the Federal Register. Metropolitan statistical areas are usually referred to as metropolitan

regions in many previous studies. The Census Bureau set the definition of the concept of a metropolitan region as "A large population nucleus (50,000 or more), together with adjacent communities having a high degree of social and economic integration with that core. Metropolitan regions comprise one or more entire counties, except in New England, where cities and towns are the basic geographic units". In other words, counties in the same metropolitan region share their industry, transportation, infrastructure, and housing. Thus, within this unit of a metropolitan region, it is important to analyze regional characteristics in terms of socio-economic and population characteristics.

There are 358 metropolitan regions in the continuous U.S (2006), and these include about eighty-three percent of the U.S. population. The metropolitan areas have a much higher population density than the rest of U.S. regions could be clear evidence that most land development occurs in metropolitan regions. Ultimately, this study includes the sample of 353 metropolitan regions, omitting five metropolitan regions because they were dropped from the Census 2010 (for the population variable) data.

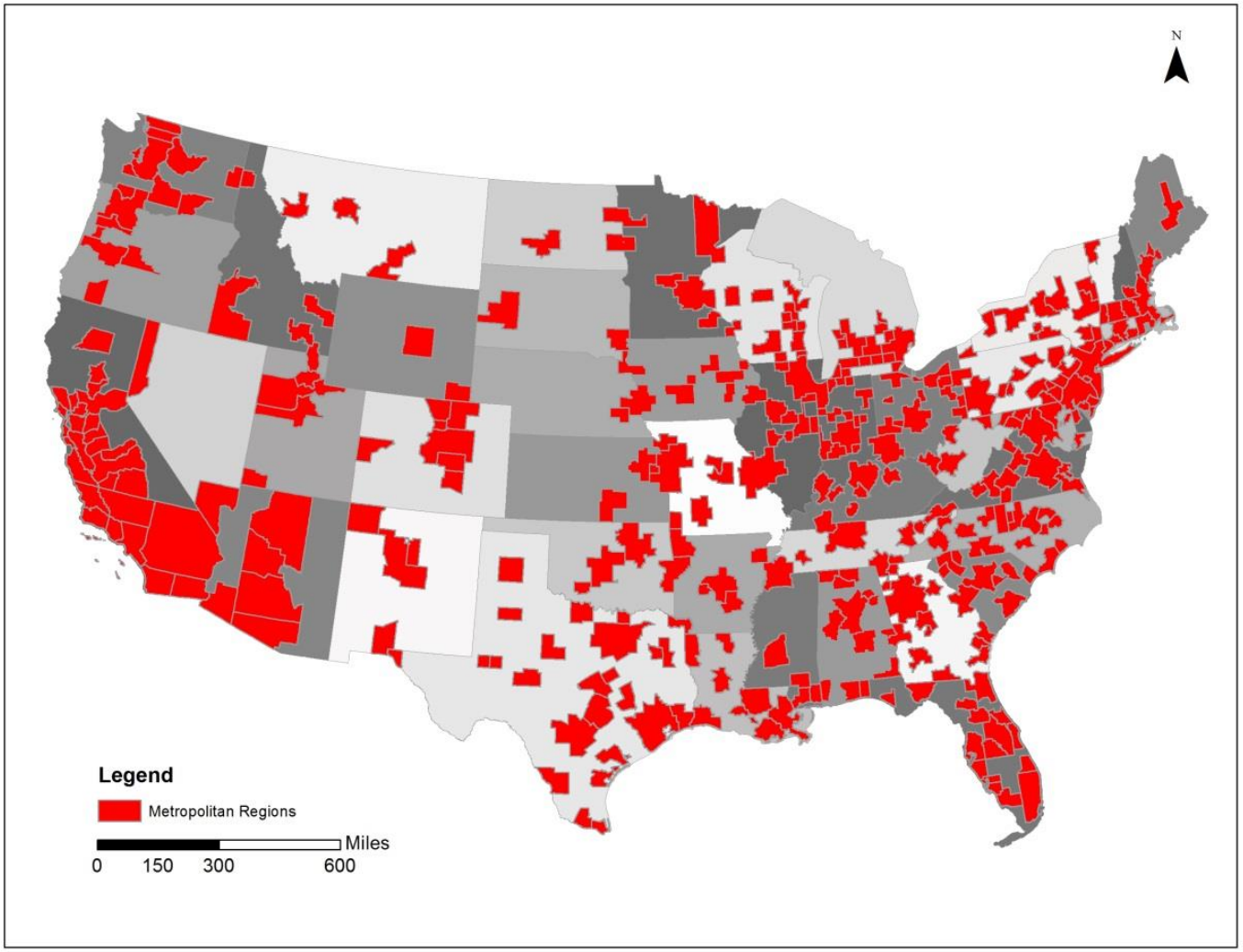

Figure 4.1. Metropolitan regions in Continuous U.S.

4.2. Measurement

4.2.1. Dependent Variable: Urban Heat Island Effect

UHIE can be determined by temperature difference between urbanized and non-urbanized areas in each metropolitan region. The larger values represent the larger magnitude of UHIE.

UHIE = Avg. Temperature $_{\text{urbanized area}}$ **- Avg. Temperature** $_{\text{non-urbanized area}}$

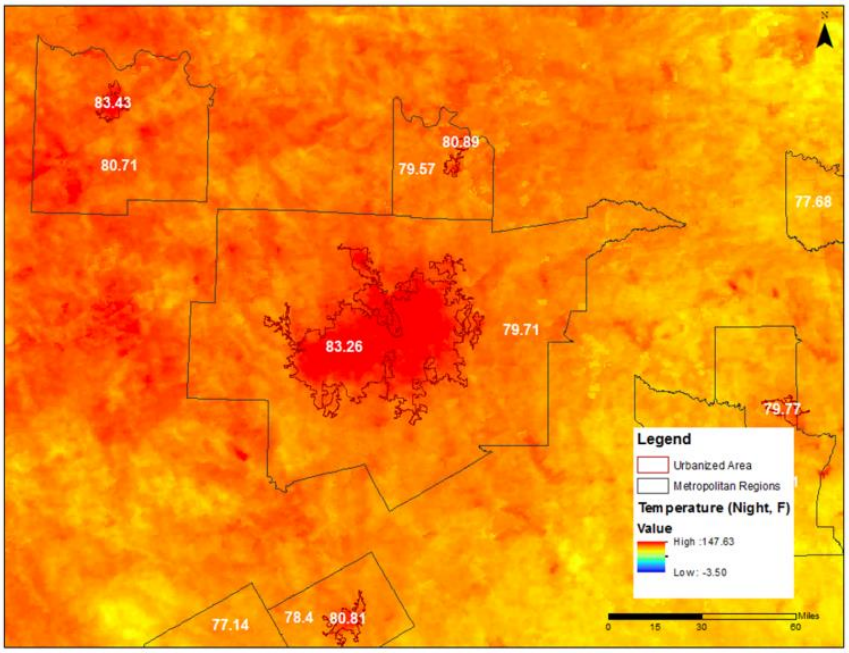

Figure 4.2. Mean temperature of urbanized and rural areas at night

There are still ongoing debates about whether to select ground temperature or air temperature when measuring UHIE since it can be measured as both surface and atmospheric phenomena (Stone and Rodgers, 2001)(See Table 4-1).

Table 4.1. Basic Characteristics of Surface and Atmospheric Urban Heat Island (EPA, 2008b)

Feature	Surface UHI	Atmospheric UHI
Temporal Development	Present at all times of the day and night Most intense during the day and in the summer	May be small or non-existent during the day Most intense at night or predawn and in the winter
Peak Intensity (Most intense UHI conditions)	More spatial and temporal variation: Day: 18 to 27 F (10 to 15 C) Night: 9 to 18 F (5 to 10 C)	Less variation: Day : -1.8 to 5.4 F (-1 to 3 C) Night: 12.6 to 21.6 F (7 to 12 C)
Typical Identification Method	Indirect measurement: Remote sensing	Direct measurement: Fixed weather stations Mobile traverses
Typical Depiction	Thermal Image	Isotherm map Temperature graph

This study will use surface temperature to quantify the influence of urban form on UHIE for the following reasons: first, air temperature is unstable because of the fluid properties of the atmosphere. Due to this characteristic, the correspondence between surface and air temperature is known to decrease with increasing altitude (Carlson et al., 1977). Therefore, air temperatures may vary depending upon the height of the measuring weather station and cannot be used as a reliable source to represent urban temperature. Second, weather stations, which are the most commonly used tool to measure air temperature, are very limited in terms of time and space. The third reason to choose surface temperature is that it can utilize remote sensing data and techniques. An advantage of remote sensing data is that it encompasses a very large number of thermal observations. This large number of observations allows for the measurement of the thermal properties of small surface features with much greater precision (Stone and Rodgers, 2001).

The magnitude of surface UHIE varies with seasons, due to changes in the sun's intensity as well as ground cover and weather. Also, surface UHIE with the greatest frequency of occurrence and intensities, is captured in the warmer half of the year, especially summer and autumn (Chandler, 1965; Lee, 1979; Unwin, 1980; Oke, 1982; EPA, 2008). As a result of these variations, surface urban heat islands are typically largest during the summer season (EPA, 2008b).

As mentioned above, UHIE will be captured by the temperature difference between urbanized and non-urbanized (i.e. rural) areas for each metropolitan region in the study area. Previous studies of land surface temperatures and thermal remote sensing of urban areas have been conducted by using various thermal imageries. This study used MODIS (Moderate Resolution Imaging Spectroradiometer) to analyze surface temperature in metropolitan regions. MODIS is a key instrument for global studies of atmosphere, land and ocean process, which is boarded the Terra Earth Observing System (EOS AM) and Aqua (EOS PM) satellite (Wan and Li, 1997). Terra MODIS and aqua MODIS are observing the entire Earth's surface every one to two days, acquiring data in 36 spectral bands, or groups of wavelengths with 1,000m, 500m and 250m spatial resolutions. Also, MODIS has various combinations in terms of spatial and temporal resolutions of land surface temperature that allows for selecting appropriate images for each research purpose. This study has utilized the MOD11A2 v.5 dataset which provides eight-day average values of clear sky land surface temperature based on daily 1-kilometer MODIS/Terra Land Surface Temperature/Emissivity product (MOD11A1). MOD11A2 is comprised of daytime and nighttime land surface temperatures, quality assessment,

observation times, view angles, bits of clear sky days and nights, and emissivity estimated in Band 31 and 32 from land cover type.

The reasons to choose this V.5 MODIS/Terra land surface temperature/emissivity products for this study are as follows: first, it was validated to Stage 2, which means that the accuracy has been assessed over a widely distributed set of locations and time periods via several ground-truth and validation efforts. Also, MOD11A2 dataset is retrieved from clear-sky (99% confidences) observations at 10:30AM (daytime) and 10:30PM (nighttime) using a generalized split-window algorithm (Imhoff et al, 2010; Wan & Dozier, 1996). In other words, this dataset is ready for use in scientific publications without further preprocessing. Second, the spatial resolution of 1,000m is quite coarse but enough to observe surface temperature patterns in metropolitan regions. Although there are much higher resolution imageries such as Landsat TM/ ETM (120m/60m) or ASTER, fine spatial resolution imageries have coarse temporal resolutions. Both datasets have a 16 day repeat interval. Since the spatial sample frame of this study covers the continuous U.S., it is hard to find specific (common) date without cloud covers for all 353 metropolitan regions. Thus, fine temporal resolution (12hr; twice a day) and an eight-day average value of temperature are key characteristics in the decision to select MODIS to measure land surface temperature.

NCDC (National Climatic Data Center) provides an online mapping service to observe the U.S. climate variability and change (U.S. Climate at a Glance). This service allows users to see the trends of average temperature and precipitation based on locations (national, regional, statewide, and cities) and periods (from 1900-2012).

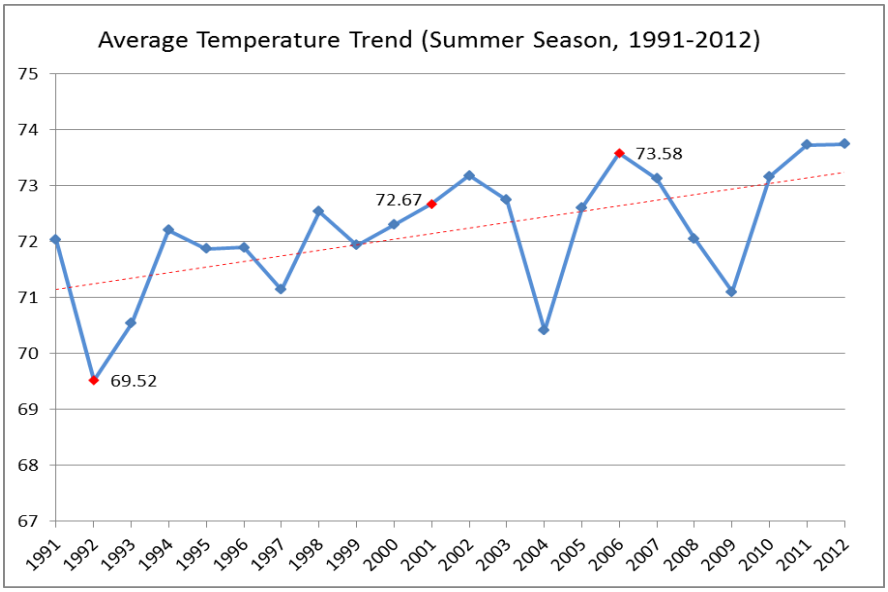

Figure 4.3. Average Temperature Trend in Summer Season (1991-2012)

To compare three candidate years, average temperatures of the summer period (June- August) for 1990-2010 are displayed as a chart (See Figure 4.3). Base temperature, 72.07 degrees Fahrenheit, is the average summer temperature from 1901-1990.The summer temperature trend for the years 1991-2010 indicates that the temperature increased 0.80 degrees Fahrenheit every decade during the summer season. The graph shows that the year 2006 records the highest average temperature among the three candidate years as well as for the last twenty years. Based on the temperature records, this study will employ the eight-day average land surface temperature of July 12, 2006 from the MODIS dataset (MOD11A2 v.5).

A total of fifteen images downloaded from USGS Global visualization viewer website and the following steps were conducted to calculate the land surface temperature of study areas.

First, a developed batch model of the MODIS Re-projection Tool (MRT tool) was used to process the re-projection of images from native MODIS projection (Sinusoidal) to Alber's Equal Area Conic Conformal to match the NLCD (National Land Cover Dataset) dataset. (See Figure 4.4). Second, fifteen downloaded MODIS images were mosaicked using ArcGIS 9.3 and their boundaries were clearly matched with each other. Third, MODIS data value was converted to temperature. MODIS provides temperature value as five-digit numbers, and these numbers were converted to real temperature (Kelvin) by multiply the scale factor of 0.02. Then, this temperature converted again from Kelvin to Fahrenheit.

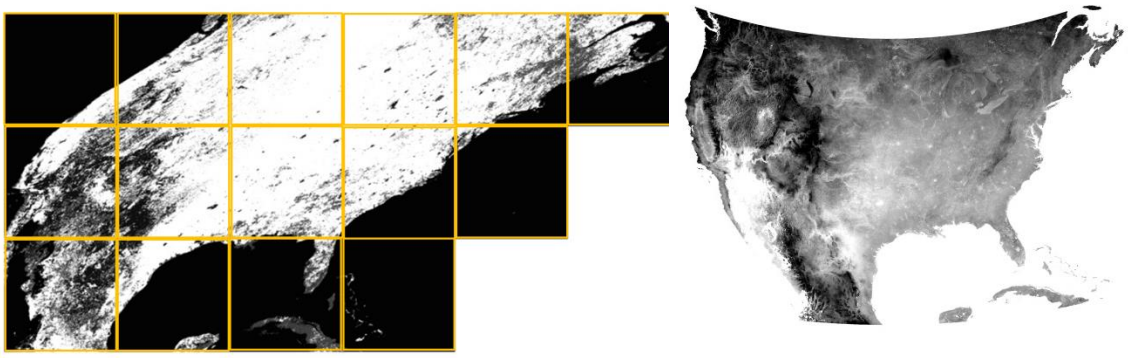

Figure 4.4. Mosaic images of nighttime temperature by MODIS
(Left: Sinusoidal projection; Right: Alber's projections)

Based on converted temperatures, temperature differences between urbanized and rural areas are calculated. To make clear (maximize) differences between urban and rural temperature, the cells on the boundaries of urbanized areas are excluded as urban-rural transition zones when calculating the average temperature. (See Figure 4.5)

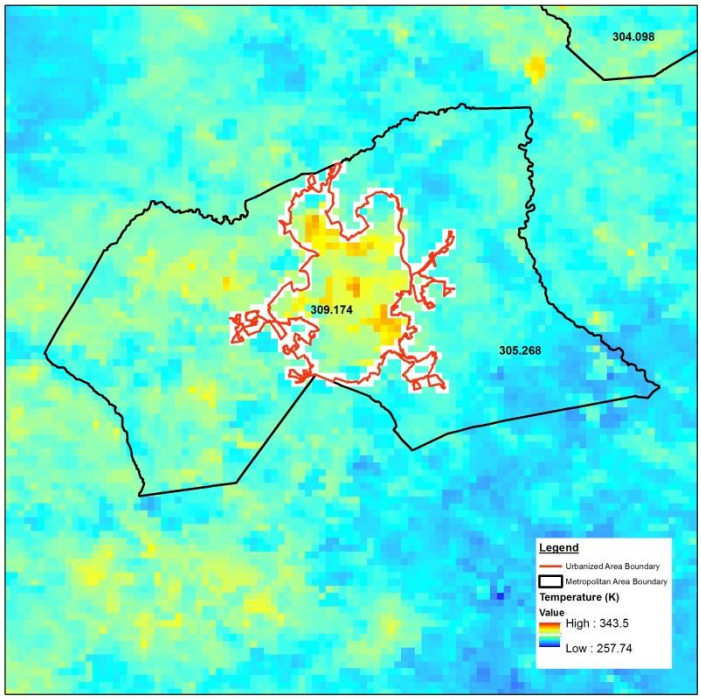

Figure 4.5. Mean temperature of urbanized and rural areas excluding boundary of urbanized area

4.2.2. Independent Variables: Spatial Development Patterns

As mentioned earlier, spatial development patterns can be measured using landscape metrics. Five landscape metrics representing spatial development patterns were selected to be measured for developed areas (i.e. impervious surfaces) (See Table 4.2). The amount of impervious surfaces is an important indicator of environmental quality (Arnold and Gibbons, 1996; Yuan and Bauer, 2007) and shows the overall footprint of development patterns. Thus, analyzing development patterns of impervious surface areas provides an alternative method for studies of urban development patterns and related surface UHIE.

Table 4.2. Intensity of development class and impervious surface
(Adopted and revised from legend of NLCD 2006 dataset)

Class	Descriptions	Percentage of Impervious Surface	Reclassify (Aggregation)
High	Highly developed area where people reside or work in high numbers. Examples include apartment complexes, row houses and commercial/industrial.	80-100	Developed Areas
Medium	Areas with a mixture of constructed materials and vegetation. These areas most commonly include single-family housing units.	50-79	
Low		20-49	
Open Space	Areas with a mixture of some constructed materials, but mostly vegetation in the form of lawn grasses. These areas most commonly include large-lot single-family housing units, parks, golf courses, and vegetation planted in developed setting for recreation, erosion control, or aesthetic purpose.	Less than 20	Excluded from Development since this area is describe as mostly vegetation.

This study measures class-level and landscape-level metrics to analyze spatial development patterns. In this study, a class is a set of land cover types and the landscape level is the metropolitan region. Since landscape metrics are commonly used to conduct an empirical analysis of landscape patterns, selecting which set of landscape metrics to utilize is an important precursor to analyzing spatial pattern. Also, it is important to select an appropriate set of metrics based on the particular purpose of each measure and the interdependence among measures because each level of landscape metrics has its own purpose and value of measurement. The measures share limited numeric information such as area and perimeter of a landscape (patch, class), and thus we should consider their correlation effect when employing two or more metrics in a statistical model.

While there are hundreds of known landscape metrics introduced and developed in the literatures, this study selected the following five metrics (See table 4.3) to measure development patterns based on the five typical characteristics of urban sprawl: PLAND (percent of land), COHESION, GYRATE_AM, PRD (patch richness density) and IJI (interspersion and juxtaposition index). A major challenge in selecting metrics was matching the concepts of development patterns to appropriate landscape metrics which traditionally measure ecological features. Metrics associated with shape, core area, and contrast can be important when targeting ecological processes, but are more difficult to relate to the notion of development patterns. However, some metrics under the concepts of area, aggregation, and diversity can be logically applied to the notion of development patterns when considering the characteristics of sprawl. If similar metrics are used to measure same concept, this study selects the simpler metric in terms of its calculation method to reduce (limit) complexity of interpretation.

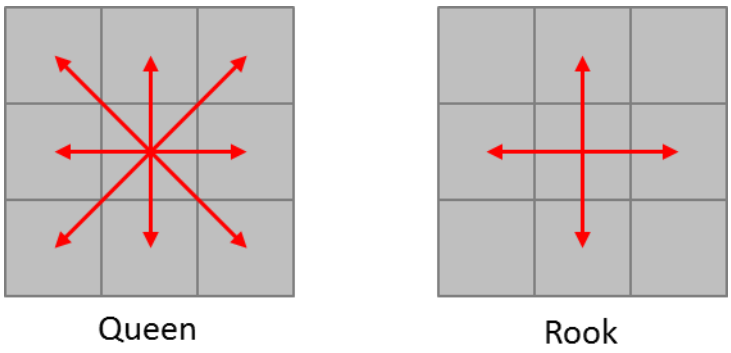

Figure 1.6. Concept of queen and rook contiguity

The Queen contiguity index was selected to analyze continuity-related index. There are two types of weight matrix that calculated based on contiguity of neighbors (See Figure 4.6). A queen weights matrix defines a location's neighbors as those with either a shared border or vertex (in contrast to a rook weights matrix, which only includes shared borders)[1].

Table 4.3. Dimensions of Development and Related Landscape Metrics

Dimensions of development	Related landscape metrics (Level)
Density	PLAND (Class)
Continuity	COHESION (Class)
Clustering	GYRATE_AM (Class)
Diversity	IJI (Landscape)
Proximity	PRD (Landscape)

Density of Development: PLAND Index

Development density can be measured by PLAND. The PLAND metric represents the sum of all the areas corresponding to a patch type, divided by total landscape area, multiplied by 100 (to convert to a percentage). PLAND measures relative amounts of developed areas (i.e. impervious surface areas) based on the size of the urbanized area. When it is applied to the built environment or impervious surface, it provides a measure of the overall extent of urban form or the community imprint on a landscape (Brody et al.,

[1] GEODA, Glossary of Key Terms: https://geodacenter.asu.edu/node/390#queen

2012). A high value of PLAND in development category indicates that the proportional abundance of development areas in urbanized area. The PLNAD index ranges between 0 and 100, as it is calculated as a percentage. PLAND approaches 0 when the corresponding class becomes rare in the landscape. Since PLAND is a relative measure, it is a more appropriate index of landscape composition than total class area: PLAND is regardless of varied size of landscape. Fragstat calculates PLAND based on the following formula:

$$\text{PLAND} = \text{P}i = \frac{\sum_{j=1}^{n} a_{ij}}{A}(100)$$

Where Pi is proportion of the landscape occupied by patch type (class); a_{ij} (m^2) is area of patch ij; A is total landscape area (m^2).

Figure 4.7 shows the hypothetical landscape transformation to explain the concept of percent landscape. The PLAND values of A, B, and C are 16%, 36%, and 81% respectively.

Figure 4.7. Hypothetical landscapes of density of development

Continuity of Development: COHESION Index

Continuity of development can be measured by the COHESION index. The COHESION index measures the physical connectedness of corresponding patch types. Patch cohesion increases as the patch type becomes more aggregated or clumped in its distribution. In other words, a high value of patch cohesion indicates a more physically connected landscape. It is actually a standardized perimeter-area ratio and it is bounded between 0 and 1, which makes it easier to interpret as well as robust enough to changes in the cell size. Therefore it has been used as a measure of continuity (Schumaker, 1996). Cohesion index is calculated for developed area using Fragstats based on the formula:

$$\text{COHESION} = \left[1 - \frac{\sum_{j=1}^{n} p_{ij}^{*}}{\sum_{j=1}^{n} p_{ij}^{*}\sqrt{a_{ij}^{*}}}\right]\left[1 - \frac{1}{\sqrt{z}}\right]^{-1} (100)$$

where p_{ij}^{*} is perimeter of patch ij in terms of number of cell surface; a_{ij}^{*} is area of patch ij in terms of number of cells; and Z is total number of cells in the landscape.

Cohesion approaching 0 means that the class patches are increasingly subdivided and less physically connected. On the other hand, cohesion increases when corresponding patch types becomes more connected and aggregated.

Figure 4.8 shows the example landscapes of connectivity. Landscape A has the lowest connectivity value since all three patches are separated (Cohesion: 68.2%). The COHESION index value of landscape B is 70% and landscape C has 100% of cohesion

with a single connected patch.

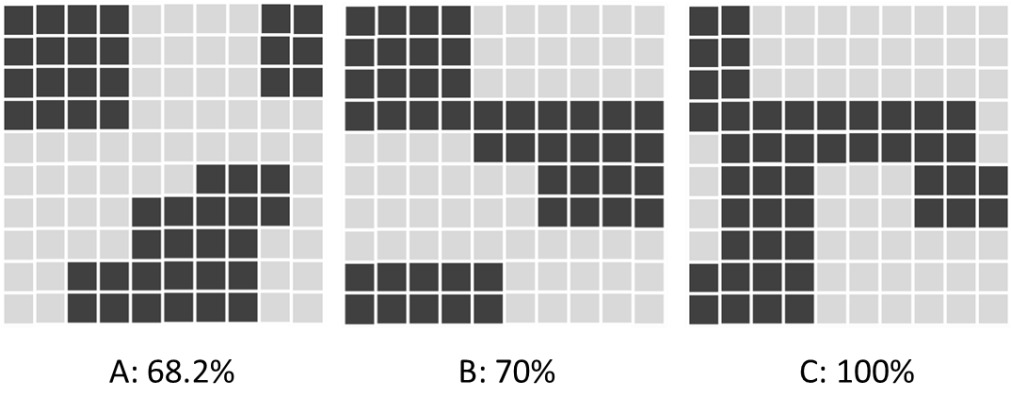

Figure 4.8. Hypothetical landscapes of continuity of development

Clustering of Development: GYRATE_AM Index

Clustering of development can be measured by the radius of gyration (GYRATE). It is the mean distance between each cell in a cluster of continuous cells (i.e. a patch) and the patch centroid (red square in Figure 4.8). GYRATE is a useful measure to analyze patch extensiveness. In other words, it provides how far across the landscape a patch extends. If the area is equal, the more elongated or far-reaching patch has the larger radius of gyration. Although GYRATE is not an explicit measure of patch shape, it can be affected by patch shape. For example, an elongated patch shape has a higher value of GYRATE than a compact and clustered patch shape, even if their patch size is same. When applied to ecological research, the value can be interpreted as the traversability of single patch (Leitao, 2006).

This study used the Area-Weighted Mean Radius of Gyration to standardize patch size, which is calculated by following equation:

$$\text{GRATE\_AM} = \sum_{j=1}^{n} \left[\sum_{r=1}^{z'} \left(\frac{h_{ijr}}{z} \right) \left(\frac{a_{ij}}{\sum_{j=1}^{n} a_{ij}} \right) \right]$$

where, h_{ijr} is a distance (m) between cell *ijr* (located within patch *ij*) and the centroid (red square point in Fig 4.9) of patch *ij* (the average location), based on cell-center-to-cell-center distance, *z* is number of cells in patch *ij*. The unit is meter and the range of values is larger than 0 without limit.

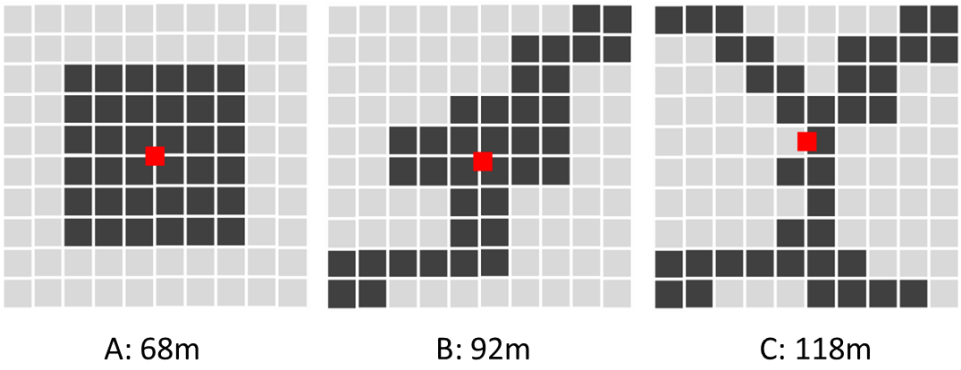

Figure 4.9. Hypothetical landscapes of clustering of development
(Adopted and revised from Leitão, 2006)

Figure 4.9 shows the examples of different GYRATE values in three hypothetical landscapes. Landscape A has the lowest GYRATE value at 68 since it has a square

configuration, which is the most compact shape possible in the grid. Landscape B (GYRATE = 92) and C (GYRATE=118) become progressively more irregular in shape and more extensive. The value of GYRATE is 0 when the patch consists of a single cell, and it reaches the maximum value when the patch comprises the entire landscape. GYRATE is calculated for each patch and can be summarized at class and landscape levels.

Diversity of Land Covers: Patch Richness Density Index

Patch richness density equals the number of different patch types present within the landscape divided by the total landscape area (m^2), then multiplied by 10,000 and 100 (to convert to 100 hectares). Patch richness is the number of different patch types present within the landscape boundary and is the simplest index showing landscape composition. It refers standardized richness to a per-area basis that facilitates comparison among landscapes.

$$\text{PRD} = \frac{m}{A}\,(10{,}000)(100)$$

Where m is number of class present in the landscape, excluding the border of landscape if present; A is total landscape area (m^2). Figure 4.10 follows hypothetical landscapes, each representing different value of patch richness. Landscapes A, B, and C have the values of PRD as 2, 3, and 5 respectively.

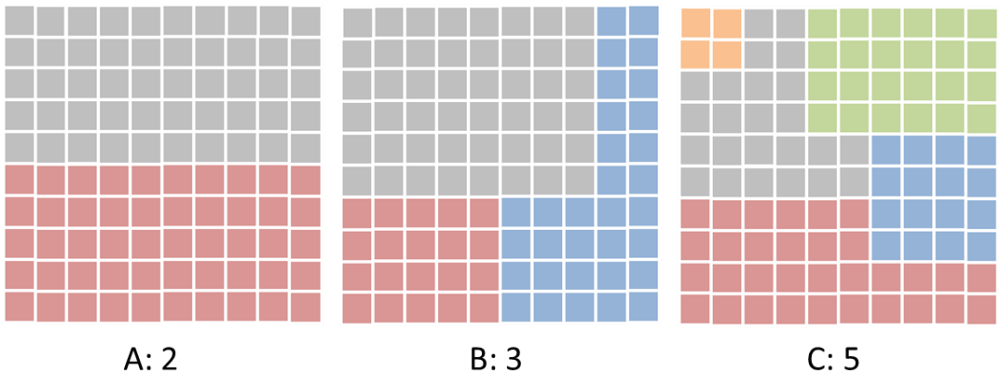

Figure 4.10. Hypothetical landscapes of diversity of land covers

Proximity of Development: Interspersion and Juxtaposition (IJI) Index

Proximity of development can be measured by the IJI index. It is based on patch adjacencies and measure the interspersion or intermixing of patch types. This index considers the neighborhood relations between patches and broadly refers to the overall texture of the landscape mosaic. This index also measures the extent to which patch types are interspersed; higher values result from landscapes in which the patch types are well interspersed, whereas lower values characterize landscapes in which the patch types have a disproportionate distribution of patch type adjacencies.

$$\text{IJI} = \frac{-\sum_{i=1}^{m}\sum_{k=i+1}^{m}\left[\left(\frac{e_{ik}}{E}\right)\ln\left(\frac{e_{ik}}{E}\right)\right]}{\ln(0.5[m(m-1)]} \ (100)$$

Where, e_{ik} is total length (m) of edge in landscape between classes i and k; E is total length (m) of edge in landscape, excluding background; m is number of classes present in the

landscape, including the landscape border, if present. IJI approaches 0 when the distribution of each patch type becomes increasingly uneven. If all patches are equally adjacent to all other patches, the value of IJI will be 100 %.

Figure 4.11 illustrates the concept of IJI. Landscape A (IJI=60.2%) shows that every patch type shares very limited borders with each other. Different patch types in landscape B share their borders more so than in landscape A, which that allows for a higher value in IJI (72.6%). In landscape C, each patch type is interspersed and shares its borders a lot more than landscape A and B. As a result, landscape C has the highest value of IJI (96.6%) and it can be interpreted as "higher proximity between land covers" in this study.

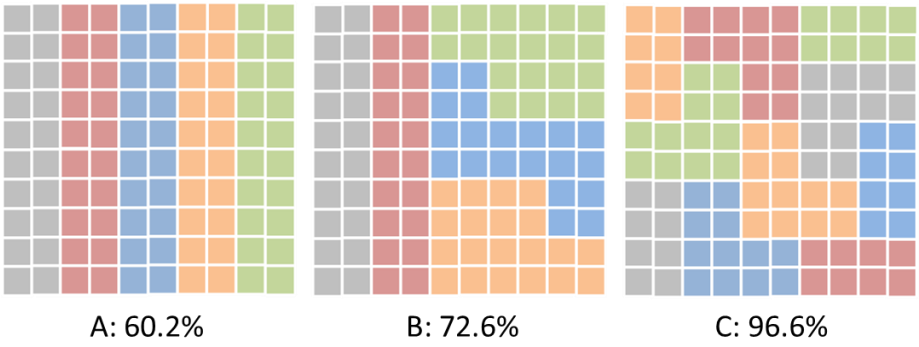

Figure 4.11. Hypothetical landscapes of proximity of land covers

4.2.3. Reclassifying the National Land Cover Database

The National Land Cover Database is a sixteen-class land cover classification scheme that has been applied consistently across the conterminous U.S. at a spatial resolution of 30 meters. NLCD 2006 is based primarily on the unsupervised classification

of Landsat Enhanced Thematic Mapper+ (ETM+) circa 2006 satellite data.[2] As shown in Table 4.2, the NLCD has four class of development based on the percentage of impervious surface. This study employs three class of development excluding open space as a developed area. Based on this aggregated land cover data, selected landscape metrics were calculated by Fragstat 4.0.

Scale is one of the most important considerations in landscape structure analysis (Forman, 1995a; McGarigal and Marks, 1995; Turner et al., 2001).The spatial data encompasses both extent and grain. Extent is the overall area of an investigation or the area included within the landscape boundary. Grain is the size of the individual units of observation (i.e. cell size). It may not be possible to know what the appropriate resolution should be. Spatial resolution of the NLCD dataset is 30m x 30m, and the size of each cell is $900m^2$. Considering that the minimum size of census block is 30,000 ft^2 (2,787.1m^2) - 40,000 ft^2 (3716.1m^2)[3], the spatial resolution of NLCD data is adequate to analyze development patterns.

The NLCD dataset was reclassified by aggregation to analyze clear impact of development pattern. In other words, total seven major land cover classes were aggregated into 5 classes. (See Table 4.4) Density, continuity, and clustering of development were analyzed using "Developed" category, while diversity and proximity of development were analyzed using all the five aggregated categories including water, open space, developed,

[2]http://www.mrlc.gov/nlcd2006.php , Also see Appendix B
[3] http://www.census.gov/geo/reference/pdfs/GARM/Ch11GARM.pdf

vegetation, and others. Since the value of diversity index (i.e. patch richness density) can be affected by the number of categories, this index was also analyzed based on original NLCD classification scheme (first order), which includes water, developed, forest, shrub land, herbaceous, planted, and wetland categories. (See Appendix C). The following table shows original and aggregated categories that were utilized in this study.

Table 4.4. Reclassification of land covers

NLCD Classification		Aggregated Categories used in this study
Class (First order)	**Sub-Class (Second order)**	
Water	Open Water	Water
	Perennial Ice/Snow	
Developed	Open Space	Open Space
	Low Intensity	Developed
	Medium Intensity	
	High Intensity	
Forest	Deciduous Forest	Vegetation
	Evergreen Forest	
	Mixed Forest	
Shrub land	Dwarf Scrub	
	Shrub/Scrub	
Herbaceous	Grassland/Herbaceous	
	Sedge/Herbaceous	
	Lichens	
	Moss	
Planted	Pasture/ Hay	Others
	Cultivated Crops	
Wetland	Woody Wetlands	
	Emergent Herbaceous Wetland	

Previous studies have pointed out the problem of correlation among different landscape metrics (Ritter et al.. 1995; Hargis et al., 1998; Seto and Fragkias, 2005). The five landscape metrics, which are the main independent variables of this study, are also highly correlated with each other since they have calculated by using same information such as patch size and perimeter (See Table 4.5). Density, continuity, and clustering are positively correlated each other, while diversity and proximity are negatively correlated to previous three measures. Thus, I analyzed different models for each development type to reduce the threat of multicorrelation. As a result, a total 10 models will be estimated: five development patterns were regressed on both day and night UHIEs, controlling for the same set of variables specified below.

Table 4.5. Correlations between spatial development pattern indexes

	Density	Continuity	Clustering	Diversity	Proximity
Density	1.0000				
Continuity	0.6937*	1.0000			
Clustering	0.4919*	0.7339*	1.0000		
Diversity	-0.0124	-0.2613*	-0.6647*	1.0000	
Proximity	-0.6390*	-0.4210*	-0.3425*	0.0800	1.0000

* $p < 0.05$

4.2.4. Control Variables

All control variables except ecoregions (dummy variables) are calculated based on the difference of percentage between urban and rural area. Since urban and rural area have physically different land size, comparing two areas based on the percentage is more

appropriate than based on their actual size. Table 4.6 is a hypothetical logic to calculate difference in percentage between urban and rural to generate control variables. For example, rural area has larger amount of vegetation than urbanized area in terms of its actual land size. However, the percentage of vegetation in urbanized area is higher than that of rural area since they are standardized by their total land size. As a result, we can compare the condition of vegetation in urbanized and rural areas based on the difference in percentage. Finally, based on the result of calculation, we can say that urbanized area has 23.3% more impervious surface, 3.4% more vegetated area and 1.67% less watered surface than rural area.

Table 4.6. Hypothetical example of calculating control variables

	Actual Amount		Standardized Amount (percentage)		Difference in Percentage (Urban-Rural)
	Urbanized	Rural	Urbanized	Rural	
Impervious surface	100	60	33.3%	10%	+23.3%
Vegetation	60	100	20%	16.6%	+3.4%
Water	10	30	3.33%	5%	-1.67%
Total Land Size	300	600			

Amount of Vegetation Cover and Watered Surfaces

The amount of vegetation is calculated as the sum of forest, shrub land, and herbaceous, Planted/Cultivated categories under the land cover dataset from the NLCD

(2006). The percentage of watered surface is also calculated as the percent of the area water category under the land cover dataset from the NLCD (2006). Vegetation cover includes three land cover classes: forest, characterized by areas covered by trees generally greater than 6 meters tall and where trees canopy accounts for 25-100% of the cover; shrub land, characterized by natural or semi-natural woody vegetation with aerial stems, generally less than 6 meters tall; and herbaceous, which are areas characterized by natural or semi-natural herbaceous vegetation that accounts for 75- 100% of the cover. Percentage of vegetation was also calculated by Fragststs 4.0.

Population Density

Population density is calculated based on 2010 census data and the total size of urbanized area in each metropolitan region. Since study year is 2006, the population in 2006 is the most appropriate data for this study. Although there is ACS (American Community Survey) data provides population in 2006, the geographic boundary of population estimated is the metropolitan region. Only the 2010 census counts the population of urbanized and rural areas separately for each metropolitan region and thus, this study used the population of 2010 to calculate population density.

Ecoregions

Ecoregions were coded as dummy variables in regression models to control for the spatial effect regarding the geographic location of each metropolitan region. As mentioned earlier,

an ecoregion includes characteristics related to geologic, landform, soil, vegetative, climatic, wildlife, water and human factors. Some metropolitan regions are situated over two or three ecoregions, and in that case each part calculated its individual percentage. Finally, the ecoregion which has the highest percentage was selected as the main ecoregion for the metropolitan region.

4.3. Data Analysis

Data analysis for this research will focus on detecting the impact of different development patterns on UHIE. The unit of analysis is metropolitan region (n=353) and the analysis took place in two major phases. The first phase of analysis aims to better understand the pattern of UHIE during the summer of 2006 and spatial development patterns in U.S. metropolitan regions based on the basic descriptive statistics and cartography. This part also provides basic descriptive statistics of development pattern analysis based on values of landscape metrics, which are calculated by Fragstats 4.0, and allow overall examination of development patterns in U.S. metropolitan regions.

Phase 2 of data analysis includes a series of regression models that were estimated to examine the relationship between development patterns and UHIE. This phase seeks to test the hypotheses mentioned in section 3.2 through the use of ordinary least square (OLS) based multivariate regression analysis. Each development pattern metric is modeled for a developed area (i.e. impervious surfaces) based on the measurements in the regression model, controlling for the same set of other variables as already specified. Additionally,

five hypotheses will be tested again using iteratively reweighted least square (IRLS) approach. STATA[4] provides the IRLS method to conduct robust regression which control potential outliers or unusual observation in my dataset (See Appendix B for more details).

The following equation represents the regression model for the dependent variable, UHIE for both day and night in 2006. The coefficients B1 represent unique effects of each independent variable (i.e. spatial development pattern) on the dependent variable.

$$DV = \alpha + \beta_1 X_1 + \beta_2 X_2 + \beta_3 X_3 + \beta_4 X_4 + \beta_5 X_5 + \beta_6 X_6 + \cdots + \beta_{12} X_{12} + \varepsilon$$

where,

DV : Dependent variables – UHIE (Day and Night: July 12, 2006)

α : Regression intercept

β_i: Partial Regression coefficients

X_1: Urban development pattern

X_2: Impervious surface

X_3: Water covered

X_4: Vegetation covered

X_5: Population Density

$X_6 - X_{12}$: Ecoregions: dummy variables

ε: Error term

[4] Statistical Analysis Package which is used in this study

A total of five urban development pattern variables were plugged in separately in each regression model to capture each variable's unique influence on UHIE. F-statistics were be conducted to check the statistical significance of the model. Post-regression specification tests of normality, multicollinearity, and heteroskedasiticity were carried out to make sure that there were no violations of the OLS regression assumptions (See Appendix F). Spatial autocorrelation was tested to check spatial autocorrelation exists in the independent variables using weight metrics based on inverse distance method since some metropolitan regions do not have neighbors, which condition is unable to create neighboring-based weight matrix.

4.4. Validity Threats

Every study design contains threats to validity and this research is no exception. Although all efforts will be made to reduce these threats, perfect study rarely can be achieved. Following is the discussions about the validity threats of this study based on four types of validity threats outlined by Cook and Campbell (1979): Statistical conclusion validity; construct validity; internal validity; external validity.

Statistical conclusion validity is important to address statistical conclusion validity because of the potential Type I and Type II error. This study may experience a lower level of statistical power due not perfectly large sample size (n = 353) and it is possible that the relationship between the independent and dependent variable may be inappropriately declared insignificant or significant (Type I or II error). In terms of potential sample size limitation, type II error–"accepting the null hypothesis when it is false"—is of more

concern because of the wider confidence interval and therefore critical region is more likely to overlap zero. In other words, this error can be presented as there are no statistically significant relationship between development patterns and UHIE even though urban development patterns are related to UHIE actually. To minimize this threat and additional issues on type I and II errors, this study analyzes all metropolitan regions of entire U.S. instead of selecting particular samples.

Internal validity may be caused when trying to control for all of the factors that may contribute to UHIE. The primary threat to internal validity in this study is that not all relevant variables influencing UHIE could be included in the statistical model. Temperature is determined by complex interrelations of natural and manmade environments and affected by various factors. Thus, this study employed control variables based on the literatures to increase internal validity.

Construct validity is perhaps the biggest validity threat of this study. Landscape metrics which is employed to measure urban development patterns is usually utilized in the ecological studies. Although applying these metrics to urban built environment is a novel approach, however, it can be a threat depends on how well these landscape metrics reflects the actual development patterns. The use of five different indices of landscape metrics with careful matching with characteristics of development pattern alleviate this threat and, to some extent, may provide insight into how well landscape metrics perfume as indicators of development patterns of urban built environment.

External validity refers to the ability to which results of this study can be generalized to other places and situation. As most of climate research, geographic location and weather condition including seasonal effect can threat to external validity when extending the outcomes of research. Since this study limited the UHIE in metropolitan regions during summer season, it is probably best generalized to the highly populated metropolitan regions in high temperature season. Another external validity threat of this research is the scale of measuring UHIE which may impose limitations on the ability to generalize the results of this study, that are based on the geographic extent of unit of analysis. The patterns and formation of urban heat island can vary by the geographic extent of observation. This study examines regional UHIE at the county level to examine and thus, the result of this study may be hard to apply to the smaller scale of UHIE (i.e. local UHIE).

CHAPTER V

RESULTS

5.1. Descriptive Statistics and Preliminary Analysis

5.1.1. Day and Night UHIE

In order to assess the statistical significance of the temperature differences between urbanized and rural areas, a paired t-test was conducted between UHIE is calculated by every paired urban-rural set for each metropolitan region. This could be a logical first step to build a dependent variable for this study**.** Results of the t-test between the two groups of urban and rural areas revealed statistically significant differences in their mean temperature.

Results of the t-test showed that urbanized areas had significantly higher temperatures than rural areas during both daytime and nighttime. During the day, the temperature difference is estimated at 4.04 F˚, while the temperature difference at night is 2.41 F˚ (See Table 5.1).

Table 5.1. The results of paired t-test

Variable	T	df	Sig (1-tailed)	Mean Difference	Std. Error Difference
DAY	16.75	353	0.0000	4.04	0.24
NIGHT	20.81	353	0.0000	2.41	0.12

Table 5.2 presents the descriptive statistics for each variable of the 353 metropolitan regions in U.S. UHIE (the mean temperature difference[5] between urbanized area and rural area in each metropolitan region) was calculated in both the daytime and nighttime.

Table 5.2. Descriptive statistics for variables

	Variable	Obs.	Mean	Std. Dev.	Min	Max
Dependent	**Urban Heat Island Day (F)**	353	4.04	4.53	-20.82	18.85
	Urban Heat Island Night (F)	353	2.41	2.18	-6.78	10.66
Independent	**Density (%)**	353	45.21	13.02	18.66	81.04
	Continuity (%)	353	99.45	.45	97.08	99.97
	Clustering (m) (Log transformed)	353	4361.05 (8.17)	3622.09 (.60)	886.71 (6.79)	30035.25 (10.31)
	Proximity (%)	353	56.74	6.83	37.78	75.06
	Diversity (n/100 ha)	353	.08	.06	.00	.30
Control	**Impervious surface (%)** (difference in Urban & Rural)	353	43.23	13.74	15.62	84.62
	Vegetation (%) (difference in Urban & Rural)	353	-29.02	22.34	-88.73	56.01
	Water surface (%) (difference in Urban & Rural, %)	353	-1.98	4.62	-49.87	4.52
	Population Density (Pop/km2) (difference in Urban & Rural)	353	924.31	402.16	-41.80	2902.753

[5] See Page 40, the formula of calculating UIHIE and Figure 4-2

The mean UHIE during the daytime was 4.04 F˚, with a standard deviation of 4.53F F˚ and a range of 38.03 F˚. On the other hand, the mean UHIE during night was 2.41 F˚ with a standard deviation of 2.18 F˚ and a range of 17.4 F˚. The average UHIE is about 1.63 F˚ higher during the daytime than at nighttime[6]. This is expected since the temperature obtained by remote sensing represents surface temperature. In other words, impervious surfaces are directly affected by the sun lights and their temperature increases rapidly, which contribute to UHIE during day. Daytime UHIE also has a larger standard deviation than nighttime UHIE, which also can be explained by the different amount of sunshine depending on geographic location and geologic characteristics of each metropolitan region.

Figure 5.1 shows the overall patterns of UHIE for daytime and nighttime. In the daytime, the larger UHIE is observed more in the northwestern and eastern U.S. than in the central U.S. This spatial pattern of daytime UHIE is briefly matched with ecoregion boundaries. On the other hand, there is no particular spatial pattern observed during nighttime. There are forty-four metropolitan regions that have negative values of UHIE during the day and seventeen have a negative value at night (colored as yellow in Figure 5.1). Negative UHIE values, indicating that an urbanized area has a lower temperature compared to surrounding rural areas (sometimes, it is called inverse UHIE), are mostly observed in the North American Desert, Mediterranean California, and some parts of Great Plains regions. Therefore, when comparing UHIE by ecoregion (Figure5.2), these three

[6] Mean difference is statistically significant based on the result of paired t-test (t = 8.0986, Pr(|T| > |t|) = 0.0000).

regions mark comparably smaller UHIE than other regions. Actually, the average UHIE of eight ecoregions for daytime (10:30 AM) and nighttime (10:30 PM) show a statistically significant difference. The Northwestern Forested Mountain region has the highest UHIE during both day (12.87 F˚) and night (5.28 F˚), while the Mediterranean California (MC), the Grate Plain (GP), and the North American Deserts have comparably lower UHIE.

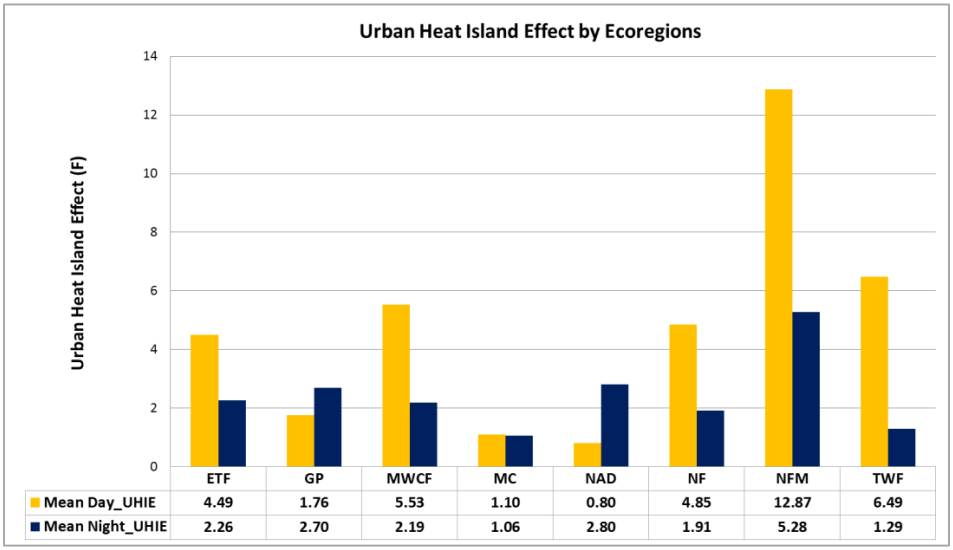

	ETF	GP	MWCF	MC	NAD	NF	NFM	TWF
Mean Day_UHIE	4.49	1.76	5.53	1.10	0.80	4.85	12.87	6.49
Mean Night_UHIE	2.26	2.70	2.19	1.06	2.80	1.91	5.28	1.29

Figure 5.1. Day and night UHIE by ecoregions

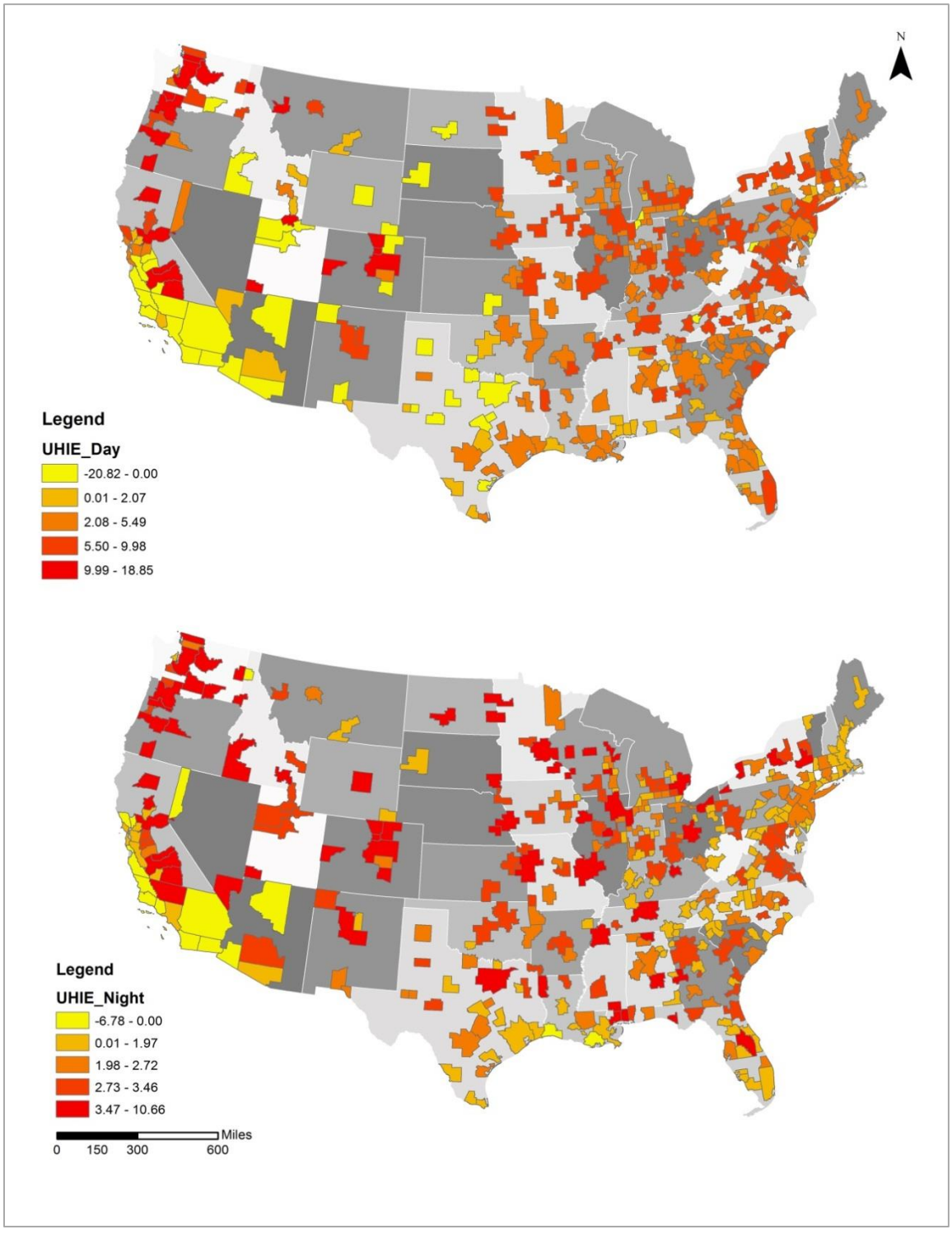

Figure 5.2. Spatial patterns of day and night UHIE

5.1.2. Spatial Development Patterns

The main independent variables, spatial development patterns, are measured by Fragstats 4.0 based on the development in urban area. The followings are the descriptive and visual results of spatial development pattern analyses.

Density of Development

Density refers to the percentage of developed land in urbanized areas in each metropolitan region. Urbanized areas in the 353 metropolitan regions studied have developed an average of 45.21% of their entire land area. Figure 5-3 shows examples of low and high density development in urban areas. The image on the left indicates low density development at 21.33% and the image on the right represents high density development at 81.04% of the entire urbanized area. This measure could also explain how urbanized areas become fully and densely developed.

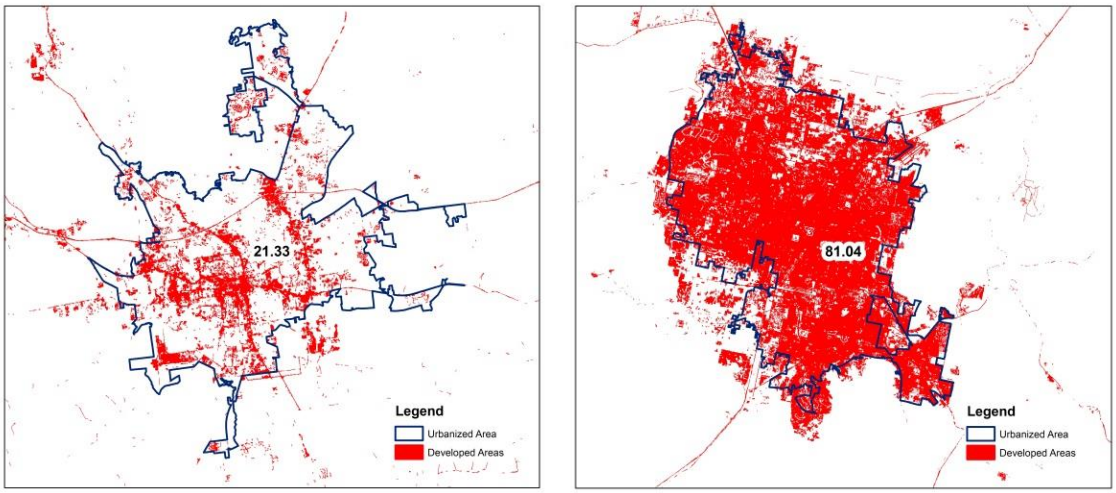

Figure 5.3. Examples of density of development
(Left: Tallahassee, FL; Low density of development
Right: Las Vegas-Paradise, NV; High density of development)

Continuity of Development

Continuity of development has a very small range between 97.08% and 99.97%, which means most of developed patches are connected together. This was expected because linear developed patches including roads can connect each separated development. Also, this study used the "8-cells rule," as neighboring cell options may affect this result of continuity. This "8-cells rule" option considers all eight adjacent cells as neighbors, including the four orthogonal and four diagonal neighbors. As shown in figure 5.4, an urban area with high connectivity has well-developed road systems, while only major roads are observed in urban area with low continuous development patterns. It is true that higher density of development in urban areas could have a higher continuity of development since they have larger possibility of being connected to developed patches

and thus, these two measures—density of development and continuity of development—are highly correlated with each other. (Table 5.3) However, they still have different distinctive characteristics to be explained as spatial development patterns. Therefore, each measure was examined in separate regression models while controlling for the same contextual variables.

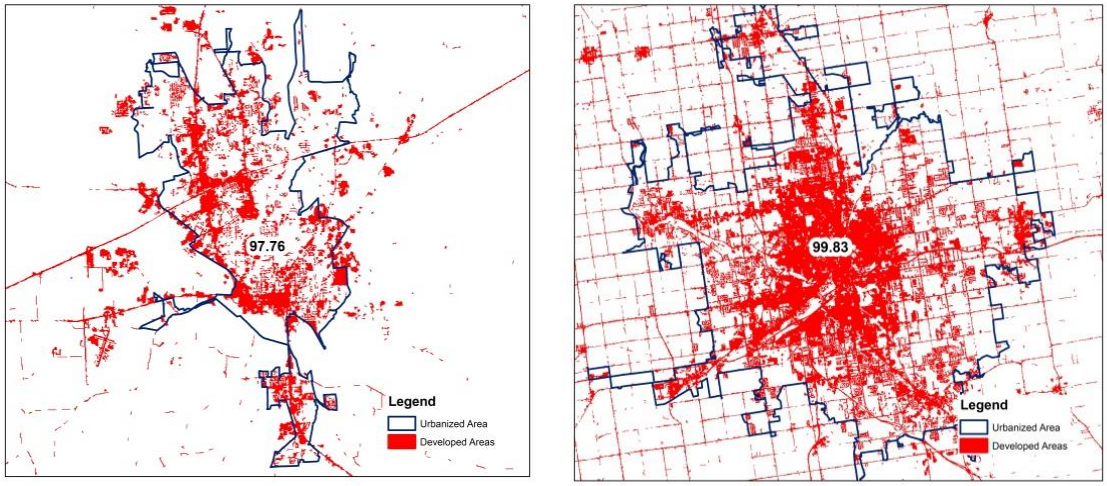

Figure 5.4. Examples of continuity of development
(Left: Jackson, TN; Low continuity of development
Right: Lansing-East Lansing, MI; High continuity of development)

Clustering of Development

Clustering of development is measured by the radius of gyration. Thus, a higher value of clustering index (i.e. GYRATE_AM) actually indicates a lower level of clustered development. In other words, when developments are not clustered, the radius of gyration will be increased, while clustered development will have a short radius of gyration. The average value of clustering index is 4361.05(m) and the maximum value is 30035.25 (m), which means that development patches in urban areas are dispersed. Figure 5.5 shows the

examples of low and high clustered development in urban areas. More clustered developments, image on the right, can minimize impervious surfaces in urbanized areas, which is probably preserving less fragmented open space and the natural environment.

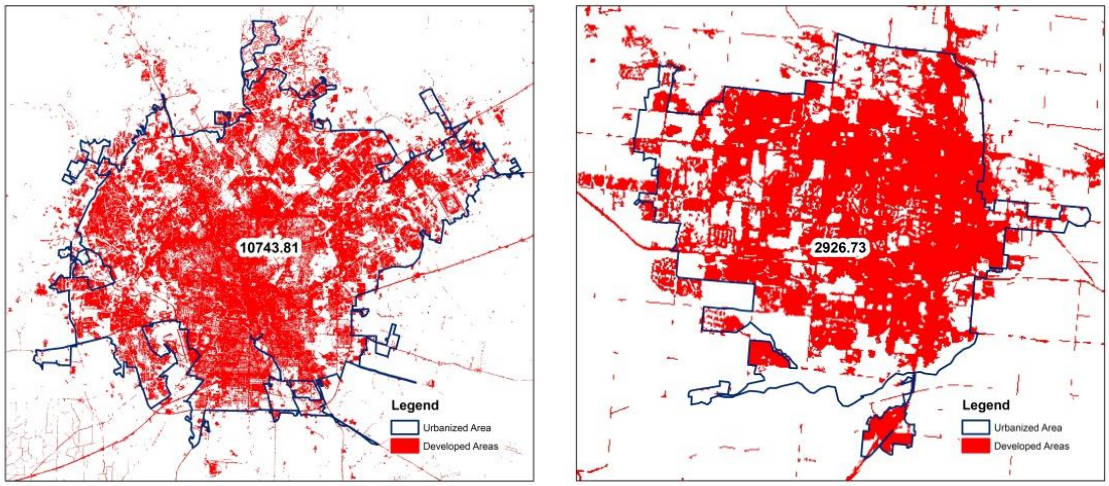

Figure 5.5. Examples of clustering of development
(Left: San Antonio, TX; Low clustering of development
Right: Greeley, CO; High clustering of development)

Diversity of Land Covers

Diversity in an urban area refers to how many land cover types exist together in the urbanized area. This index simply calculates the number of land cover type in each unit area (10 ha). When this index is used for ecological study, higher diversity (i.e. biodiversity) indicates a healthier ecological system. When applied to an urban area, diversity of land cover shows that the urban area includes various land cover types (e.g. vegetation, water, and wetlands) other than development. Figure 5.6 shows two urbanized areas with different patch richness densities. Supposing that two regions in the figure 5.6 have same size of urbanized area as 10,000 hectares, there will be two types of land cover

in the left region and thirty types of land cover in the right images, conceptually (because the unit area is 100ha). In this sense, although the actual value from PRD index looks small, it reflects meaningful information in terms of diversity of land covers.

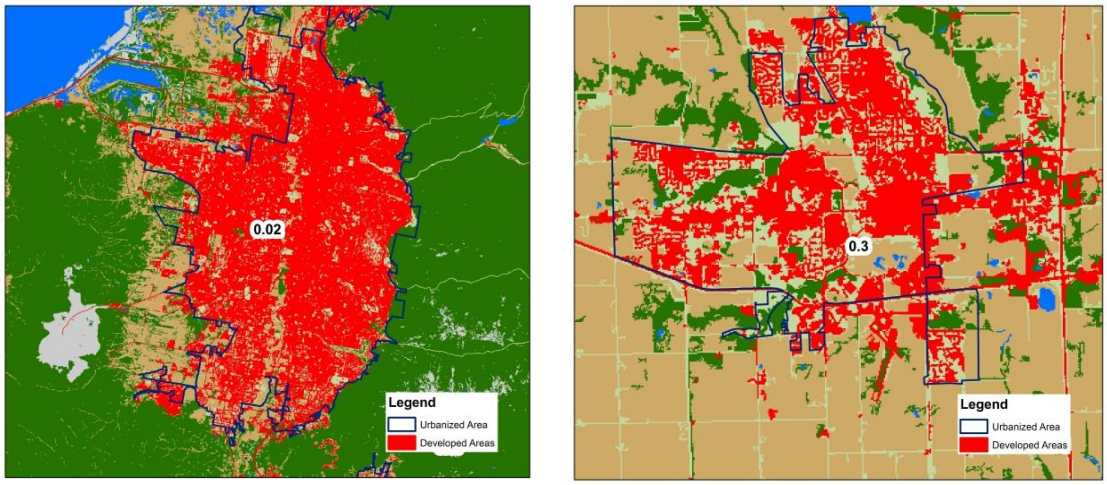

Figure 5.6. Examples of diversity of land covers
(Left: Salt Lake City; Low diversity of land covers
Right: Ames, IA; High diversity of land covers)

Proximity of Land Covers

The proximity index refers that how well each land cover types are connected with each other. Thus, an urbanized area with a high value of proximity provides good accessibility between the built and natural environments. Figure 5.7 shows the examples of urbanized areas with high and low proximities of land covers. Although two urban areas include a pretty good amount of vegetation, they have different spatial distributions (configurations) of vegetation. The area with high proximity (the image on the right) has good accessibility to natural environments from development and development and other land covers share these boundaries frequently. In contrast, the urban area with a low

proximity value (the image on the left) has very poor accessibility to other land covers from developed areas.

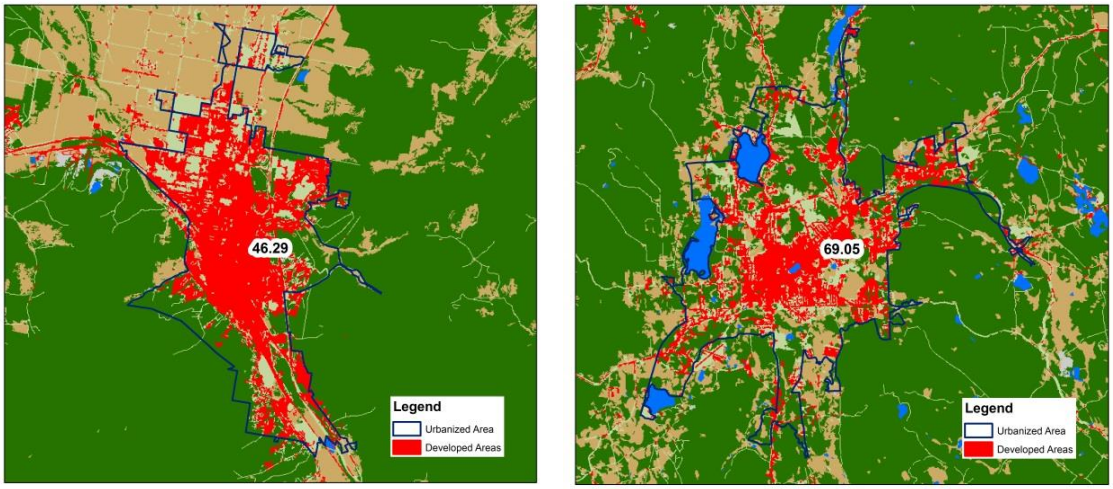

Figure 5.7. Examples of proximity of land covers
(Left: Pocatello, ID; Low proximity of land covers
Right: Pittsfield, MA; High proximity of land covers)

5.2. Examining Impact of Development Patterns on UHIE

5.2.1. Individual Impact of Each Spatial Development Pattern on UHIE

As mentioned briefly in the methods section (Data Analysis), this study tries to use two different versions of robust regression techniques to analyze the impact of development patterns on UHIE: OLS regression and IRLS approach. However, I decided to focus on and interpret the results of robust regression models since post estimations of OLS regression analyses did not detect any violations of OLS regression assumptions except heteroscedasticity and spatial autocorrelation which exists only for day UHIE models (Moran's I value for daytime UHIE: 0.12, p-value < 0.01). To be consistent for

both daytime and nighttime models in terms of comparing day and night UHIE, this study employs regional dummy variables instead of using spatial regression models to control for the spatial effect on the dependent variable (i.e. UHIE). Also, I believe that robust regression is able to handle the heteroscedasticity issue in OLS regression models with the use of robust standard error. The results and discussions of the IRLS approach will be presented in Appendix B.

Multiple regression analyses for UHIE illustrate the impact of different development patterns on day and night UHIE, while controlling for the amount of impervious surface and environmental variables. Generally, the five independent variables representing development patterns show the expected results in terms of their impact on UHIE (See Table 5.3).

Table 5.3. The effect of spatial development patterns on day and night UHIE

	OLS regression with robust standard error	
UHIE	Day	Night
Density	.0691***	0.0285***
Continuity	1.0524**	0.4319*
Non-Clustering	0.5531*	0.2276
Diversity	-3.4378	-2.2247
Proximity	-0.0467	0.0021

***P< 0.01 **p< 0.05 *p< 0.1

All significance tests are one tailed because the hypotheses of this study clearly indicated the direction of effect for the independent and control variables.

The followings provide the closer examination of the robust regression analysis results for each index of spatial development pattern.

Density of Development and UHIE

Table 5.4 shows the effect of density of development on day and night UHIE. Due to impervious surface variable has detected as variance inflation factor (VIF=80.89), it is excluded in density models. Density models are significant overall and explain nearly 33 percent and 19 percent of the variance in day and night UHIE respectively. The density of development acts to increase UHIE during both day and night. Increasing the percent of development in urban areas significantly ($p < 0.01$) increases both day and night UHIE in metropolitan regions. Results indicate that development density is a more effective factor involved in increasing UHIE during day than night. A 1 percent increase in developed area leads to a 0.07 F˚ and 0.03 F˚ higher day and night UHIE respectively. ***Sub-Hypothesis 1****, Metropolitan regions with a higher ratio of development in urbanized areas will have a higher UHIE than metropolitan regions that have a lower ratio of development in urbanized areas*, is supported by this density model.

The control variables are also significant predictors of UHIE and generally behaved as expected. Control variables that represent the natural environment have a significant impact on UHIE. For example, vegetation has a negative effect on UHIE but is only significant ($p < 0.01$) during nighttime. However, water shows an interesting result in that it reduces UHIE during daytime but increases UHIE during nighttime.

This could be possible because water has large "specific heat" than any other materials that covered urban surface. Thus, water should be cooler than other surface materials during daytime but warmer than others during nighttime. Population density is non-significant regression coefficient in both day and night robust regression models. All dummy variables of ecoregions are all statistically significant. Based on the reference category, the Northwestern Forest Mountain (NFM) region, all other ecoregions have significantly lower values of UHIE. In other words, NFM has the largest UHIE during both daytime and nighttime compared to all other regions in the U.S. (See Figure 3.2 and Figure 5.2)

Table 5.4. Density of development and UHIE

UHIE	Day				Night				
	Coefficient (Robust Std. Error)	P-value (One-tailed)	95% confidence Interval		Coefficient (Robust Std. Error)	P-value (One-tailed)	95% confidence Interval		VIF
Density	.0691 (0.0241)	0.00	.0217	.1166	0.0285 (0.0116)	0.0070	0.0058	0.0513	2.60
Impervious									
Vegetation	-.0215 (0.0235)	0.18	-0.0677	0.0248	-0.0290 (0.0119)	0.0080	-0.0525	-0.0055	1.60
Water	-.2546 (0.1117)	0.01	-0.4743	-0.0349	0.0831 (0.0696)	0.1165	-0.0538	0.2201	1.17
Population Density	.0002 (0.0008)	0.42	-0.0014	0.0018	0.0000 (0.0005)	0.4970	-0.0009	0.0009	2.35
Marine West Coast Forests	-6.415 (1.4061)	0.00	-9.1808	-3.6494	-2.5100 (1.0734)	0.0100	-4.6213	-0.3987	1.31
Mediterranean California	-12.2287 (2.1294)	0.00	-16.4171	-8.0403	-4.2239 (1.2239)	0.0005	-6.6312	-1.8166	2.51
North American Deserts	-12.1843 (1.8663)	0.00	-15.8553	-8.5133	-2.1900 (1.0224)	0.0165	-4.2009	-0.1790	2.57
Northern Forests	-6.2908 (1.2494)	0.00	-8.7483	-3.8332	-2.7178 (0.7891)	0.0005	-4.2699	-1.1658	1.48
Great Plains	-11.2006 (1.2763)	0.00	-13.7110	-8.6901	-2.5280 (0.7414)	0.0005	-3.9863	-1.0697	3.51
Northern Forests	-7.2346 (1.1732)	0.00	-9.5423	-4.9270	-2.4977 (0.7353)	0.0005	-3.9439	-1.0515	5.83
Tropical Wet Forests	-6.4882 (1.3677)	0.00	-9.1783	-3.7980	-4.6020 (0.8638)	0.0000	-6.3010	-2.9030	1.14
Constant	9.6116 (1.9082)	0.00	5.8583	13.3649	4.0499 (1.0397)	0.0000	2.0049	6.0949	
	Number of obs = 353 R-squared = 0.3283		F(11, 341) = 11.68 Prob > F = 0.0000		Number of obs = 353 R-squared = 0.1907		F(11, 341) = 5.61 Prob > F = 0.0000		

* All significance tests are one tailed because the hypotheses of this study clearly indicated the direction of effect for the independent and control variables

Continuity of Development and UHIE

Continuity is one of the typical spatial forms related to the sprawl development pattern. Continuity models are significant overall and explain nearly 33 percent and 19 percent of the variance in day and night UHIE respectively. As shown in Table 5.5, the continuity of development also appears to have a significant effect on UHIE in both daytime ($p < 0.05$) and nighttime ($p < 0.1$). As expected, the increasing continuity of development in urban areas contributes to the creation of more heat, which results in a large UHIE. A positive percent change in the continuity of development significantly increases day UHIE at 1.05 ˚F but only marginally increases night UHIE at 0.43˚F. ***Sub-Hypothesis 2****, Metropolitan regions with a higher continuity of development in urbanized areas will have a higher Urban Heat Island Effect than the metropolitan regions with a lower continuity of development in urbanized area*, is supported by this continuity model.

As listed in Table 5.5, estimates of control variables in the continuity models remain essentially unchanged when compared to density models. Impervious surface area has a positive effect on UHIE, but is only marginally significant in both day and night UHIE models. Vegetation and water both reduce UHIE, but vegetation is a strong predictor of night UHIE while water is a significant predictor of day UHIE. Population density is still non-significant factor to estimate UHIE.

Table 5.5. Continuity of development and UHIE

UHIE	Day				Night				
	Coefficient (Robust Std. Error)	P-value (One-tailed)	95% confidence Interval		Coefficient (Robust Std. Error)	P-value (One-tailed)	95% confidence Interval		VIF
Continuity	1.0524 (0.5919)	0.04	-0.1118	2.2166	0.4319 (0.3185)	0.09	-0.1945	1.0584	1.99
Impervious	0.0380 (0.0233)	0.05	-0.0078	0.0838	0.0137 (0.0114)	0.11	-0.0086	0.0361	3.30
Vegetation	-0.0229 (0.0236)	0.17	-0.0693	0.0235	-0.0305 (0.0119)	0.01	-0.0538	-0.0071	1.55
Water	-0.2556 (0.1063)	0.01	-0.4647	-0.0465	0.0842 (0.0716)	0.12	-0.0566	0.2251	1.17
Population Density	0.0002 (0.0008)	0.42	-0.0014	0.0018	0.0000 (0.0005)	0.47	-0.0009	0.0010	2.33
Marine West Coast Forests	-6.5490 (1.4318)	0.00	-9.3652	-3.7327	-2.5751 (1.0774)	0.01	-4.6944	-0.4559	1.31
Mediterranean California	-12.1327 (2.1357)	0.00	-16.3337	-7.9318	-4.2002 (1.2315)	0.00	-6.6225	-1.7780	2.53
North American Deserts	-12.2096 (1.8841)	0.00	-15.9156	-8.5036	-2.2016 (1.0265)	0.02	-4.2208	-0.1824	2.58
Northern Forests	-6.4566 (1.2810)	0.00	-8.9764	-3.9369	-2.8028 (0.7929)	0.00	-4.3623	-1.2432	1.49
Great Plains	-11.3022 (1.3130)	0.00	-13.8848	-8.7197	-2.5716 (0.7459)	0.00	-4.0387	-1.1046	3.55
Northern Forests	-7.3575 (1.1978)	0.00	-9.7134	-5.0015	-2.5653 (0.7426)	0.00	-4.0260	-1.1046	5.89
Tropical Wet Forests	-6.7787 (1.4680)	0.00	-9.6660	-3.8914	-4.7406 (0.8298)	0.00	-6.3728	-3.1083	1.15
Constant	-93.5276 (58.3732)	0.06	-208.3457	21.2905	-38.1920 (31.3684)	0.11	-99.8926	23.5085	
	Number of obs = 353 R-squared = 0.3321		F(12, 340) = 10.23 Prob > F = 0.0000		Number of obs = 353 R-squared = 0.1919		F(11, 341) = 5.72 Prob > F = 0.0000		

* All significance tests are one tailed because the hypotheses of this study clearly indicated the direction of effect for the independent and control variables

Clustering of Development and UHIE

Clustering models are significant overall and it explains nearly 33 percent and 19 percent of the variance in day and night UHIE respectively. Non-clustering of development appears to have a positive impact on UHIE, but it is a significant predictor only for day UHIE. In other words, more clustered development patterns can decrease day UHIE. Thus, sub-Hypothesis 3*, Metropolitan region with a higher clustering of development in urbanized area will have a lower Urban Heat Island Effect than the metropolitan region has a lower clustering of development in urbanized area*, is partially supported by this clustering model. The index of clustering development patterns is GYRATE_AM which is calculate by the radius of gyration of each development patch. Since the value of GYRATE_AM is mean distance between each cell in a cluster of continuous cells (i.e. a patch) and the patch centroid, and the GYRATE_AM is a logged variable, the regression coefficient of clustering can be interpreted as a 0.006% increase in the GYRATE_AM increase 1°F of day UHIE and a 0.002% increase in the GYRATE_AM increase 1°F of day UHIE.[7] (See Table 5.6)

Impervious surfaces in urbanized areas are a significant factor in the amplification of UHIE in daytime ($p < 0.01$) and nighttime ($p < 0.05$). As expected, vegetation reduces day and night UHIE. Water has negatively significant impact on day UHIE while its effect is positive for night UHIE even though it is no longer significant factor at night.

[7] Level(Y)-Log(X) Interpretation: ΔUHIE=(Coefficient/100)% Δnon-clustering

Table 5.6. Clustering of development and UHIE

UHIE	Day				Night				
	Coefficient (Robust Std. Error)	P-value (One-tailed)	95% confidence Interval		Coefficient (Robust Std. Error)	P-value (One-tailed)	95% confidence Interval		VIF
Non-Clustering	0.5531 (0.4161)	0.09	-0.2653	1.3716	0.2276 (0.2635)	0.19	-0.2906	0.7459	1.54
Impervious	0.0517 (0.0220)	0.01	0.0085	0.0949	0.0193 (0.0102)	0.03	-0.0006	0.0393	2.66
Vegetation	-0.0269 (0.0232)	0.12	-0.0726	0.0187	-0.0321 (0.0115)	0.00	-0.0547	-0.0096	1.55
Water	-0.2929 (0.1092)	0.00	-0.5076	-0.0782	0.0689 (0.0709)	0.17	-0.0706	0.2083	1.19
Population Density	-0.0001 (0.0009)	0.46	-0.0018	0.0016	-0.0001 (0.0005)	0.45	-0.0011	0.0010	2.58
Marine West Coast Forests	-6.4815 (1.4257)	0.00	-9.2858	-3.6772	-2.5475 (1.0784)	0.01	-4.6687	-0.4263	1.31
Mediterranean California	-12.0845 (2.1540)	0.00	-16.3213	-7.8478	-4.1803 (1.2382)	0.00	-6.6159	-1.7447	2.53
North American Deserts	-12.1442 (1.8760)	0.00	-15.8342	-8.4542	-2.1748 (1.0258)	0.02	-4.1925	-0.1571	2.57
Northern Forests	-6.3557 (1.2530)	0.00	-8.8204	-3.8911	-2.7614 (0.7922)	0.00	-4.3196	-1.2032	1.48
Great Plains	-11.2005 (1.2872)	0.00	-13.7325	-8.6686	-2.5300 (0.7436)	0.00	-3.9926	-1.0673	3.53
Northern Forests	-7.3783 (1.1779)	0.00	-9.6952	-5.0614	-2.5741 (0.7438)	0.00	-4.0372	-1.1110	5.93
Tropical Wet Forests	-7.1416 (1.3777)	0.00	-9.8514	-4.4317	-4.8902 (0.9091)	0.00	-6.6782	-3.1021	1.17
Constant	6.3522 (3.4928)	0.04	-0.5180	13.2224	2.7982 (2.0701)	0.09	-1.2736	6.8700	
	Number of obs = 353 R-squared = 0.3302		F(12, 340) = 10.70 Prob > F = 0.0000		Number of obs = 353 R-squared = 0.1905		F(11, 341) = 5.02 Prob > F = 0.0000		

* All significance tests are one tailed because the hypotheses of this study clearly indicated the direction of effect for the independent and control variables

Diversity of Land Covers and UHIE

Diversity models are significant overall and it explains nearly 33 percent and 19 percent of the variance in day and night UHIE respectively. Diversity of development refers to standardized patch richness (i.e. number of land cover types existing) per unit area (100 hectares). Thus, this measure includes all land cover types based on the reclassification of NLCD dataset. (See Table 4.4)

Shown in Table 5.7, increasing the number of land cover types has a negative effect on UHIE during both day and night. However, this indicator is not significant for daytime UHIE and only marginally significant for nighttime UHIE. This weak relationship may be caused because the diversity index only counts the number of land cover types and does not consider the size and amount of each land cover type. For example, although there are very small amounts of vegetation and large amounts development in urbanized areas, they only count as two different types of land covers. Therefore, ***Sub-Hypothesis 4,*** *Metropolitan regions with a higher diversity of land covers in urbanized areas will have a lower Urban Heat Island Effect than metropolitan regions with a lower diversity of land covers in urbanized area*, is not statistically supported by this diversity model.

As with previous models, control variables in the diversity models are also significant predictors of day and night UHIE. Impervious surface area significantly increases day ($p < 0.01$) and night UHIE ($p < 0.05$). Vegetation is still a good source in decreasing day and night UHIE although the impact is more statistically significant during nighttime. Water significantly reduces day UHIE but shows a positive effect on night

UHIE like in the previous models. Population density remains insignificant factor in this model as it is predicted in previous models. Ecoregions are all significant although they have slightly changed their coefficient from previous models.

To test the robustness of the diversity index depending on land cover classification, this study analyzed an additional regression model using a more detailed land cover classification scheme (i.e. first order classification of NLCD). The land cover categories of first order classification include water, developed, forest, shrub land, herbaceous, planted, and wetland. Shown in Appendix C, the result indicates that this alternate diversity index measure is still insignificant for both day and night UHIE.

Table 5.7. Diversity of land covers and UHIE

UHIE	Day				Night				
	Coefficient (Robust Std. Error)	P-value (One-tailed)	95% confidence Interval		Coefficient (Robust Std. Error)	P-value (One-tailed)	95% confidence Interval		VIF
Diversity	-3.4378 (3.5134)	0.16	-10.3484	3.4729	-2.2247 (2.1099)	0.15	-6.3749	1.9254	1.09
Impervious	0.0609 (0.0224)	0.00	0.0168	0.1050	0.0232 (0.0105)	0.01	0.0025	0.0439	2.46
Vegetation	-0.0265 (0.0235)	0.13	-0.0727	0.0196	-0.0323 (0.0116)	0.00	-0.0552	-0.0094	1.55
Water	-0.2850 (0.1118)	0.01	-0.5049	-0.0650	0.0673 (0.0710)	0.17	-0.0723	0.2070	1.19
Population Density	0.0001 (0.0008)	0.45	-0.0015	0.0018	0.0000 (0.0005)	0.49	-0.0010	0.0009	2.39
Marine West Coast Forests	-6.5005 (1.4401)	0.00	-9.3332	-3.6678	-2.5680 (1.0849)	0.01	-4.7019	-0.4341	1.31
Mediterranean California	-12.2870 (2.1439)	0.00	-16.5040	-8.0700	-4.2822 (1.2279)	0.00	-6.6975	-1.8670	2.53
North American Deserts	-12.2047 (1.8816)	0.00	-15.9058	-8.5035	-2.2135 (1.0241)	0.02	-4.2280	-0.1991	2.58
Northern Forests	-6.2689 (1.2437)	0.00	-8.7152	-3.8227	-2.7176 (0.7947)	0.00	-4.2807	-1.1545	2.58
Great Plains	-11.1999 (1.2884)	0.00	-13.7342	-8.6656	-2.5479 (0.7382)	0.00	-3.9999	-1.0960	3.53
Northern Forests	-7.3637 (1.1804)	0.00	-9.6855	-5.0418	-2.6010 (0.7352))	0.00	-4.0471	-1.1549	5.97
Tropical Wet Forests	-6.7927 (1.4281)	0.00	-9.6016	-3.9837	-4.8096 (0.8555)	0.00	-6.4924	-3.1268	1.15
Constant	10.5265 (1.9263)	0.00	6.7375	14.3156	4.6432 (1.0473)	0.00	2.5832	6.7033	
	Number of obs = 353 R-squared = 0.3286		F(12, 340) = 10.55 Prob > F = 0.0000		Number of obs = 353 R-squared = 0.1914		F(11, 341) = 5.08 Prob > F = 0.0000		

* All significance tests are one tailed because the hypotheses of this study clearly indicated the direction of effect for the independent and control variables

Proximity of Land Covers and UHIE

Proximity models are significant overall and explain nearly 33 percent and 19 percent of the variance in day and night UHIE respectively. Shown in Table 5.9, the results of robust regression analysis indicates that increasing value of proximity between different land cover types reduces daytime UHIE, but increases UHIE during the nighttime. However, the effect of proximity is not statistically significant for both day and night UHIE. Therefore, Sub-Hypothesis 5*, Metropolitan region with a higher proximity among different land covers in urbanized area will have a lower Urban Heat Island Effect than the metropolitan region has a lower proximity among different land covers in urbanized area*, is not supported by this proximity model.

Shown in Table 5.8, control variables remain essentially unchanged when compared to previous models. Impervious surface area has a positive impact on both day and night UHIE. Vegetation has a negative effect but is only a statistically significant coefficient of daytime UHIE. On the contrary, water is only statistically significant coefficient of nighttime UHIE with a negative effect. Population density and regional dummies act same as previous models.

Table 5.8. Proximity of land covers and UHIE

UHIE	Day				Night				
	Coefficient (Robust Std. Error)	P-value (One-tailed)	95% confidence Interval		Coefficient (Robust Std. Error)	P-value (One-tailed)	95% confidence Interval		VIF
Proximity	-0.0467 (0.0382)	0.11	-0.1219	0.0284	0.0021 (0.0216)	0.46	-0.0404	0.0446	1.93
Impervious	0.0507 (0.0234)	0.02	0.0048	0.0967	0.0234 (0.0103)	0.01	0.0031	0.0437	2.79
Vegetation	-0.0200 (0.0240)	0.20	-0.0672	0.0271	-0.0316 (0.0121)	0.00	-0.0554	-0.0078	1.61
Water	-0.2247 (0.1135)	0.02	-0.4480	-0.0013	0.0788 (0.0744)	0.15	-0.0675	0.2252	1.22
Population Density	0.0002 (0.0008)	0.39	-0.0014	0.0018	0.0001 (0.0005)	0.44	-0.0009	0.0010	2.33
Marine West Coast Forests	-6.3996 (1.4562)	0.00	-9.2639	-3.5353	-2.5352 (1.0815)	0.01	-4.6624	-0.4079	1.31
Mediterranean California	-12.3485 (2.1395)	0.00	-16.5569	-8.1401	-4.2249 (1.2293)	0.00	-6.6428	-1.8070	2.54
North American Deserts	-12.4672 (1.9385)	0.00	-16.2801	-8.6542	-2.1612 (1.0676)	0.02	-4.2611	-0.0613	2.71
Northern Forests	-6.2461 (1.2601)	0.00	-8.7247	-3.7675	-2.7424 (0.7877)	0.00	-4.2917	-1.1930	1.48
Great Plains	-11.2848 (1.3063)	0.00	-13.8543	-8.7153	-2.4907 (0.7488)	0.00	-3.9637	-1.0178	3.57
Northern Forests	-7.3015 (1.1966)	0.00	-9.6552	-4.9478	-2.5070 (0.7426)	0.00	-3.9676	-1.0465	5.88
Tropical Wet Forests	-6.8362 (1.4490)	0.00	-9.6864	-3.9861	-4.6228 (0.8704)	0.00	-6.3348	-2.9108	1.15
Constant	13.0502 (3.2146)	0.00	6.7271	19.3732	4.1586 (1.7375)	0.01	0.7409	7.5762	
	Number of obs = 353 R-squared = 0.3293		F(12, 340) = 10.55 Prob > F = 0.0000		Number of obs = 353 R-squared = 0.1879		F(11, 341) = 5.08 Prob > F = 0.0000		

* All significance tests are one tailed because the hypotheses of this study clearly indicated the direction of effect for the independent and control variables

5.2.2. Combined Impact of Spatial Development Patterns on UHIE

In this section, I explore additional regression models to see if there are other scenarios that include all of the independent variables (spatial development patterns) together in the model. The previous section employs only one key independent variable at a time because of high correlations among independent variables, but this approach could omit variables based on assumed potential multicollinearity. Thus, this section tested an additional three models which attempt to include all of the key independent variables in one single model, and then selectively dropped one variable at a time to reduce multicollinearity issues. Also, the robust regression method was used for an additional three models since heteroscedasticity was detected in these models (See Appendix F).

Table 5.9 presents the results of daytime UHIE regression models with several combinations of key independent variables. Model 1 is significant overall, with F (16,336) =7.96; Prob > F = 0.00, and it explains thirty-four percent of the variance. Among the five spatial pattern variables tested in Model 1, only continuity was marginally significant at the 0.1 level. Water is still a significant factor that decreases daytime UHIE, as it has also done in previous models. Some variables in the model, including density (93.27), clustering (5.80), and impervious surface (85.18), showed high VIF[8]. Thus, I selectively dropped impervious surface [9] and then potentially one other variable to reduce

[8] Except dummy variable (i.e. EFT region)

[9] Model 1 was also tested with dropping density instead of impervious surface but the net results of other variables are not changed with when density was dropped in the model. Thus, I decided to drop impervious surface to reduce multicollinearity issues since density is one of the key independent variables in this study.

multicollinearity issues. Model 2 was also significant overall, with F (15,337) =8.45; Prob > F = 0.00, although this model excludes impervious surface. The VIF value of density was clearly dropped from 93.27 to 4.27; however there were not substantial changes in coefficients and significance for other variables in the Model 1. In Model 2, clustering still has a high VIF at 5.79, and thus it was dropped in Model 3. As a result, there no critical multicollinearity issues were detected in Model 3. This model was also statistically significant, with F (14,338) =9.06; Prob > F = 0.00. The result of Model 3 indicated that density and continuity show marginal significance (0.097 and 0.07 respectively) at the 0.1 level. Similar to previous models with single independent variables, water is a very significant factor in decreasing UHIE during the daytime across all models.

Table 5.10 presents the results of the nighttime UHIE regression model. The same steps are performed for the nighttime UHIE models as with the daytime UHIE models based on the post-regression test of VIF. Model 1 was significant overall, with F (16,336) =4.47; Prob > F = 0.00. Density was a significant factor at the 0.05 level, and impervious surface was also significant at the 0.10 level. However, similar to the results of the daytime UHIE model, density, clustering, and impervious surface showed high values of VIF. Thus, impervious surface was dropped in Model 2 and clustering was later dropped in Model 3. Model 2 was significant overall, with F (15,337) =4.91; Prob > F = 0.00, as was Model 3, with F (14,338) =5.00; Prob > F = 0.00. Density was significant at the 0.05 level in both Model 2 and Model 3. In addition, vegetation was a very significant factor in decreasing nighttime UHIE across all models.

Table 5.9. Single and combined models for day UHIE

Day UHIE	Density Coefficient (P-value)	Continuity Coefficient (P-value)	Clustering Coefficient (P-value)	Diversity Coefficient (P-value)	Proximity Coefficient (P-value)	Model 1 Coefficient (P-value)	VIF	Model 2 Coefficient (P-value)	VIF	Model 3 Coefficient (P-value)	VIF
Density	0691 (0.002)					0.1115 (0.245)	93.27	0.0365 (0.097)	4.27	0.0365 (0.097)	4.27
Continuity		1.0524 (0.038)				1.0166 (0.095)	3.80	0.9907 (0.102)	3.78	0.9617 (0.070)	2.30
Clustering			0.5531 (0.093)			-0.0502 (0.471)	5.80	-0.0427 (0.476)	5.79		
Diversity				-3.4378 (0.165)		-1.2496 (0.400)	2.67	-1.2503 (0.400)	2.67	-1.0402 (0.394)	1.28
Proximity					-0.0467 (0.111)	-0.0380 (0.174)	2.15	-0.0426 (0.135)	2.06	-0.0425 (0.137)	2.05
Impervious surface		0.0380 (0.052)	0.0517 (0.010)	0.0609 (0.004)	0.0507 (0.016)	-0.0698 (0.318)	85.18				
Vegetation	-.0215 (0.181)	-0.0229 (0.166)	-0.0269 (0.124)	-0.0265 (0.130)	-0.0200 (0.202)	-0.0151 (0.271)	1.72	-0.0166 (0.251)	1.69	-0.0167 (0.253)	1.67
Water	-.2546 (0.012)	-0.2556 (0.009)	-0.2929 (0.004)	-0.2850 (0.006)	-0.2247 (0.025)	-0.2092 (0.032)	1.30	-0.2203 (0.025)	1.28	-0.2217 (0.024)	1.25
Population Density	.0002 (0.422)	0.0002 (0.417)	-0.0001 (0.458)	0.0001 (0.446)	0.0002 (0.391)	0.0001 (0.466)	2.79	0.0001 (0.461)	2.78	0.0001 (0.466)	2.42
MWCF	-6.415 (0.000)	-6.5490 (0.000)	-6.4815 (0.000)	-6.5005 (0.000)	-6.3996 (0.000)	-6.4935 (0.000)	1.31	-6.4970 (0.000)	1.31	-6.4937 (0.000)	1.31
MC	-12.2287 (0.000)	-12.1327 (0.000)	-12.0845 (0.000)	-12.2870 (0.000)	-12.3485 (0.000)	-12.3548 (0.000)	2.65	-12.3091 (0.000)	2.64	-12.2964 (0.000)	2.55
NAD	-12.1843 (0.000)	-12.2096 (0.000)	-12.1442 (0.000)	-12.2047 (0.000)	-12.4672 (0.000)	-12.5554 (0.000)	2.74	-12.5405 (0.000)	2.73	-12.5341 (0.000)	2.71
NF	-6.2908 (0.000)	-6.4566 (0.000)	-6.3557 (0.000)	-6.2689 (0.000)	-6.2461 (0.000)	-6.4016 (0.000)	1.49	-6.3665 (0.000)	1.49	-6.3687 (0.000)	1.49
GP	-11.2006 (0.000)	-11.3022 (0.000)	-11.2005 (0.000)	-11.1999 (0.000)	-11.2848 (0.000)	-11.5791 (0.000)	3.68	-11.5023 (0.000)	3.62	-11.4981 (0.000)	3.60
ETF	-7.2346 (0.000)	-7.3575 (0.000)	-7.3783 (0.000)	-7.3637 (0.000)	-7.3015 (0.000)	-7.5055 (0.000)	6.01	-7.4593 (0.000)	5.96	-7.4588 (0.000)	5.96
TWF	-6.4882 (0.000)	-6.7787 (0.000)	-7.1416 (0.000)	-6.7927 (0.000)	-6.8362 (0.000)	-7.0437 (0.000)	1.19	-7.0711 (0.000)	1.19	-7.0945 (0.000)	1.16
Constant	9.6116 (0.000)	-93.5276 (0.055)	6.3522 (0.035)	10.5265 (0.000)	13.0502 (0.000)	-87.4159 (0.118)		-84.4122 (0.127)		-81.8907 (0.101)	
	R-squared =0.3286	R-squared =0.3321	R-squared =0.3302	R-squared =0.3286	R-squared =0.3293	R-squared =0.3361		R-squared =0.3356		R-squared =0.3356	

* All significance tests are one tailed because the hypotheses of this study clearly indicated the direction of effect for the independent and control variables

Table 5.10. Single and combined models for night UHIE

Night UHIE	Density Coefficient (P-value)	Continuity Coefficient (P-value)	Clustering Coefficient (P-value)	Diversity Coefficient (P-value)	Proximity Coefficient (P-value)	Model 1 Coefficient (P-value)	VIF	Model 2 Coefficient (P-value)	VIF	Model 3 Coefficient (P-value)	VIF
Density	0.0285 (0.007)					0.1479 (0.041)	93.27	0.0253 (0.030)	4.27	0.0250 (0.031)	4.27
Continuity		0.4319 (0.088)				0.4348 (0.149)	3.80	0.3923 (0.177)	3.78	0.2533 (0.224)	2.30
Clustering			0.2276 (0.194)			-0.2176 (0.322)	5.80	-0.2053 (0.331)	5.79		
Diversity				-2.2247 (0.146)		-2.8098 (0.177)	2.67	-2.8109 (0.178)	2.67	-1.8010 (0.210)	1.28
Proximity					0.0021 (0.462)	0.0153 (0.245)	2.15	0.0078 (0.358)	2.06	0.0084 (0.350)	2.05
Impervious surface		0.0137 (0.114)	0.0193 (0.029)	0.0232 (0.014)	0.0234 (0.012)	-0.1141 (0.071)	85.18				
Vegetation	-0.0290 (0.008)	-0.0305 (0.006)	-0.0321 (0.003)	-0.0323 (0.003)	-0.0316 (0.005)	-0.0271 (0.027)	1.72	-0.0295 (0.011)	1.69	-0.0302 (0.010)	1.67
Water	0.0831 (0.117)	0.0842 (0.120)	0.0689 (0.166)	0.0673 (0.172)	0.0788 (0.145)	0.0911 (0.120)	1.30	0.0729 (0.164)	1.28	0.0666 (0.186)	1.25
Population Density	0.0000 (0.497)	0.0000 (0.468)	-0.0001 (0.448)	0.0000 (0.488)	0.0001 (0.443)	0.0000 (0.485)	2.79	0.0000 (0.498)	2.78	-0.0001 (0.435)	2.42
MWCF	-2.5100 (0.010)	-2.5751 (0.009)	-2.5475 (0.010)	-2.5680 (0.009)	-2.5352 (0.010)	-2.5811 (0.008)	1.31	-2.5868 (0.008)	1.31	-2.5712 (0.008)	1.31
MC	-4.2239 (0.001)	-4.2002 (0.001)	-4.1803 (0.001)	-4.2822 (0.001)	-4.2249 (0.001)	-4.3536 (0.000)	2.65	-4.2790 (0.001)	2.64	-4.2179 (0.001)	2.55
NAD	-2.1900 (0.017)	-2.2016 (0.017)	-2.1748 (0.018)	-2.2135 (0.016)	-2.1612 (0.022)	-2.2312 (0.019)	2.74	-2.2069 (0.020)	2.73	-2.1760 (0.021)	2.71
NF	-2.7178 (0.001)	-2.8028 (0.000)	-2.7614 (0.001)	-2.7176 (0.001)	-2.7424 (0.001)	-2.7917 (0.000)	1.49	-2.7344 (0.001)	1.49	-2.7446 (0.001)	1.49
GP	-2.5280 (0.001)	-2.5716 (0.001)	-2.5300 (0.001)	-2.5479 (0.001)	-2.4907 (0.001)	-2.7238 (0.000)	3.68	-2.5982 (0.001)	3.62	-2.5781 (0.001)	3.60
ETF	-2.4977 (0.001)	-2.5653 (0.001)	-2.5741 (0.001)	-2.6010 (0.000)	-2.5070 (0.001)	-2.6634 (0.000)	6.01	-2.5879 (0.000)	5.96	-2.5855 (0.001)	5.96
TWF	-4.6020 (0.000)	-4.7406 (0.000)	-4.8902 (0.000)	-4.8096 (0.000)	-4.6228 (0.000)	-4.5880 (0.000)	1.19	-4.6328 (0.000)	1.19	-4.7454 (0.000)	1.16
Constant	4.0499 (0.000)	-38.1920 (0.112)	2.7982 (0.089)	4.6432 (0.000)	4.1586 (0.009)	-38.1715 (0.166)		-33.2582 (0.200)		-21.1349 (0.259)	
	R-squared =0.1907	R-squared =0.1919	R-squared =0.1905	R-squared =0.1914	R-squared =0.1879	R-squared =0.2024		R-squared =0.1963		R-squared =0.1958	

* All significance tests are one tailed because the hypotheses of this study clearly indicated the direction of effect for the independent and control variables

CHAPTER VI

DISCUSSIONS AND CONCLUSIONS

Results from the statistical analyses lead to topics that are worthy of further discussion. This section examines and expands on the results of the multivariate regression analyses and discusses the key findings as the answers for the research objectives of this study. The policy implications of these research findings are discussed and synthesized into recommendations. Finally, I describe research limitations and conclusions of the study.

6.1. Key Findings Regarding Research Objectives

Although there are several previous studies that examine UHIE, this study is one of the few that explore the overall patterns of regional UHIE across the U.S. This study uses the basic concept of UHIE, the temperature difference between urban and rural areas, to compare these regions while adjusting for different climates and natural environments.

The key findings regarding the first research objective, which is to investigate UHIE at a regional scale in the metropolitan regions, are as follows:

First, the descriptive analysis of UHIE shows that the mean UHIE is 4.04˚F during day and 2.41˚F at night. Although there are variations of UHIE depending on the location and ecological context of each metropolitan region, the results of this study reveal that generally the magnitude of day UHIE and night UHIE are different, and daytime UHIE is

larger than nighttime UHIE. This finding is consistent with previous research on surface UHIE suggesting that surface UHIE is most intense during the day and in the summer (Roth et al., 1989; EPA, 2008; Imhoff et al., 2010). Moreover, this result can be a reasonable justification of this study in that examining the impact of spatial patterns of development on surface UHIE is relevant since surface temperature is directly affected by sun-light and the surface materials that cover urban areas.

Second, the results indicate that ecological context is a statistically significant modulator that helps to explain the spatial distribution of the UHIE. When summarizing UHIE by ecoregions, each ecoregion shows different patterns for daytime and nighttime (See Figure 5.2). Although the average UHIE of daytime is larger than that of the nighttime, there are some exceptional regions which have larger nighttime UHIE than daytime UHIE. For example, two ecoregions have larger UHIE at nighttime: the Great Plains region and the North American Desert region. These two regions have similar characteristics in terms of summer climate. The climate of the Great Plains region is dry and continental, characterized by short, hot summers and long, cold winters. Similarly, the North American Desert region has a desert and steppe climate: arid to semi-arid, with marked seasonal temperature extremes (ECE, 1997). Also, The North American Desert region traditionally have small population centers, but some urban areas like Las Vegas have recently experienced rapid growth (ECE, 1997). During the daytime, temperature is increased in both urban and rural areas by an extremely hot and dry climate as well as limited vegetation. However, in the nighttime without sun-light, temperatures in rural areas decrease rapidly as compared to the urban areas with development. This discussion

can be extended to another finding that some metropolitan regions that have a negative UHIE, especially in daytime. Negative UHIE is observed in the North American Desert, the Mediterranean California, and the Great Plains regions. With some exceptions of coastal metropolitan regions, extremely high temperatures in both urban and rural areas due to their climatic, environmental, and demographic settings lead to small or negative UHIE in these ecoregions. This finding is supported by a previous study on UHIE and biomes, which suggests that UHIE responses for eight different biomes are all significantly different ($p = 0.01$) and clearly show the effect of ecological context on UHIE (Imhoff et al., 2010). Although the previous study employs a slightly different ecoregion classification scheme by Olson et al. (2001), their results also reveal that urban areas surrounded by desert and xeric shrublands show much smaller temperature contrast or even a reverse of UHIE.

Regarding the results of this study and the findings of Imhoff et al. (2010) that are related to ecoregions and UHIE, additional tests were conducted to see if each ecoregion has a statistically different effect in the model, in which case regional clusters would exist (See Appendix G). The results show that there are three regional clusters of ecoregions that differ substantially from each other in the analysis. Except when using the Northeastern Forested Mountain region as a base region, two regional clusters were generated differently for daytime UHIE and nighttime UHIE. For daytime UHIE, the

ecoregions of the MWCF[10], NF, ETF, and TWF showed the same pattern for daytime UHIE, and the ecoregions of the MC, NAD, and GP had a similar effect in the regression model. On the other hand, the ecoregions of the MWCF, NAD, NF, GP, and ETF showed similar patterns for nighttime UHIE, and TWF and MC were grouped as another regional cluster in the nighttime UHIE model. Regional clusters for daytime UHIE are affected by the geographic location of ecoregions, while regional clusters for nighttime UHIE are more affected by the characteristics of the location. For example, each regional cluster for daytime UHIE is geographically linked, however regional clusters for nighttime UHIE, especially in Ecoregion 2, are not geographically linked. Yet both ecoregions are located in coastal areas and show similar patterns for nighttime UHIE.

Although there were no substantive changes in key independent variables when three new regional clusters were employed as regional dummy variables instead of eight ecoregions of the Level I ecoregion classification (See Appendix G), this additional test suggests that we could generate regional clusters when considering UHIE as an additional indicator of ecoregions.

Regarding the second research objective, measuring spatial patterns of development in urban areas based on the concepts of landscape metrics, this study analyzes spatial development patterns in urban areas using five selected land scape metrics to examine not only composition but also configuration. The results indicate that each

[10] MWCF: Marine West Coast Forest / NAD: North American Desert / NF: Northern Forests/ GP: Great Plains/ ETF: Eastern Temperate Forests/ TWF: Tropical Wet Forests/ NFM: Northeastern Forested Mountains/ MC: Mediterranean California

urban area has different spatial development pattern even though they are uniformly designated as "urbanized areas" in metropolitan regions because of their large population. In short, every urbanized area can have different spatial patterns in terms of development.

There is another discussion point in the selection and measurement process of development patterns using landscape metrics. Previous research mentioned that the selection of landscape metrics is a critical step, since there are hundreds of landscape indexes (Leitão, A. B, 2006; Ji et al., 2006; Wu et al., 2011). The selected metrics in this study also correlate with each other, including PLAND (density of development), COHESION (continuity of development), GYRATE_AM (clustering of development), PRD (diversity of development), and IJI (proximity of development). For example, PLAND and COHESION are highly and positively correlated with each other, since the large amount of land developed in any given area could lead to connected development. As a result, this study builds several individual regression models for each landscape index to avoid multicollinearity and complexity of interpretation.

With regard the third research objective—examine the relationship between spatial development patterns and UHIE—the results of statistical analyses reveal that density, continuity and clustering (only for daytime) have significant impacts on UHIE when each of the indexes is tested separately in the model.

Density of development has a positive impact on both day and night UHIE; a higher density of development significantly increases day and night UHIE (See Table 5.5). Since impervious surface is a crucial element needed to increase urban temperature and

UHIE, this result agrees with most of previous studies about UHIE. For example, Streutker (2002), and Yoshida et al. (2004) reveal that large amounts of impervious surface and dense built environment create more heat, which results in a large UHIE. There is no objection to the general consensus of previous studies that reducing and minimizing impervious surface are the primary solution to decreased UHIE. However, the population is continuously growing and has been more concentrated on urban areas. Therefore, we cannot avoid developing land and creating more impervious surfaces in urban areas. Thus, we need to think about how we can develop land wisely in terms of reducing UHIE and providing a comfortable thermal environment, which is the main research question of this study. The following contains several discussions emphasizing which types of spatial development pattern can reduce UHIE based on the findings of this study.

Increasing continuity of development can also significantly also enhance UHIE. Continuity of development is even more informative when it is considered as one characteristic of sprawl because it indicates a land consumptive development pattern rather than planned and concentrated pattern. Thus, continuous and widespread development patterns are major contributors to producing large amounts of impervious surface while diminishing the natural environment. Moreover, highly continuous development patterns are usually observed in urbanized areas with sophisticated road systems. It is true that well-developed road systems are convenient and provide good accessibility, but they are also paved by asphalts that create large amounts of heat and sometimes aggravate fragmentation of the natural environment.

Less clustered development patterns increase UHIE, especially during daytime.

The research of Stone and Norman (2006) has also supported the benefit of clustering development on UHIE. They conclude that lower density and dispersed patterns of urban residential development contribute more surface energy to regional heat island formation than do higher density, compact forms. Clustered or stacked development is frequently used as an opposite concept of sprawl since it could minimize the ecological footprint in the areas of land associated with them (Gordon and Richardson, 1997a). Thus, low clustering development has been linked to several negative effects such as flooding and erosion because of the creation of impervious surface (Galster et al., 2001; Brody et al., 2013). For example, Brody et al. (2013) argued that clustered medium-intensity development significantly reduces residential flood damage. In this sense, clustering is clear evidence of reducing hazard vulnerability and an effective planning strategy to minimize impervious surface areas which will contribute in reducing not only UHIE but also other natural hazards.

While the effect is negative, diversity and proximity of land covers in urbanized areas does not significantly impact UHIE. In fact, the diversity index is an insignificant predictor under two different land cover classification schemes. One possible reason for this weak impact is that the diversity measure (i.e. patch richness density) does not consider the size of each land cover but only the number of land covers per unit area (100ha). Thus, small hints of vegetation or water can be counted to calculate patch richness even though they cannot have much effect on temperature if they are squeezed between massive areas of impervious surface.

Another expected reason for the result of the proximity index is that this is more

related to the functional aspect of land cover (i.e. land uses). For example, high proximity between different land uses including residential, commercial, and industrial, should minimize construction of roads and reduce travel distance. As a result, UHIE will be decreased if high proximity is attained between different land uses.

On the other hand, when tests combined the impacts of indexes, density and impervious surface are the most important factors that are consistently working in the combined models although continuity have potential impacts on UHIEs across regions at the metropolitan level of analysis. Since density is measured by the percentage of impervious surface in an urban area and the impervious surface variable is measured by the difference in percentage of impervious surface between urban and rural areas[11], these two variables (density and impervious surface) have almost the same values. Therefore, the VIF values of both variables are high when they exist together.

Based on the results of five landscape indexes, low-density, discontinued, and un-clustered development patterns are recommended to reduce UHIE when single effect of each spatial development pattern were tested in the model. As mentioned earlier, the landscape indexes were selected based on the characteristics of sprawl and compact development patterns. Visual analysis with maps revealed that each landscape metrics clearly describe overall spatial patterns in urbanized area (See Figure 5.3 - 5.7). However, there was a particular spatial pattern which represents both sprawl and compact types of development. For example, the high continuity is observed in continuous and ribbon types

[11] Very few impervious surfaces exist in rural areas.

development which is a typical sprawl-type development, and it is also observed in the grid pattern of road systems which is preferred road networks of compact-type development. In other words, high continuity of development is associated with both sprawl and compact development types in opposite direction. Thus, continuous development can be rejected in terms of UHIE but it could come with other undesirable outcomes such as low accessibility to roads. This finding suggests that we need careful considerations to decide and suggest specific spatial development patterns for enhancing environmental quality (e.g. thermal comfort) and mobility (e.g. accessibility) at the same time.

The results of the regression analysis of this study suggest some additional interesting findings. First, although both vegetation and water have negative effects on UHIE, vegetation is a more significant factor of UHIE at night while water is a more significant factor of UHIE during the day. This result is consistent across all regression models. Another finding is also about water: although it failures to become significant indicator in regression models, it continuously shows a positive sign during the nighttime. In other words, water possibly increases temperature in urbanized areas and UHIE at night. This result can be explained with the concept of specific heat; water has one of the highest specific heats of any substance. Thus, water can be an influential factor in decreasing UHIE in daytime, but it seems to be a factor that increases UHIE in the nighttime (although it is not statistically significant). These finding can be very useful concepts in terms of urban design and land use planning.

6.2. Planning Implications and Recommendations

Spatial planning is considered to be the primary tool used to guide development in a sustainable manner and also to safeguard inhabitants from various hazards (Berke, Godschalk, Kaiser, & Rodriguez, 2006; Brody & Highfield, 2005; Gadschalk, Edward J. Kaiser, & Berke, 1998).

The results of this study indicate that spatial development patterns can significantly affect both daytime and nighttime UHIE, even when controlling for multiple environmental, demographic, and regional contextual variables. In other words, UHIE is associated with not only the amount of development but also the spatial configuration of development. The statistical analyses of the five landscape metrics reveal that specific spatial development patterns mitigate UHIE, suggesting a way for regional planners and decision-makers to facilitate the emergence of more heat-resilient communities in terms of spatial planning. In general, the results of this study support less sprawling development patterns in order to be more resilient to regional UHIE. These findings are generalizable to U.S. metropolitan regions and thus, this study recommends at least four specific spatial planning strategies that may reduce the increased UHIE from both existing and future urban development.

6.2.1. Reducing Impervious Surface through Reconfiguring the Development

The finding of a positive relationship between the amount of impervious surface and UHIE confirms the well-established effect of paving materials in UHIE formation.

The widely accepted approach to mitigating the thermal impact of impervious surface is the reduction in the total amount of paved surface. In the same sense, the findings of this study suggest that a 1% increase in development in urbanized areas is associated with a 0.07 ˚F and 0.03 ˚F higher day UHIE and night UHIE, respectively. Stone (2006) suggests several ways to reduce UHIE with no loss in living space, especially for residential structures. For new developments, multistory construction provides a straightforward method to minimizing the building footprint area. Another recommended strategy to reduce new impervious surface area is infill development. The reuse of abandoned or underused areas and renovation and adaptive reuse of existing older structures could accommodate future population and housing growth without increasing the total area of impervious surface (People for Open Space, 1983; Beatley and Manning, 1997).

6.2.2. Limiting Continuity of Development through a Clustering Strategy

Continuous development pattern is another contributor to UHIE. This connected pattern that spreads outward from urban centers creates large amounts of impervious surface, which produce heat in various ways. The results of this study reveal that more continuous development increases UHIE while more clustered development reduces UHIE. These two findings can be applied together to land development policy. More clustered and compact development patterns will lead to a smaller physical footprint for a city and less impact on adjacent hinterlands. On the other hand, more sparse and sprawled development patterns will need more transportation networks that will produce more heat

as well as fragment natural environments. Design guidelines for clustering development at the city or even regional level can be established, along with minimum open space and density standards. There are a couple of tools and policies that planners and developers can choose from to encourage the development of a more concentrated built environment. One potentially powerful strategy to reduce sprawl-type development is to create financial incentives to build and grow in more compact patterns (Beatley and Manning, 1997). For example, overlay zoning is allowed for cluster and compact developed area. Also tax incentives and grants for specific development projects can be used

6.2.3. Placing Vegetation and Water Appropriately

Vegetation and water are traditional elements used to decrease and manage the urban thermal environment. The results of this study also reveal that they have a negative effect on UHIE. However, each element is more influential at different times of day: water becomes a more significant factor during daytime while vegetation becomes a more significant factor at night. The impact of these natural features could be used as a good guideline when designing urban spaces. For example, water can be used more efficiently as a temperature reducer where population congregates during the daytime, such as business or commercial districts; Vegetation could be added to the residential areas where people usually gather at night. In this way, strategic placement of vegetation and water throughout the urban landscape could provide better thermal comfort for residents.

6.3 Limitations and Future Research

While this study provides a greater understanding of regional UHIE across the U.S. and offers insights on the effect of spatial development patterns on the intensity of UHIE, it should be considered only a starting point for more thorough research on this topic. Thus, it is important to highlight several limitations of this study.

First, this study considers only a single class of land cover-aggregated developed areas which, while representative of urban growth and impervious surfaces, does not fully considered the functional aspect of developed areas. Future research could analyze the spatial patterns for sub-categories of developed areas (e.g. high, medium, and low intensities of development) or more detailed land use data. This approach allows for more detailed policy recommended for each different land use.

Second, this study examines only five landscape metrics as measures of spatial development patterns. Although these five indices were selected based on existing literature and with careful consideration, it may be that certain measures do not fully capture the spatial development pattern across a landscape. For example, diversity of land cover in this study was expected to affect UHIE based on the existing literature, but this study found it to be an insignificant predictor even under different classification schemes. There are many alternate measures of diversity that could be used for future research. Examining additional metrics would allow for a more comprehensive understanding of the role development patterns play in the UHIE.

Third, the scale at which development patterns were measured is another limitation of this study. Since the scale of ecological data is defined by extent and grain (Forman and Godron, 1986; Turner et al. 1989; Wiens 1989), it is critical that spatial scales are defined appropriately to represent the ecological phenomenon (Cushman and McGarigal, 2008). Extent and grain size of analysis used in this study are determined by the spatial resolution of the USGS land cover dataset (30m x 30m) and technical capabilities of the computing environment. However, it is more meaningful to define scale from the perspective of the organism or ecological phenomenon under consideration (Cushman and McGarigal, 2008). Future research should use data at different spatial scales to allow the selection of potentially more appropriate extent and grain sizes.

Forth, although spatial autocorrelation was tested to detect a potential spatial effect in the regression model, it was relevant only for daytime UHIE, not for nighttime UHIE. To be consistent for both daytime and nighttime models in terms of comparing day and night UHIE, this study employed regional dummy variables instead of using spatial regression models to control for the spatial effect on the dependent variable (i.e. UHIE). I believe that the spatial effect can be effectively reduced by regional dummies. Future research, however, could use more advanced statistical approaches, such as spatially weighted regression to identify and deal with potentially confounding spatial effects.

Fifth, the spatial scale of this study is limited to metropolitan regions since this study focuses on examining regional UHIE. However, it is well known that there are finer scales of UHIE, such as cities, neighborhoods, and even at the block level. Future study on the impact of spatial development patterns should be done at finer spatial scales to detect the

more localized impact of spatial development patterns on UHIE, while also considering the environmental and social contexts of each particular region. In addition, the availability of finer spatial resolution of thermal remote sensing data should create additional opportunities to analyze local scale UHIE.

6.4.Conclusions and Contributions on Planning Research

The results of this study demonstrate that spatial development patterns in urbanized areas affect regional UHIE. There has been a general consensus that urbanization with increasing impervious surfaces has a positive effect on urban temperature. In addition, land cover and land use are the most significant factors in determining surface UHIE. However, most previous studies are more focused on the amount and composition of land cover, while there has been very limited research attempting to measure how spatial configuration is important to mitigate regional UHIE.

Despite the limitations noted above, my research addresses this critical gap by identifying the statistical variation of regional UHIE across different spatial development patterns on a regional scale. I believe the results of this study make three important contributions to the planning literature associated with UHIE.

First, although it is limited to particular spatial patterns of development, regional UHIE is associated with not only the amount of development but also its spatial arrangement. In other words, when contextual heat contributors are held constant, UHIE can differ depending on the configuration of development in urban areas, especially for

continuity and clustering. This notion can be used as a policy-relevant measure to guide more heat-resilient communities. In this sense, planners can suggest the spatial rearrangement of development or regulate land-cover alteration in urbanized areas to enhance their thermal performance.

Second, this study analyzes regional UHIE and spatial development patterns across all U.S. metropolitan regions. Although there is variation in the UHIE among different ecoregions and some particular metropolitan regions act differently in regression analyses, generally, UHIE in metropolitan regions are significantly related to each region's spatial development patterns. Since this finding is not limited to one particular region, it can be generalized to spatial planning and urban design guidelines on a regional scale development.

Last, this study uses ecologically-based landscape metrics to examine the relationship between spatial development form and UHIE. This is an important contribution to the urban planning and natural hazard research field because it provides a comprehensive approach on both spatial land development and hazard-resistant planning through alternative ways of measuring and modeling spatial development patterns.

REFERENCES

Arnold, C.L., and Gibbons, J., (1996). Impervious Surface Coverage: the Emergence of a Key Environmental Indicator. J. Am. Plan. Assoc. 62(2):243-285.

Beatley, T. and Manning, K. (1997). The Ecology of Place: Planning for Environment, Economy and Community. Washington, DC: Island Press.

Berke, P. R., Godschalk, D. R., Kaiser, E. J., & Rodriguez, D. (2006). Urban Land Use Planning: 5th Edition. Champaign, IL: University of Illinois Press.

Blaine, T. W. and Schear, P. (1998). Cluster Development Fact Sheet, Ohio State University Extension Land Use Fact Sheet Series.

Brody, S. D., &Highfield, W. F. (2005). Does Planning Work? Testing the Implementation of Local Environmental Planning in Florida. Journal of American Planning Association, 71(2), 159-175.

Brody, S.D., Kim, H., and Gunn, J. (2013). The Effect of Urban Form on Flood Damage along the Gulf of Mexico Coast. Urban Studies, 50(4):789-806.

Carlson, T. N., Augustine, J.A., & Boland, F. E. (1977). Potential Application of Satellite Temperature Measurements in the Analysis of Land Use over Urban Areas. Bulletin of the American Meteorological Society, 58(12): 1301-1303.

Cardelino C.A. and Chameides W.L. (2000). Application of Data from Photochemical Assessment Monitoring Stations to the Observation-based Model. Atmospheric Environment, 34(12):2325-2332.

Champion, T. and Hugo, G. (2004). Introduction: Moving Beyond the Urban-Rural Dichotomy. In: Champion, T. and Hugo, G. (Ed.), New Forms of Urbanization (pp.3-24). Ashgate Publishing Company: Burlington

Chandler, T. J. (1965). The climate of London, Hutchinson, London, 292pp.

Chander, G. and Markham, B. (2003). Revised Landsat-5 TM Radiometric Calibration Procedure and Postcalibration Dynamic Ranges. IEEE Transactions on Geosciences and Remote Sensing, 41(11), 2674-2677.

Chen, Z., Gong, C., Wu, J., and Yu, S. (2011). The Influence of Socioeconomic and Topographic Factors on Nocturnal Urban Heat Islands: A Case Study in Shenzhen, China. International Journal of Remote Sensing. 33(12):3834-3849

Clarke, J. K. (1972). Some Effects of the Urban Structure on Heat Mortality. Environmental Research, 5:93-104.

Clawson (1962). Urban Sprawl and Speculation in Suburban Land. Land Economics 38(2):94-111.

Conti, S., Meli, P., Minelli, G., Solimini, R., Toccaceli, V., Vichi, M., Beltrono, C., &Perini, L. (2005). Epidemiologic Study of Mortality During the Summer: 2003 Heat Wave in Italy. Environ Res. 98(3):390–399.

Crossett, K., T. J. Culliton, P. Wiley, and T. R. Goodspeed. (2004). Population Trends Along the Coastal United States, 1980-2008, National Oceanic and Atmospheric Administration, Administration Coastal Trends Report Series.

Cushman, S. A. and McGarigal, K. (2008). Landscape Metrics, Scale of Resoution. In: K. von Gadow, T. Pukkala (eds.), Designing Green Landscapes, pp. 33-51, Springer, New York

ECE. (1997). Ecological Regions of North America: Toward a Common Perspective.

EPA (2008a). Latest Findings on National Air Quality: Status and Trends through 2006

EPA (2008b). Reducing Urban Heat Islands: Compendium of Strategies.

Ewing, R. (2008).Chracteristics, Causes, and Effects of Sprawl: A Literature Review. Urban Ecology, in: Marzluff, J., et al. (Eds) Urban Ecology: An International Perspective on the interaction between humans and nature. Pp. 519-535. New York, NY: Springer.

Forman, R. T. T., and M. Godron. (1986). Landscape Ecology. John Wiley & Sons, New York.

Freilich, R., Sitkowski, R.J., and Menillo, S.D. (2010). Form Sprawl to Sustainability: Smart Growth, New Urbanism, Green Development, and Renewable Energy. Chicago, IL: American Bar Association.

Gallo, K.P. and Owen, T.W. (1998). Assessment of Urban Heat Island: A Multi-Sensor Perspective for the Dallas-Ft. Worth, USA regions, Geocarto International, 13(4):35-41.

Galster, G., Hanson, R., Ratcliffe, M. R., Wolman, H., Coleman, S., &Freihage, J. (2001). Wrestling Sprawl to the Ground: Defining and Measuring an Elusive Concept. Housing Policy Debate, 12(4), 681–717.

Gedzelman SD, Austin S, Cermak R, Stefano N, Partridge S, Quesenberry S, Robinson DA (2003). Mesoscale Aspects of the Urban Heat Island Around New York City. Theory Appl Climatol 75:29-42.

Gober, P., Brazel, A. Quay, R., Myint S., Grossman-Clarke, S., Miller A., & Rossi, S. (2010). Using Watered Landscapes to Manipulate Urban Heat Island Effects: How Much Water Will It Take to Cool Phoenix? Journal of the American Planning Association, 76 (1):109-121.

Godschalk, D., Edward J. Kaiser, &Berke, P. R. (1998). Integration Hazard Mitigation and Local Land Use Planning. In R. J. Burby (Ed.), Cooperating with nature (pp. 85-118). Washington, DC: Joseph Henry Press.

Golany G.S. (1995). Urban Design Morphology and Thermal Performance, Atmospheric Environment, 30: 455-465.

Gong, C. F., Chen, J. Q., and Yu, S.X., (2011). Spatiotemporal Dynamics of Urban Forest Conversion Through Model Urbanization in Shenzhen, China. International Journal of Remote Sensing, 32, pp. 9071-9092.

Gorden, P. and H.W. Richardson (1997a). Are Compact Cities a Desirable Planning Goal? Journal of the American Planning Association. 63(1):95-106

Gorden, P. and H.W. Richardson (1997b). Where's the Sprawl? Journal of the American Planning Association. 63(2):275-278

Grimm, N. B., Faeth, S. H., Golubiewski, N. E., Redman, C. L., Wu, J.G., Bai, X. M., Briggs, J. M. (2008). Global Change and the Ecology of Cities. Science, 319: 756–760.

Grover, H. (2010) Local Response to Global Climate Change: The Role of Local Development Plans in Climate Change Management. Doctoral Dissertation at Texas A&M University

Hargis, C. D., Bissonette, J.A., and David, J. L. (1998). The Behavior of Landscape Metrics Commonly Used in the Study of Habitat Fragmentation. Landscape Ecology. 13:167-186.

Hanson, S., and G. Pratt. (1988). Reconceptualizing the Links between Home and Work in Urban Geography. Economic Geography. 64:299-321

Herold, M., Goldstein, N.C., and Clarke, K.C. (2003). The Spatiotemporal Form of Urban Growth: Measurement, Analysis and Modeling. Remote Sensing of Environment, 86 286–302.

Horner, M. W. (2004). Spatial Dimensions of Urban Commuting: A Review of Major Issues and Their Implications for Future Geographic Research. The Processional Geographer. 56:160-73

Hu, YonghongandJia, Gensuo (2010). Influence of Land Use Change on Urban Heat Island Derived from Multi-sensor Data. Int. J. climatol,. 30: 1382-1395.

Jenerette, G.D., Harlan, S.L., Brazel, A., Jones, N., Larsen, L., and Stefanov, W.L. (2007). Regional Relationships Between Vegetation, Surface Temperature, and Human Settlement in a Rapidly Urbanizing Ecosystem. Landscape Ecology, 22(3):353-365.

Kalnay E. & Cai M. (2003). Impact of Urbanization and Land-use Change on Climate. Nature, 423, 528-531.

Katsoulis, B. D., and Theoharatos, G. A., (1985). Indications of the Urban Heat Island in Athens, Greece, Journal of climate and Applied Meteorology, 24: 1296-1302.

Klinenberg, E., (2002). Heat Wave: A Social Autopsy of Disaster in Chicago. University of Chicago Press: Chicago.

Landsberg, H. E. (1981). The Urban Climate. Academic Press: NY

Lee, D. D. (1979). Contrasts in Warming and Cooling Rates at an Urban and a Rural site. Weather, 34: 60-66

Lee, S., & French, S. P. (2009). Regional Impervious Surface Estimation: An Urban Heat Island Application. Journal of Environmental Planning and Management, 52(4):477-496.

Leitão, A. B., Miller, J., Ahern, J., and McGarigal, K. (2006). Measuring Landscapes: A Planner's Handbook. Washington D.C: Island Press.

Lo, C. P., &Quattrochi, D. A. (2003). Land-use and Land-cover change, Urban Heat Island Phenomenon, and Health Implications: A Remote Sensing Approach. Photogrammetric Engineering & Remote Sensing, 69(9):1053-1063.

Marc L. Imhoff, Ping Zhang, Robert E. Wolfe, Lahouari Bounoua. (2010). Remote Sensing of the Urban Heat Island Effect Across Biomes in the Continental USA. Remote sensing of Environment. 114:504-531

Marina Alberti, Erik Botsford, and Alex Cohen (2001). Quantifying the Urban Gradient: Linking Urban Planning and Ecology In J. M. Marzluff, R. Bowman, R. McGowan, R. Donnelly, Eds. *Avian Ecology in an Urbanizing World.* Kluwer, New York.

Mcgarigal, K. and Marks, B. J. (1995). Fragstats: Spatial Pattern Analysis Program for Quantifying Landscape Structure. United States Department of Agriculture

McGarigal, K., Cushman, S. A., Neel, M. C., and Ene, E. (2002). FRAGSTATS: Spatial Pattern Analysis Program for Categorical Maps.

McGarigal, K., SA Cushman, and E Ene. (2012). FRAGSTATS v4: Spatial Pattern Analysis Program for Categorical and Continuous Maps. Computer Software Program Produced by the Authors at the University of Massachusetts, Amherst. Available at the following web site: http://www.umass.edu/landeco/research/fragstats/fragstats.html

McGarigal, K. (2012). Characterizing Landscape Patterns – Conceptual Foundation. http://www.umass.edu/landeco/teaching/landscape_ecology/schedule/landeco_schedule.html.

Mileti, D.S (1999) Disasters by Design: A Reassessment of Natural Hazards in the United States. Joseph Henry Press: Washington D.C.

National Climate Data Center (NCDC). (2004). Billion-Dollar Weather Disasters, 1980–2004. Website: http://www.ncdc.noaa.gov/ol/reports/billionz.html

Nichol, J.E., (1994). A GIS-Based Approach to Micro Climate Monitoring in Singapore's High-Rise Housing Estates. Photogrammetric Engineering & Remote Sensing, 60:1225-1232.

Oke, T. R. (1973). City Size and the Urban Heat Island. Atmospheric Environment, 7:769–779.

People for Open Space (1983). Room Enough: Housing and Open Space in Bay Area. San Francisco: People for Open Space

Porter, D. R. and Kinsey, J. (2000). The Practice of Sustainable Development. Washington D. C: Urban Land Institute.

Quattrochi, D. A., Luvall, J. C., Rickman, D. L., Estes, M. G., Laymon, C. A., & Howell, B. F. (2000). A Decision Support Information System for Urban Landscape Management using Thermal Infrared Data. Photogrammetric Engineering and Remote Sensing, 66 (10): 1195–1207.

Ritters K.H., Oneill R. V., Hunsker C. T., Wickham J.D., Yankee D.H., Timmins S.P., Jones K.B. and Jackson B.L. (1995). A Factor-Analysis of Landscape Pattern and Structure Metrics. Landscape Ecology 10:23-39.

Roth, M., Oke, T.R. and Emery, W.J. (1989). Satellite Derived Urban Heat Islands from Three Coastal Cities and the Utilization of Such Data in Urban Climatology, International Journal of Remote Sensing, 10:1699-1720.

Rosenziweig, C., Solecki, W. D., Parshall, L., Chopping, M., Pope, G., & Goldberg, R. (2005). Characterizing the Urban Heat Island in Current and Future Climates in New Jersey. Environmental Hazards, 6:51-62.

Sartor, F., Snacken, R., Demuth, C. and Walckiers, D. (1995). Temperature, Ambient Ozone Levels, and Mortality During Summer 1994 in Belgium. Environmental Research, 70:105-113.

Schneider A and Woodcock C. (2008). Compact, Dispersed, Fragmented, Extensive? A Comparison of Urban Expansion in Twenty-Five Global Cities Using Remotely Sensed, Data Patter Metrics and Census Information. Urban Studies. 45:659-92

Sultana, S. and Weber, J. (2007). Journey-to-Work Patterns in the Age of Sprawl: Evidence from Two Midsize Southern Metropolitan regions. The Professional Geographer, 59(2):193-208.

Seto, K.C., and Fragkias, M. (2005). Quantifying Spatiotemporal Patterns of Urban Land-Use Change in Four Cities of China with Time Series Landscape Metrics. Landscape Ecology. 20:871-888.

Sillman, S. and Samson, P.J. (1995). Impact of Temperature on Oxidant Photochemistry in Urban, Polluted Rural, and Remote Environments. Journal of Geophysical Research, 100: 11497-11508.

Smoyer, K.E., Rainham, D. G., and Hewko, J. N. (2000). Heat-Stress-Related Mortality in Five Cities in Southern Ontario: 1980–1996. Int J Biometeorol, 44(4):190–197.

Song, Y. and Knaap G. J. (2004). Measuring Urban Form: Is Portland Winning the War on Sprawl? Journal of American Planning Association, 70(2): 210-225

Squires, G. (2002). Urban Sprawl and Uneven Development of Metropolitan America, in: Squires, G. (Ed.) Urban Sprawl: Causes, Consequences and Policy Response, pp. 1-22. Washington, D.C: The Urban Land Institute.

Stabler, L. B., Martin, C. A., Brazel, A. J. (2005). Microclimates in a Desert City were Related to Land Use and Vegetation Index. Urban Forestry & Urban Greening, 3: 137–147

Stankowski, S. J. (1972). Population Density as an Indirect Indicator of Urban and Suburban Land-Surface Modifications. Professional Paper: Report 800B. (pp. B219-B224). U.S. Geological survey.

Stevermer, A. J. (2002). Recent Advances and Issues in Meteorology. Greenwood Press: Westport, CT.

Stone, B. Jr., & Rodgers, M. O. (2001). Urban Form and Thermal Efficiency: How the Design of Cities Can Influence the Urban Heat Island Effect. Journal of the American Planning Association, 67(2): 186-98.

Stone, B., & Norman, J. M. (2006). Land use Planning and Surface Heat Island Formation: A Parcel-Based Radiation Flux Approach. Atmospheric Environment, 40, 3561-3573.

Stone, B., Hess, J. J., & Frumkin, H. (2010). Urban Form and Extreme Heat Events: Are Sprawling Cities More Vulnerable to Climate Change Than Compact Cities? Environmental Health Perspectives, 118(10):1425-1428.

Streutker, D. R. (2002). A Remote Sensing Study of the Urban Heat Island of Houston, TX. American Geophysical Union, Fall Meeting 2001, Abstract #A12A-0050.

Emily Talen. (2005). Evaluating Good Urban Form in an Inner-City Neighborhood: An Empirical Application. Journal of Architectural and Planning Research, 22(3):204-228.

Tan, J., Zheng, Y., Tang, X., Guo, C., Li, L., Song, G., Zhen, X., Yuan, D., Kalkstein, A. J., Li, F., & Chen, H. (2010).The Urban Heat Island and Its Impact on Heat Waves and Human Health in Shanghai. Int. J. Biometeorology, 54:75–84.

Turner, M. G. R. V. O'Nell, R. H. Gardner, and B.T. Milne. (1989). Effects of Changing Spatial Scale on the Analysis of Landscape Configuration. Landscape Ecology. 3:153-162

Unwin, D. J. (1980). The Synoptic Climatology of Birmingham's Urban Heat Island, 1965-74. Weather. 35:43-50

U.S. Global change research program (2009).Global Climate Change Impact in the United States Southeast section pp. 111-116.

Vermont Forum on Sprawl (1999). Sprawl Defined. World Wide Web page http://www. vtsprawl.org/sprawldef.htm

Voogt, J.A., & Oke, T. R. (2003). Thermal Remote Sensing of Urban Climate. Remote Sensing of Environment, 86:370-384.

Vukovich, F. M. (1983). An Analysis of the Ground Temperature and Reflectivity Pattern about St. Louis, Missouri, using HDMM satellite data. Journal of Applied Meteorology, 22: 560-571.

Wan, Z., and Dozier, J. (1996). A Generalized Split-Window Algorithm for Retrieving Land-Surface Temperature from Space. IEEE Transactions on Geoscience and Remote Sensing, 34(4): 892-905.

Wei Ji, J. M., Rima WahabTwibell and Karen Underhil. (2006).Characterizing Urban Sprawl Using Multi-stage Remote Sensing Images and Landscape Metrics. Computers, Environment and Urban Systems, 30:861-879.

Weng, Q. (2001). A Remote Sensing-GIS Evaluation of Urban Expansion and Its Impact on Surface Temperature in the Zhujiang Delta, China. International Journal of Remote Sensing, 22 (10): 1999-2014.

Weng, Q. and Quattrochi, D. A. (2006). Thermal Remote Sensing of Urban Areas: An Introduction to the Special Issue, Remote Sensing of Environment, 104, 119-122.

Weng, Q., Lu, D., and Liang, B. (2006). Urban Surface Biophysical Descriptors and Land Surface Temperature Variations. Photogrammetric engineering & Remote Sensing. 72(11):1275-1286.

Wiens. J. A. (1989). Spatial Scaling in Ecology. Funct. Ecology. 3:385-397

Wu, J., Jemerette, G. D., Buyantuyev, A., and Redman, C. L. (2011). Quantifying spatiotemporal patterns of urbanization: The case of the two fastest growing metropolitan regions in the United States. Ecological Complexity, 8:1-8.

Wu, J., Buyantuyev, A., Jenerette, G. D., Litteral, J., Neil, K., and Shen, W. (2011). Ch.4 Quantifying Spatiotemporal Patterns and Ecological Effects of Urbanization: A Multiscale Landscape Approach. In: Richter, M. and Weiland, U. (Eds) Applied Urban Ecology: A Global Framework, pp. 35-53. Chichester, UK: John Wiley & Sons, Ltd.

Yoshida, T., Antake, T., & Wang. (2004). Measurement of thermal environment in Kyoto city and its prediction by CFD simulation. Energy & Buildings, 36(8): 771-779.

Yuan, F. and Bauer M. E. (2007). Comparison of impervious surface area and normalized difference vegetation index as indicators of surface urban heat island effect in Landsat imagery. Remote Sensing of Environment, 106: 375-386.

Sierra club: http://www.sierraclub.org/sprawl/report98/report.asp

Wan, Z. and Li, Z. (1997). A Physics-Based Algorithm for Retrieving Land-Surface Emissivity and Temperature from EOS/MODIS data. IEEE Transaction of Geoscience and remote sensing. 35(4):980-996

APPENDIX A

LEGEND OF NATIONAL LAND COVER DATABASE 2006

Table A.1. Land Cover Classification (Adopted from http://www.mrlc.gov/nlcd06_leg.php)

Class\ Value	Classification Description
Water	*Areas of open water or permanent ice/snow cover.*
11	**Open Water** - areas of open water, generally with less than 25% cover of vegetation or soil.
12	**Perennial Ice/Snow** - areas characterized by a perennial cover of ice and/or snow, generally greater than 25% of total cover.
Developed	*Areas characterized by a high percentage (30% or greater) of constructed materials (e.g. asphalt, concrete, buildings, etc.).*
21	**Developed, Open Space** - areas with a mixture of some constructed materials, but mostly vegetation in the form of lawn grasses. Impervious surfaces account for less than 20% of total cover. These areas most commonly include large-lot single-family housing units, parks, golf courses, and vegetation planted in developed settings for recreation, erosion control, or aesthetic purposes.
22	**Developed, Low Intensity** - areas with a mixture of constructed materials and vegetation. Impervious surfaces account for 20% to 49% percent of total cover. These areas most commonly include single-family housing units.
23	**Developed, Medium Intensity –** areas with a mixture of constructed materials and vegetation. Impervious surfaces account for 50% to 79% of the total cover. These areas most commonly include single-family housing units.
24	**Developed High Intensity** -highly developed areas where people reside or work in high numbers. Examples include apartment complexes, row houses and commercial/industrial. Impervious surfaces account for 80% to 100% of the total cover.
Barren	*Areas characterized by bare rock, gravel, sand, silt, clay, or other earthen material, with little or no "green" vegetation present regardless of its inherent ability to support life. Vegetation, if present, is more widely spaced and scrubby than that in the green vegetated categories; lichen cover may be extensive.*
31	**Barren Land (Rock/Sand/Clay)** - areas of bedrock, desert pavement, scarps, talus, slides, volcanic material, glacial debris, sand dunes, strip mines, gravel pits and other accumulations of earthen material. Generally, vegetation accounts for less than 15% of total cover.
Forest	*Areas characterized by tree cover (natural or semi-natural woody vegetation, generally greater than 6 meters tall); tree canopy accounts for 25% to 100% of the cover.*
41	**Deciduous Forest** - areas dominated by trees generally greater than 5 meters tall, and greater than 20% of total vegetation cover. More than 75% of the tree species shed foliage simultaneously in response to seasonal change.
42	**Evergreen Forest** - areas dominated by trees generally greater than 5 meters tall, and greater than 20% of total vegetation cover. More than 75% of the tree species maintain their leaves all year. Canopy is never without green foliage.

43	**Mixed Forest** - areas dominated by trees generally greater than 5 meters tall, and greater than 20% of total vegetation cover. Neither deciduous nor evergreen species are greater than 75% of total tree cover.
Shrubland	*Areas characterized by natural or semi-natural woody vegetation with aerial stems, generally less than 6 meters tall, with individuals or clumps not touching to interlocking. Both evergreen and deciduous species of true shrubs, young trees, and trees or shrubs that are small or stunted because of environmental conditions are included.*
51	**Dwarf Scrub** - Alaska only areas dominated by shrubs less than 20 centimeters tall with shrub canopy typically greater than 20% of total vegetation. This type is often co-associated with grasses, sedges, herbs, and non-vascular vegetation.
52	**Shrub/Scrub** - areas dominated by shrubs; less than 5 meters tall with shrub canopy typically greater than 20% of total vegetation. This class includes true shrubs, young trees in an early successional stage or trees stunted from environmental conditions.
Herbaceous	*Areas characterized by natural or semi-natural herbaceous vegetation; herbaceous vegetation accounts for 75% to 100% of the cover.*
71	**Grassland/Herbaceous** - areas dominated by gramanoid or herbaceous vegetation, generally greater than 80% of total vegetation. These areas are not subject to intensive management such as tilling, but can be utilized for grazing.
72	**Sedge/Herbaceous** - Alaska only areas dominated by sedges and forbs, generally greater than 80% of total vegetation. This type can occur with significant other grasses or other grass like plants, and includes sedge tundra, and sedge tussock tundra.
73	**Lichens** - Alaska only areas dominated by fruticose or foliose lichens generally greater than 80% of total vegetation
74	**Moss** - Alaska only areas dominated by mosses, generally greater than 80% of total vegetation.
Planted/Cultivated	*Areas characterized by herbaceous vegetation that has been planted or is intensively managed for the production of food, feed, or fiber; or is maintained in developed settings for specific purposes. Herbaceous vegetation accounts for 75% to 100% of the cover.*
81	**Pasture/Hay** – areas of grasses, legumes, or grass-legume mixtures planted for livestock grazing or the production of seed or hay crops, typically on a perennial cycle. Pasture/hay vegetation accounts for greater than 20% of total vegetation.
82	**Cultivated Crops** – areas used for the production of annual crops, such as corn, soybeans, vegetables, tobacco, and cotton, and also perennial woody crops such as orchards and vineyards. Crop vegetation accounts for greater than 20% of total vegetation. This class also includes all land being actively tilled.
Wetlands	*Areas where the soil or substrate is periodically saturated with or covered with water as defined by Cowardin et al., (1979).*
90	**Woody Wetlands** - areas where forest or shrubland vegetation accounts for greater than 20% of vegetative cover and the soil or substrate is periodically saturated with or covered with water.
95	**Emergent Herbaceous Wetlands** - Areas where perennial herbaceous vegetation accounts for greater than 80% of vegetative cover and the soil or substrate is periodically saturated with or covered with water.

APPENDIX B

DATA ANALYSIS USING IRLS APPROACH

Additional phase of data analysis includes a series of regression models using alternative robust regression approach. This phase also seeks test five hypotheses use of iteratively reweighted least square (IRLS). STATA[12] provides IRLS method to conduct robust regression. IRLS analysis begins by estimating OLS and then any observations so influential that they have Cook's D values greater than 1 (i.e. influential outliers) are excluded from sample after this first step. Based on OLS estimation, the residuals are examined and each observation is given a "weight" between 0 and 1 based on the size of its residual. Then, regression equation is re-estimated using weighted least square regression method based on Huber weights and Biweights. IRLS employs both weighting function because Huber weighting deals with severe outliers, whereas biweights sometimes fail to converge or have multiple solutions. These re-estimating processes are repeated (i.e. iterations) until the "weights" and parameter estimates change by amounts that are so small that the changes are no longer significant.

Although OLS is an efficient estimator given normally distributed residuals, it cannot retain efficiency when there are small violations of assumptions about the underlying population, e.g., an error term is not really a "normal distribution". Robust regression using IRLS is an alternative method to Least Square Regression. Treiman (2009,

[12] Statistical Analysis Package which is used in this study

p. 237) explains that when "we have no clear basis for modifying or omitting particular observations ... we need an alternative way of handling outliers ...One alternative is robust regression, which does not in general discard observations [although the approach we will use does discard very extreme outliers] but rather downweights them, giving less influence to highly idiosyncratic observations. Robust estimators are attractive because they are nearly as efficient as OLS estimators when the error distribution is normal and are much more efficient when the errors are heavy-tailed, as is typical with high leverage points and outliers."

Thus, each development pattern metric was modeled using IRLS approaches, controlling for the same set of other variables as already specified.

As mentioned earlier, IRLS works interactively: calculate case weights from absolute residuals, and regress again using those weights. In general, cases with large residuals are given low weights and the weight can be "0" when residuals are very large. To see which observation given weight as "0" and how they are located spatially, the calculated weights are joined to each metropolitan region in ArcGIS (See Fig C.1). The metropolitan regions that received a weight of "0" for at least one model are colored as yellow in the map. Most of them are located in west region in U.S. and they are considered as outliers in IRLS models. Although it is better to include all observations in the U.S. to explain overall patterns of UHIE, analysis excluding some unusual observations (pretended as outliers in IRLS model) allows to estimate general trends of UHIE in U.S.

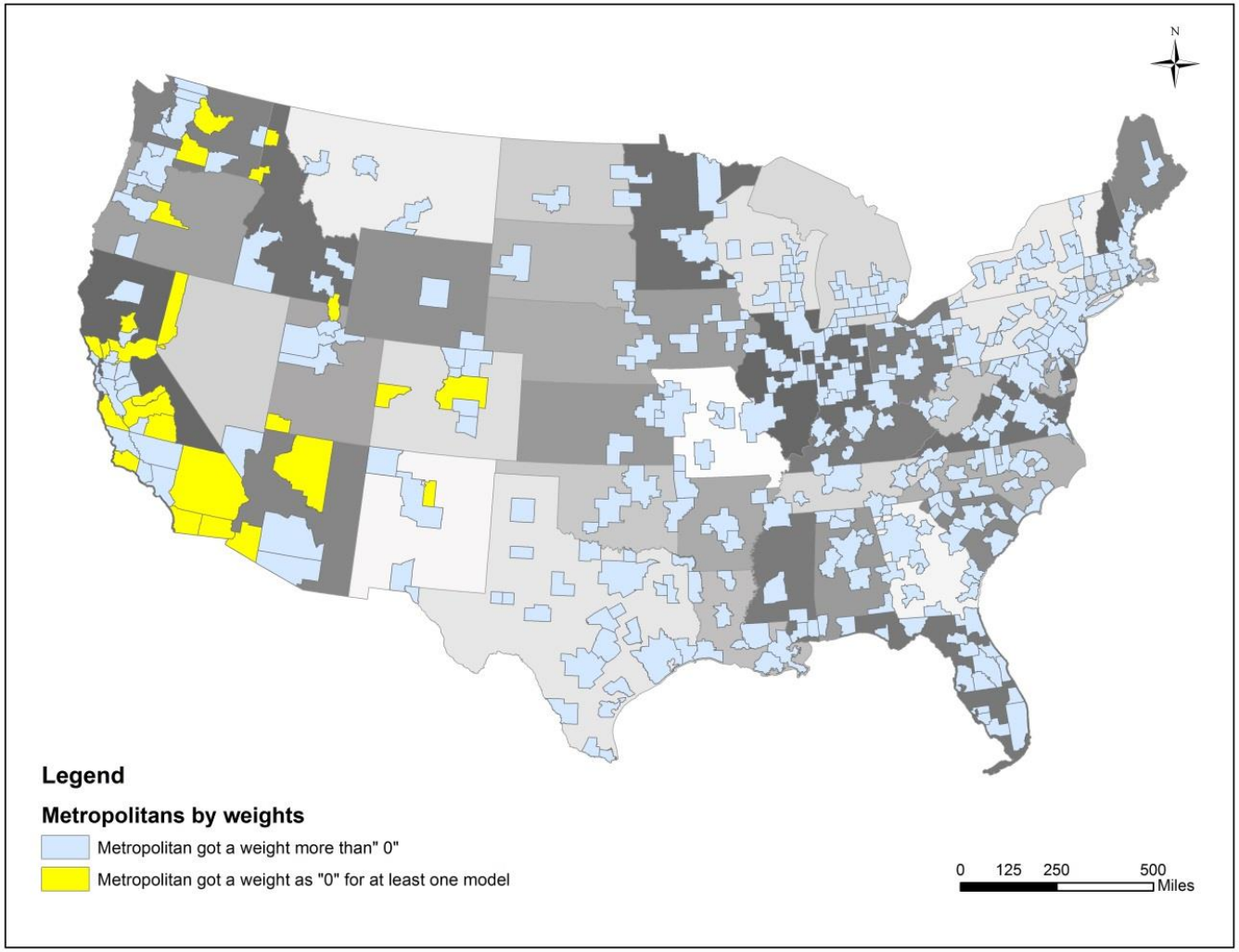

Figure B.1. Unusual observations detected from IRLS models (Weight = 0)

Table B.1. – B.5. Show comparisons of robust regression (OLS with robust standard error) and IRLS (Iteratively Reweighted Least Square) results.

When using the IRLS approach, most of the development pattern indexes affect both day and night UHIE. (See Table 5.4) For example, a non-clustering pattern of development has a positive, but non-significant effect on night UHIE in the robust regression model. In contrast, the non-clustering development turns out to be significant factor in the increase of night UHIE ($p < 0.01$) in the IRLS model. Except for density (day and night) and proximity (night), keep the same significance level in both models, all development indexes become more significant indicators to predict UHIE when using the IRLS models. Although the IRLS approach enhances the significance of the major independent variables (i.e. development patterns),

When some unusual observations in the western U.S. are controlled (Figure 5.8), each development pattern and control variables turned out to be more significant factors affecting UHIE. Development density is still a highly significant factor to increase UHIE, but their coefficients are reduced. Continuity of development becomes a more obvious factor to increase night UHIE in the IRLS models. The coefficient and significance of this indicator (i.e. continuity of development) are increased for the night UHIE. Non-clustering development patterns becomes a very significant factor that increases both day and night UHIE. Despite the limitations associated with the diversity index, it becomes a marginally significant factor impacting both day and night UHIE in the IRLS model. Proximity of land covers also turns out to be a more significant factor that increases daytime UHIE.

Table B.1. Density of development and UHIE

	Robust regression with robust standard error		Iteratively Reweighted Least Squared	
UHIE	Day	Night	Day	Night
Density	.0691*** (2.87)	0.0285*** (2.46)	.0443*** (2.59)	0.0261*** (3.24)
Impervious	**High value of VIF**			
Vegetation	-.0215 (-0.91)	-0.0290*** (-2.43)	-.0147 (-1.00)	-0.0105* (-1.52)
Water	-.2546** (-2.28)	0.0831† (1.19)	-.3246*** (-2.84)	0.0994** (1.85)
Population Density	.0002 (0.2)	0.0000 (0.01)	.0020*** (3.71)	0.0004* (1.45)
MWCF	-6.415*** (-4.56)	-2.5100** (-2.34)	-7.9770*** (-5.97)	-1.5467*** (-2.46)
MC	-12.2287*** (-5.74)	-4.2239*** (-3.45)	-17.7667*** (-19.63)	-4.1069*** (-9.66)
NAD	-12.1843*** (-6.53)	-2.1900** (-2.14)	-17.4893*** (-20.64)	-0.8539** (-2.15)
NF	-6.2908*** (-5.03)	-2.7178*** (-3.44)	-7.5301*** (-6.25)	-2.4333*** (-4.30)
GP	-11.2006*** (-8.78)	-2.5280*** (-3.41)	-12.1837*** (-16.29)	-2.2458*** (-6.39)
ETF	-7.2346*** (-6.17)	-2.4977*** (-3.4)	-8.4986*** (-12.25)	-2.0776*** (-6.38)
TWF	-6.4882*** (-4.74)	-4.6020*** (-5.33)	-8.1338*** (-4.14)	-4.0125*** (-4.35)
Constant	9.6116*** (5.04)	4.0499*** (3.9)	10.4845*** (9.00)	3.0773*** (5.63)
	Number of obs = 353 F(11, 341) = 11.68 Prob > F = 0.0000 R-squared = 0.3283	Number of obs = 353 F(11, 341) = 5.61 Prob > F = 0.0000 R-squared = 0.1907	Number of obs = 353 F(11, 341) = 56.99 Prob > F = 0.0000	Number of obs = 353 F(11, 341) = 17.90 Prob > F = 0.0000

***P< 0.01 **p<0.05 *p<0.1 †p<0.15

Table B.2. Continuity of development and UHIE

	Robust regression		IRLS	
UHIE	Day	Night	Day	Night
Continuity	1.0524** (1.78)	0.4319* (1.36)	0.8897** (2.07)	0.5347*** (2.63)
Impervious	0.0380* (1.63)	0.0137† (1.21)	0.0189† (1.04)	0.0104† (1.22)
Vegetation	-0.0229 (-0.97)	-0.0305*** (-2.57)	-0.0138 (-0.96)	-0.0108* (-1.60)
Water	-0.2556*** (2.40)	0.0842† (1.18)	-0.3214*** (-2.83)	0.0967** (1.81)
Population Density	0.0002 (0.21)	0.0000 (0.08)	0.0019*** (3.66)	0.0003* (1.37)
MWCF	-6.5490*** (-4.57)	-2.5751*** (-2.39)	-8.1986*** (-6.19)	-1.6196*** (-2.60)
MC	-12.1327*** (-5.68)	-4.2002*** (-3.41)	-17.6274*** (-19.63)	-4.0079*** (-9.46)
NAD	-12.2096*** (-6.48)	-2.2016** (-2.14)	-17.4981*** (-20.84)	-0.8712** (-2.20)
NF	-6.4566*** (-5.40)	-2.8028*** (-3.53)	-7.7802*** (-6.51)	-2.4980*** (-4.43)
GP	-11.3022*** (-8.61)	-2.5716*** (-3.45)	-12.4294*** (-16.70)	-2.2893*** (-6.52)
ETF	-7.3575*** (-6.14)	-2.5653*** (-3.45)	-8.7166*** (-12.61)	-2.1383*** (-6.56)
TWF	-6.7787*** (-4.62)	-4.7406*** (-5.71)	-8.4061*** (-4.31)	-4.1153*** (-4.48)
Constant	-93.5276* (-1.60)	-38.1920† (-1.22)	-76.6510** (-1.81)	-49.3250** (-2.47)
	Number of obs = 353 F(12, 340) = 10.23 Prob > F = 0.0000 R-squared = 0.3321	Number of obs = 353 F(12, 340) = 5.72 Prob > F = 0.0000 R-squared = 0.1919	Number of obs = 353 F(12, 340) = 53.03 Prob > F = 0.0000	Number of obs = 353 F(12, 340) = 16.51 Prob > F = 0.0000

***P< 0.01 **p<0.05 *p<0.1 †p<0.15

Table B.3. Non-clustering of development and UHIE

	Robust regression		IRLS	
UHIE	Day	Night	Day	Night
Non-Clustering	0.5531* (1.33)	0.2276 (0.86)	0.5447** (1.92)	0.3241*** (2.45)
Impervious	0.0517*** (2.36)	0.0193** (1.90)	0.0294** (1.80)	0.0170** (2.22)
Vegetation	-0.0269† (-1.16)	-0.0321*** (-2.80)	-0.0180† (-1.25)	-0.0142** (-2.11)
Water	-0.2929*** (-2.68)	0.0689 (0.97)	-0.3561*** (-3.10)	0.0764* (1.43)
Population Density	-0.0001 (-0.11)	-0.0001 (-0.13)	0.0016*** (2.98)	0.0001 (0.51)
MWCF	-6.4815*** (-4.55)	-2.5475*** (-2.36)	-8.1202*** (-6.11)	-1.4406** (-2.32)
MC	-12.0845*** (-5.61)	-4.1803*** (-3.38)	-17.6027*** (-19.47)	-3.8356*** (-9.10)
NAD	-12.1442*** (-6.47)	-2.1748** (-2.12)	-17.6638*** (-20.95)	-0.7848** (-2.00)
NF	-6.3557*** (-5.07)	-2.7614*** (-3.49)	-7.6818*** (-6.40)	-2.3604*** (-4.22)
GP	-11.2005*** (-8.7)	-2.5300*** (-3.40)	-12.3504*** (-16.57)	-2.1384*** (-6.15)
ETF	-7.3783*** (-6.26)	-2.5741*** (-3.46)	-8.7293*** (-12.53)	-2.0619*** (-6.35)
TWF	-7.1416*** (-5.18)	-4.8902*** (-5.38)	-8.7937*** (-4.44)	-4.2606*** (-4.61)
Constant	6.3522* (1.82)	2.7982* (1.35)	7.2683*** (3.33)	1.0948† (1.08)
	Number of obs = 353 F(12, 340) = 10.70 Prob > F = 0.0000 R-squared = 0.3302	Number of obs = 353 F(12, 340) = 5.02 Prob > F = 0.0000 R-squared = 0.1905	Number of obs = 353 F(12, 340) = 16.51 Prob > F = 0.0000	Number of obs = 353 F(12, 340) = 15.96 Prob > F = 0.0000

***P< 0.01 **p<0.05 *p<0.1 †p<0.15

Table B.4. Diversity of land covers and UHIE

	Robust regression		IRLS	
UHIE	Day	Night	Day	Night
Diversity	-3.4378 (-0.98)	-2.2247† (-1.05)	-3.6885* (-1.53)	-1.6648* (-1.48)
Impervious	0.0609*** (2.72)	0.0232** (2.21)	0.0378*** (2.39)	0.0219*** (2.95)
Vegetation	-0.0265† (-1.13)	-0.0323*** (-2.78)	-0.0199* (-1.37)	-0.0138** (-2.04)
Water	-0.2850*** (-2.55)	0.0673 (0.95)	-0.3495*** (-3.02)	0.0867* (1.60)
Population Density	0.0001 (0.14)	0.0000 (-0.03)	0.0019*** (3.52)	0.0003† (1.27)
MWCF	-6.5005*** (-4.51)	-2.5680*** (-2.37)	-8.0510*** (-6.02)	-1.4919*** (-2.38)
MC	-12.2870*** (-5.73)	-4.2822*** (-3.49)	-17.8324*** (-19.62)	-4.1001*** (-9.62)
NAD	-12.2047*** (-6.49)	-2.2135** (-2.16)	-17.6639*** (-20.80)	-0.8501** (-2.14)
NF	-6.2689*** (-5.04)	-2.7176*** (-3.42)	-7.5034*** (-6.22)	-2.4119*** (-4.26)
GP	-11.1999*** (-8.69)	-2.5479*** (-3.45)	-12.2779*** (-16.35)	-2.2232*** (-6.32)
ETF	-7.3637*** (-6.24)	-2.6010*** (-3.54)	-8.6532*** (-12.30)	-2.1242*** (-6.44)
TWF	-6.7927*** (-4.76)	-4.8096*** (-5.62)	-8.4650*** (-4.28)	-4.1422*** (-4.47)
Constant	10.5265*** (5.46)	4.6432*** (4.43)	11.3934*** (9.56)	3.5433*** (6.34)
	Number of obs = 353 F(12, 340) = 10.55 Prob > F = 0.0000 R-squared = 0.3286	Number of obs = 353 F(12, 340) = 5.08 Prob > F = 0.0000 R-squared = 0.1914	Number of obs = 353 F(12, 340) = 52.97 Prob > F = 0.0000	Number of obs = 353 F(12, 340) = 16.26 Prob > F = 0.0000

***P<0.01 **p<0.05 *p<0.1 †p<0.15

Table B.5. Proximity of land covers and UHIE

	Robust regression		IRLS	
UHIE	Day	Night	Day	Night
Proximity	-0.0467† (-1.22)	0.0021 (0.10)	-0.0528** (-1.87)	0.0014 (0.11)
Impervious	0.0507** (2.17)	0.0234** (2.26)	0.0271* (1.60)	0.0219*** (2.74)
Vegetation	-0.0200 (-0.84)	-0.0316*** (-2.61)	-0.0123 (-0.83)	-0.0131** (-1.88)
Water	-0.2247** (-1.98)	0.0788† (1.06)	-0.2886*** (-2.46)	0.0973** (1.75)
Population Density	0.0002 (0.28)	0.0001 (0.14)	0.0019*** (3.68)	0.0004* (1.59)
MWCF	-6.3996*** (-4.39)	-2.5352** (-2.34)	-7.9891*** (-5.97)	-1.6072*** (-2.54)
MC	-12.3485*** (-5.77)	-4.2249*** (-3.44)	-17.8224*** (-19.54)	-4.1542*** (-9.62)
NAD	-12.4672*** (-6.43)	-2.1612** (-2.02)	-18.1013*** (-20.79)	-0.8291** (-2.01)
NF	-6.2461*** (-4.96)	-2.7424*** (-3.48)	-7.5532*** (-6.25)	-2.4758*** (-4.33)
GP	-11.2848*** (-8.64)	-2.4907*** (-3.33)	-12.4150*** (-16.42)	-2.2370*** (-6.25)
ETF	-7.3015*** (-6.1)	-2.5070*** (-3.38)	-8.6653*** (-12.40)	-2.1065*** (-6.37)
TWF	-6.8362*** (-4.72)	-4.6228*** (-5.31)	-8.5694*** (-4.33)	-4.0615*** (-4.34)
Constant	13.0502*** (4.06)	4.1586*** (2.39)	14.3659*** (6.64)	3.2257*** (3.15)
	Number of obs = 353 F(12, 340) = 10.55 Prob > F = 0.0000 R-squared = 0.3293	Number of obs = 353 F(12, 340) = 5.08 Prob > F = 0.0000 R-squared = 0.1879	Number of obs = 353 F(12, 340) = 53.05 Prob > F = 0.0000	Number of obs = 353 F(12, 340) = 16.26 Prob > F = 0.0000

Most of control variables do not change when compared to the results of robust regression models, except population density and water. Population density is not significant in the robust model but it seems to be a significant factor to increase day UHIE,

even though its effect is very small. Water becomes a more significant factor, but still shows a different sign for day UHIE and night UHIE.

APPENDIX C

RESULT OF DIVERSITY INDEX MODEL USING FIRST ORDER OF NLCD SCHEME

Table C.1. Result of diversity index model

UHIE	Day				Night			
	Coefficient (Robust Std. Error)	P-value (One-tailed)	95% confidence Interval		Coefficient (Robust Std. Error)	P-value (One-tailed)	95% confidence Interval	
Diversity	-0.7118 (2.3911)	0.38	-5.4151	3.9915	-0.8697 (1.2873)	0.25	-3.4018	1.6624
Impervious	0.0607 (0.0224)	0.00	0.0166	0.1047	0.0232 (0.0106)	0.01	0.0024	0.0440
Vegetation	-0.0256 (0.0235)	0.14	-0.0718	0.0207	-0.0320 (0.0116)	0.00	-0.0548	-0.0091
Water	-0.2721 (0.1136)	0.01	-0.4955	-0.0486	0.0714 (0.0712)	0.16	-0.0687	0.2114
Population Density	0.0002 (0.0008)	0.41	-0.0014	0.0018	0.0000 (0.0005)	0.50	-0.0009	0.0010
MWCF	-6.4696 (1.4277)	0.00	-9.2779	-3.6614	-2.5613 (1.0830)	0.01	-4.6915	-0.4311
MC	-12.2217 (2.1443)	0.00	-16.4395	-8.0040	-4.2479 (1.2306)	0.00	-6.6684	-1.8273
NAD	-12.1507 (1.8771)	0.00	-15.8430	-8.4585	-2.1815 (1.0226)	0.02	-4.1929	-0.1700
NF	-6.2977 (1.2496)	0.00	-8.7556	-3.8399	-2.7330 (0.7920)	0.00	-4.2909	-1.1751
GP	-11.1445 (1.2904)	0.00	-13.6826	-8.6065	-2.5247 (0.7382)	0.00	-3.9767	-1.0727
ETF	-7.2721 (1.1834)	0.00	-9.5998	-4.9443	-2.5695 (0.7348)	0.00	-4.0147	-1.1242
TWF	-6.6110 (1.4345)	0.00	-9.4326	-3.7894	-4.7413 (0.8566)	0.00	-6.4262	-3.0564
Constant	10.1678 (1.9435)	0.00	6.3450	13.9905	4.5151 (1.0385)	0.00	2.4724	6.5578
	Number of obs = 353		F(12, 340) = 10.63		Number of obs = 353		F(11, 341) = 5.06	
	R-squared = 0.3269		Prob > F = 0.0000		R-squared = 0.1893		Prob > F = 0.0000	

* All significance tests are one tailed because the hypotheses of this study clearly indicated the direction of effect for the independent and control variables

APPENDIX D

INTERCORRELATION MATRIX

	Variables	1	2	3	4	5	6	7	8	9	10	11	12	13	14	15	16	17	18	19
1	d_uhi	1.00																		
2	n_uhi	0.56*	1.00																	
3	density	0.09*	0.25*	1.00																
4	continuity	0.11*	0.22*	0.69*	1.00															
5	proximity	0.00	-0.13*	-0.64*	-0.42*	1.00														
6	clustering	0.09*	0.15*	0.49*	0.73*	-0.34*	1.00													
7	diversity	-0.01	-0.02	-0.01	-0.26*	0.08	-0.66*	1.00												
8	Impervious	0.10*	0.25*	0.99*	0.69*	-0.61*	0.49*	-0.01	1.00											
9	Vegetation	-0.15*	-0.25*	-0.56*	-0.42*	0.41*	-0.26*	-0.01	-0.54*	1.00										
10	Water	0.06	0.07	-0.04	-0.02	0.22*	0.10*	-0.11*	-0.02	-0.09*	1.00									
11	Population	-0.05	0.09	0.65*	0.45*	-0.47*	0.46*	-0.11*	0.64*	-0.32*	-0.18*	1.00								
12	mwcf	0.04	-0.01	-0.01	-0.01	0.07	-0.02	0.03	0.00	0.06	0.00	0.01	1.00							
13	nfm	0.43*	0.29*	0.15*	0.06	-0.01	0.01	0.11*	0.16*	-0.08	0.00	0.06	-0.03	1.00						
14	mc	-0.17*	-0.16*	0.21*	0.07	-0.17*	0.05	-0.03	0.20*	-0.11*	-0.18*	0.45*	-0.03	-0.06	1.00					
15	nad	-0.20*	0.05	0.20*	0.12*	-0.30*	0.07	0.03	0.20*	0.08	-0.19*	0.27*	-0.03	-0.06	-0.07	1.00				
16	nf	0.03	-0.03	-0.08	-0.05	0.14*	-0.05	0.09*	-0.07	0.08	0.15*	-0.07	-0.02	-0.03	-0.04	-0.04	1.00			
17	gp	-0.20*	0.05	0.28*	0.25*	-0.22*	0.11*	0.05	0.27*	-0.10*	-0.11*	0.17*	-0.05	-0.09	-0.10*	-0.11*	-0.06	1.00		
18	etf	0.13*	-0.09*	-0.47*	-0.30*	0.37*	-0.15*	-0.11*	-0.46*	0.11*	0.22*	-0.52*	-0.16*	-0.29*	-0.34*	-0.38*	-0.19*	-0.54*	1.00	
19	twf	0.04	-0.04	0.06	0.07	-0.09	0.17*	-0.08	0.07	-0.12*	0.09*	0.07	-0.01	-0.02	-0.02	-0.02	-0.01	-0.03	-0.10*	1.00

*** P < 0**

APPENDIX E

RESULT OF FULL REGRESSION MODELS FOR ALL INDEPENDENT VARIABLES

Table E.1. Full regression model for Day UHIE

	Coefficient (Robust Std. Error)	P-value (one-tailed)	95% confidence Interval		VIF
Density	0.1115 (0.1611)	0.24	-0.2054	0.4283	93.27
Continuity	1.0166 (0.7727)	0.09	-0.5033	2.5366	3.8
Clustering	-0.0502 (0.6924)	0.47	-1.4123	1.3118	5.8
Diversity	-1.2496 (4.8991)	0.40	-10.8863	8.3871	2.67
Proximity	-0.0380 (0.0404)	0.17	-0.1175	0.0414	2.15
Impervious	-0.0698 (0.1470)	0.32	-0.3589	0.2194	85.18
Vegetation	-0.0151 (0.0247)	0.27	-0.0636	0.0335	1.72
Water	-0.2092 (0.1124)	0.03	-0.4302	0.0119	1.30
Population density	0.0001 (0.0009)	0.47	-0.0016	0.0018	2.79
MWCF	-6.4935 (1.4469)	0.00	-9.3397	-3.6473	1.31
MC	-12.3548 (2.1468)	0.00	-16.5777	-8.1318	2.65
NAD	-12.5554 (1.9610)	0.00	-16.4128	-8.6979	2.74
NF	-6.4016 (1.2848)	0.00	-8.9288	-3.8744	1.49
GP	-11.5791 (1.3279)	0.00	-14.1912	-8.9670	3.68
ETF	-7.5055 (1.1946)	0.00	-9.8553	-5.1556	6.01
TWF	-7.0437 (1.5150)	0.00	-10.0237	-4.0637	1.19
Constant	-87.4159 (73.4386)	0.12	-231.8732	57.0414	MEAN VIF=13.61
				Number of obs = 353	
				F(16, 336) = 7.96	
				Prob > F = 0.0000	
				R-squared = 0.3361	

Table E.2. Full regression model for Night UHIE

	Coefficient (Robust Std. Error)	P-value (one-tailed)	95% confidence Interval		VIF
Density	0.1479 (0.0848)	0.04	-0.0188	0.3146	93.27
Continuity	0.4348 (0.4171)	0.15	-0.3857	1.2553	3.8
Clustering	-0.2176 (0.4694)	0.32	-1.1409	0.7057	5.8
Diversity	-2.8098 (3.0227)	0.18	-8.7556	3.1360	2.67
Proximity	0.0153 (0.0221)	0.24	-0.0282	0.0588	2.15
Impervious	-0.1141 (0.0772)	0.07	-0.2660	0.0378	85.18
Vegetation	-0.0271 (0.0140)	0.03	-0.0546	0.0004	1.72
Water	0.0911 (0.0774)	0.12	-0.0611	0.2433	1.30
Population density	0.0000 (0.0006)	0.49	-0.0012	0.0011	2.79
MWCF	-2.5811 (1.0512)	0.01	-4.6488	-0.5133	1.31
MC	-4.3536 (1.2291)	0.00	-6.7713	-1.9360	2.65
NAD	-2.2312 (1.0703)	0.02	-4.3364	-0.1260	2.74
NF	-2.7917 (0.8224)	0.00	-4.4094	-1.1741	1.49
GP	-2.7238 (0.7671)	0.00	-4.2328	-1.2149	3.68
ETF	-2.6634 (0.7387)	0.00	-4.1164	-1.2103	6.01
TWF	-4.5880 (0.9350)	0.00	-6.4272	-2.7488	1.19
Constant	-38.1715 (39.1935)	0.17	-115.2671	38.9241	MEAN VIF=13.61

Number of obs = 353
F(16, 336) = 4.47
Prob > F = 0.0000
R-squared = 0.2024

APPENDIX F

VALIDITY TESTS FOR VARIABLES

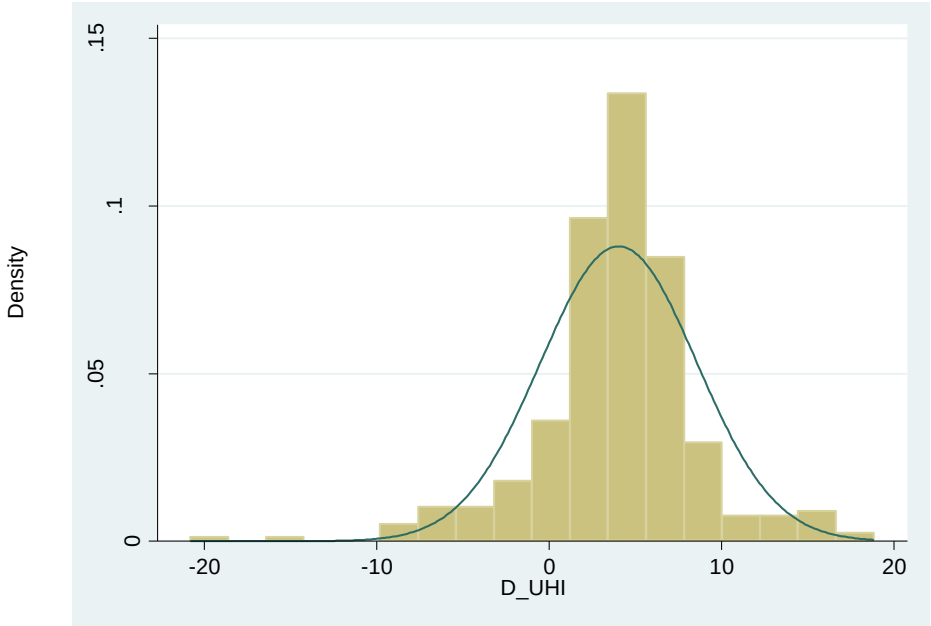

Figure F.1. Normality for dependent variable (Day UHIE)

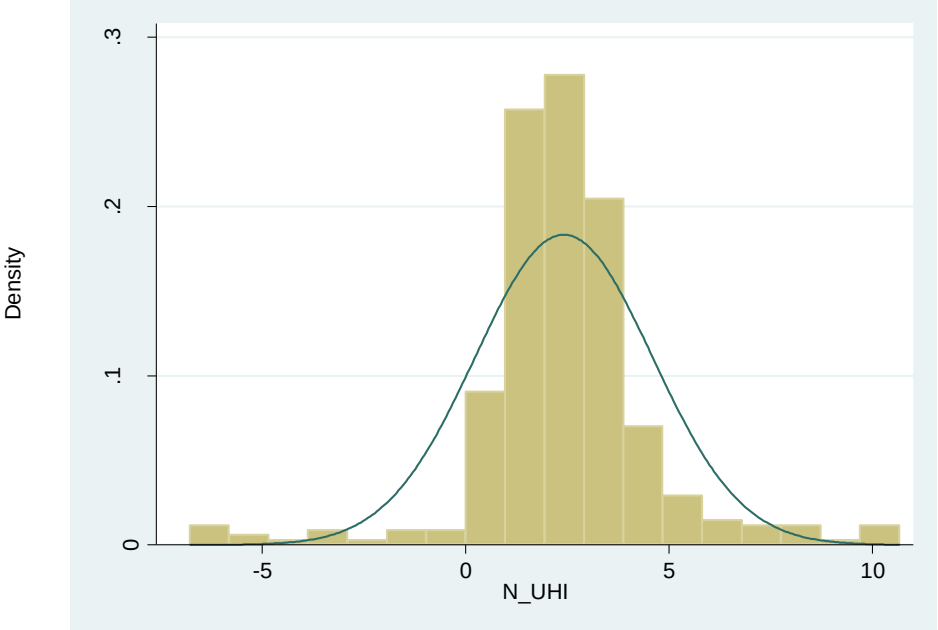

Figure F.2. Normality for dependent variable (Night UHIE)

Table F.1. Heteroskadasticity test: White test

	Day UHIE	Night UHIE
Density Model	chi2(57) = 148.22 Prob > chi2 = 0.0000	chi2(57) = 145.73 Prob > chi2 = 0.0000
Continuity Model	chi2(57) = 141.93 Prob > chi2 = 0.0000	chi2(57) = 135.74 Prob > chi2 = 0.0000
Clustering Model	chi2(57) = 149.79 Prob > chi2 = 0.0000	chi2(57) = 136.08 Prob > chi2 = 0.0000
Diversity Model	chi2(57) = 156.34 Prob > chi2 = 0.0000	chi2(57) = 138.53 Prob > chi2 = 0.0000
Proximity Model	chi2(57) = 143.37 Prob > chi2 = 0.0000	chi2(57) = 145.44 Prob > chi2 = 0.0000
Model 1	chi2(108) = 200.90 Prob > chi2 = 0.0000	chi2(108) = 175.49 Prob > chi2 = 0.0000
Model 2	chi2(94) = 186.51 Prob > chi2 = 0.0000	chi2(94) = 166.66 Prob > chi2 = 0.0000
Model 3	chi2(81) = 175.89 Prob > chi2 = 0.0000	chi2(81) = 152.36 Prob > chi2 = 0.0000

* White's test for Ho: homoskedasticity against Ha: unrestricted heteroskedasticity

APPENDIX G

TEST DIFFERENCES AMONG ECOREGIONS

- Day UHIE (H0: Ecoregion A = Ecoregion B, for example H0: MWCF=MC)
- Gray colored cell means that two ecoregions have statistically same effect in regression model since they cannot reject null hypothesis.

Table G.1. Test results of differences of day UHIE among ecoregion

	MWCF[13]	MC	NAD	NF	GP	ETF
MC	F(1, 336) = 8.14 Prob > F = 0.0046					
NAD	F(1, 336) = 11.08 Prob > F = 0.0010	F(1, 336) = 0.01 Prob > F = 0.9291				
NF	F(1, 336) = 0.01 Prob > F = 0.9280	F(1, 336) = 8.69 Prob > F = 0.0034	F(1, 336) = 12.15 Prob > F = 0.0006			
GP	F(1, 336) = 21.42 Prob > F = 0.0000	F(1, 336) = 0.17 Prob > F = 0.6841	F(1, 336) = 0.36 Prob > F = 0.5502	F(1, 336) = 32.27 Prob > F = 0.0000		
ETF	F(1, 336) = 1.28 Prob > F = 0.2590	F(1, 336) = 6.36 Prob > F = 0.0121	F(1, 336) = 10.00 Prob > F = 0.0017	F(1, 336) = 3.42 Prob > F = 0.0651	F(1, 336) = 36.45 Prob > F = 0.0000	
TWF	F(1, 336) = 0.15 Prob > F = 0.6959	F(1, 336) = 6.47 Prob > F = 0.0114	F(1, 336) = 9.84 Prob > F = 0.0019	F(1, 336) = 0.26 Prob > F = 0.6082	F(1, 336) = 13.74 Prob > F = 0.0002	F(1, 336) = 0.19 Prob > F = 0.6640

Day Ecoregion 1: MWCF=NF=ETF=TWF

Day Ecoregion 2: MC=NAD=GP

Day Ecoregion 3: NFM (Base region)

[13] MWCF: Marine West Coast Forest / NAD: North American Desert / NF: Northern Forests/ GP: Great Plains/ ETF: Eastern Temperate Forests/ TWF: Tropical Wet Forests (Also, see the map of the ecoregion in page 5)

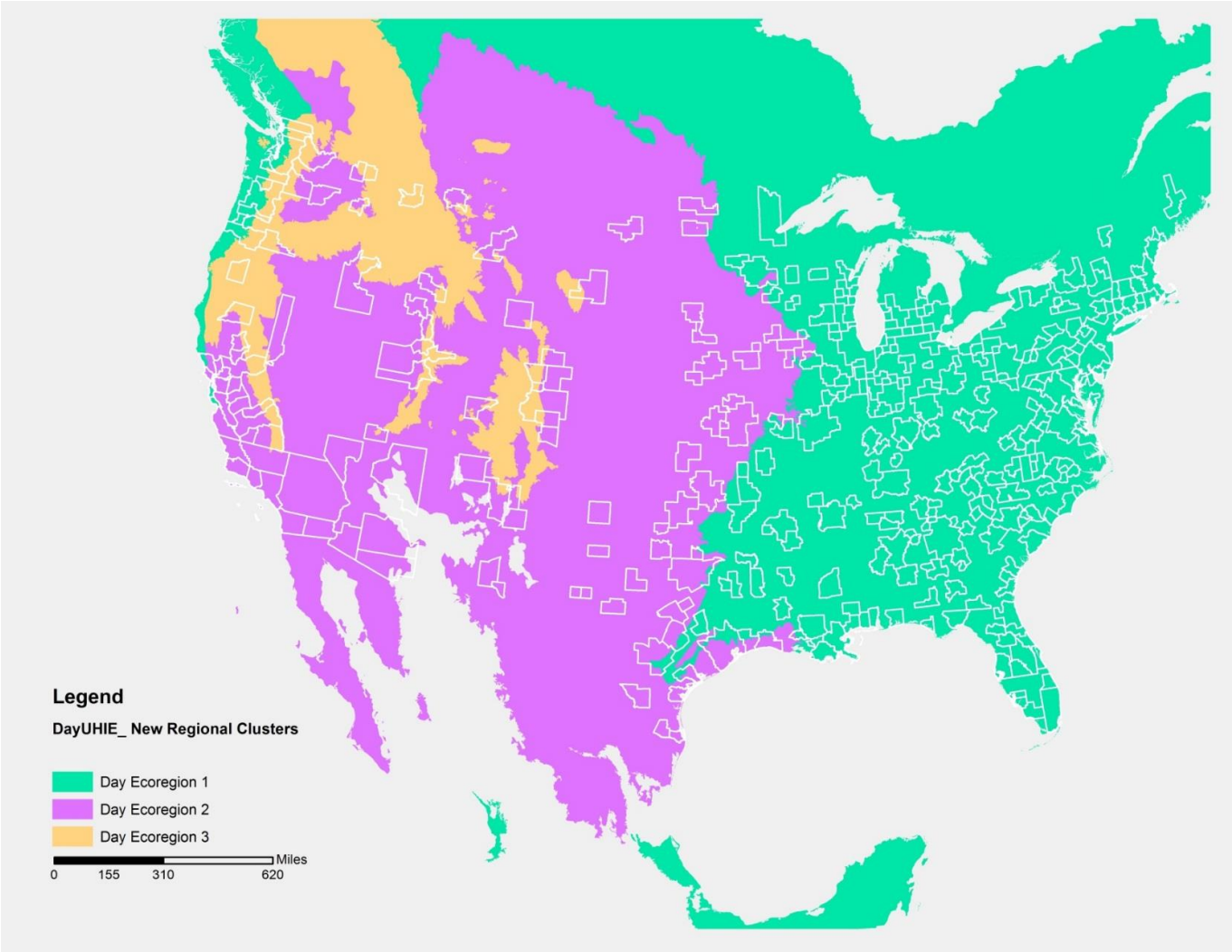

Figure G.1. New Group of Ecoregions by Day UHIE

Full model with level I ecoregion as dummies (base region = Northwestern Forested Mountains)

Linear regression

Number of obs	353
F(16, 336)	7.96
Prob > F	0.0000
R-squared	0.3361
Root MSE	3.7818

d_uhi	Coef.	Robust Std. Err.	t	P>|t|	[95% Conf.	Interval]
density	.1114646	.1610839	0.69	0.489	-.2053954	.4283246
continuity	1.016648	.7727159	1.32	0.189	-.5033226	2.536618
clustering	-.0502158	.6924325	-0.07	0.942	-1.412265	1.311833
diversity	-1.249575	4.899055	-0.26	0.799	-10.88626	8.387108
proximity	-.0380337	.0404005	-0.94	0.347	-.1175036	.0414361
pct_d_developed	-.0697557	.1469983	-0.47	0.635	-.3589087	.2193973
pct_d_vege	-.0150726	.0246949	-0.61	0.542	-.0636488	.0335035
pct_d_water	-.2091968	.1123757	-1.86	0.064	-.4302453	.0118517
d_popden_km	.0000729	.000857	0.09	0.932	-.0016128	.0017587
mwcf	-6.4935	1.44692	-4.49	0.000	-9.339662	-3.647338
mc	-12.35476	2.146833	-5.75	0.000	-16.57768	-8.131829
nad	-12.55536	1.961031	-6.40	0.000	-16.41281	-8.697918
nf	-6.401594	1.284754	-4.98	0.000	-8.928769	-3.874419
gp	-11.5791	1.32794	-8.72	0.000	-14.19122	-8.966973
etf	-7.505455	1.194604	-6.28	0.000	-9.8553	-5.155611
twf	-7.043686	1.514957	-4.65	0.000	-10.02368	-4.063692
_cons	-87.41592	73.43858	-1.19	0.235	-231.8732	57.04139

Full model with new common ecoregions as dummies (base region = Day Ecoregion 3 (NFM))

Linear regression

Number of obs	353
F(11, 341)	9.92
Prob > F	0.0000
R-squared	0.3320
Root MSE	3.7655

d_uhi	Coef.	Robust Std. Err.	t	P>|t|	[95% Conf.	Interval]
density	.1247889	.1670805	0.75	0.456	-.2038493	.453427
continuity	1.047756	.7652572	1.37	0.172	-.4574626	2.552975
clustering	.0551152	.6963204	0.08	0.937	-1.314509	1.424739
diversity	-.292071	5.127369	-0.06	0.955	-10.37732	9.793182
proximity	-.0292323	.0405176	-0.72	0.471	-.1089283	.0504637
pct_d_developed	-.0806327	.1513156	-0.53	0.594	-.3782621	.2169967
pct_d_vege	-.0160031	.0247131	-0.65	0.518	-.0646125	.0326063
pct_d_water	-.1835848	.111052	-1.65	0.099	-.402018	.0348484
d_popden_km	-.0001375	.0008505	-0.16	0.872	-.0018104	.0015354
day_eco1	-7.459696	1.174452	-6.35	0.000	-9.769779	-5.149613
day_eco2	-11.91398	1.321243	-9.02	0.000	-14.51279	-9.315164
_cons	-91.8988	72.79501	-1.26	0.208	-235.0826	51.28499

- Night UHIE (H0: Ecoregion A = Ecoregion B, for example H0: MWCF=MC)
- Gray colored cell means that two ecoregions have statistically same effect in regression model since they cannot reject null hypothesis.

Table G.2. Test results of differences of night UHIE among ecoregion

	MWCF[14]	MC	NAD	NF	GP	ETF
MC	F(1, 336) = 1.79 Prob > F = 0.1814					
NAD	F(1, 336) = 0.09 Prob > F = 0.7633	F(1, 336) = 2.69 Prob > F = 0.1018				
NF	F(1, 336) = 0.06 Prob > F = 0.8041	F(1, 336) = 1.85 Prob > F = 0.1747	F(1, 336) = 0.37 Prob > F = 0.5443			
GP	F(1, 336) = 0.03 Prob > F = 0.8642	F(1, 336) = 2.41 Prob > F = 0.1211	F(1, 336) = 0.37 Prob > F = 0.5431	F(1, 336) = 0.02 Prob > F = 0.8833		
ETF	F(1, 336) = 0.01 Prob > F = 0.9174	F(1, 336) = 2.46 Prob > F = 0.1176	F(1, 336) = 0.29 Prob > F = 0.5928	F(1, 336) = 0.12 Prob > F = 0.7291	F(1, 336) = 0.04 Prob > F = 0.8377	
TWF	F(1, 336) = 3.90 Prob > F = 0.0490	F(1, 336) = 0.04 Prob > F = 0.8450	F(1, 336) = 5.65 Prob > F = 0.0180	F(1, 336) = 5.97 Prob > F = 0.0151	F(1, 336) = 6.88 Prob > F = 0.0091	F(1, 336) = 9.57 Prob > F = 0.0021

Night Ecoregion 1: MWCF=NAD=NF=GP=ETF

Night Ecoregion 2: TWF=MC (Actually, MC looks like same as all other regions but I decided MC is more similar to TWF than Night Ecoregion 1 group based on its F-value and significance)

Night Ecoregion 3: NFM (Base region)

[14] MWCF: Marine West Coast Forest / NAD: North American Desert / NF: Northern Forests/ GP: Great Plains/ ETF: Eastern Temperate Forests/ TWF: Tropical Wet Forests/ NFM: Northeastern Forested Mountains/ MC: Mediterranean California (Also, see the map of the ecoregion in page 35)

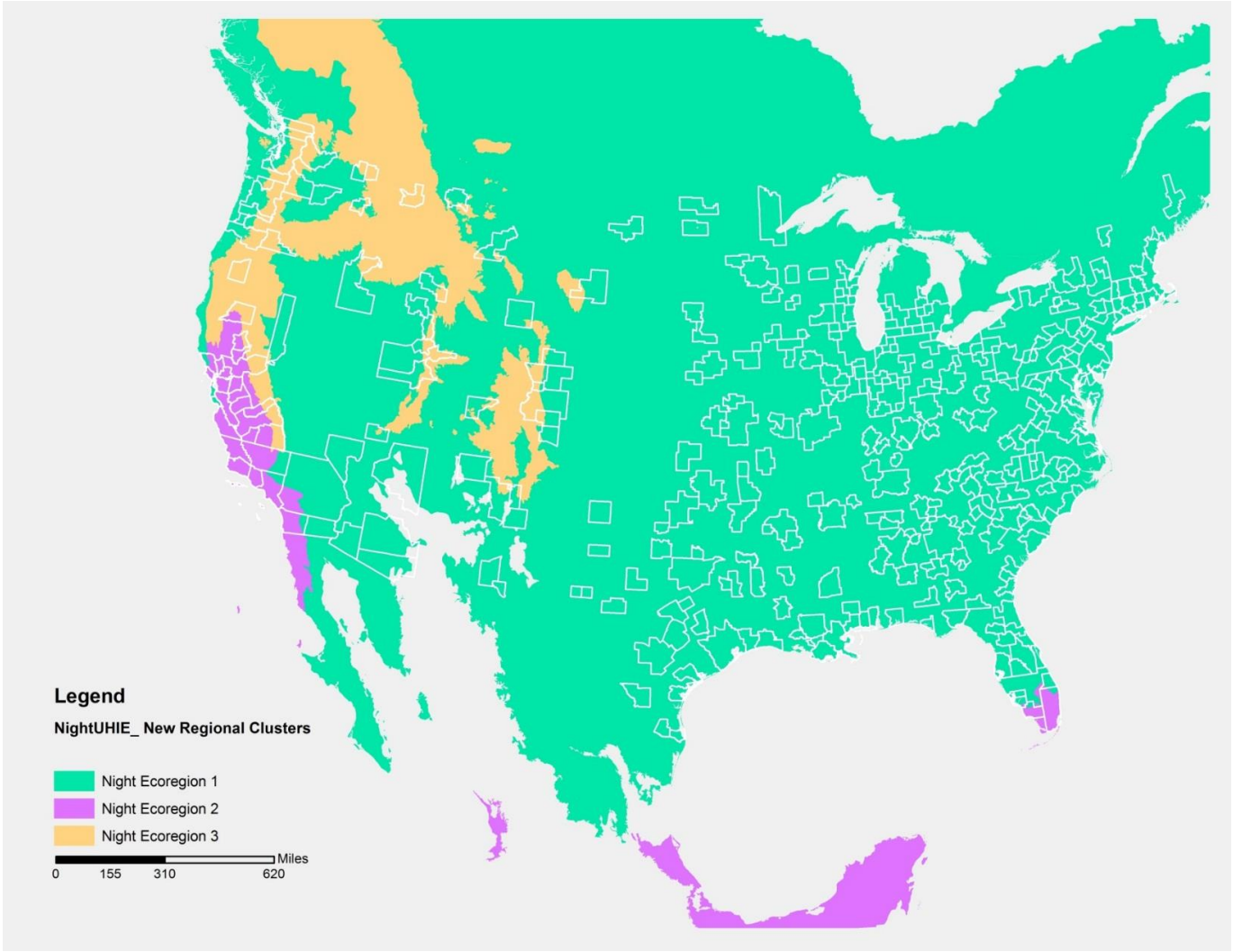

Figure G.2. New Group of Ecoregions by Night UHIE

Full model with level I ecoregion as dummies (base region = Northwestern Forested Mountains)

```
Linear regression                               Number of obs =     353
                                                F( 16,   336) =    4.47
                                                Prob > F      =  0.0000
                                                R-squared     =  0.2024
                                                Root MSE      =  1.9896
```

n_uhi	Coef.	Robust Std. Err.	t	P>|t|	[95% Conf.	Interval]
density	.1478953	.0847626	1.74	0.082	-.018837	.3146276
continuity	.4348314	.4171238	1.04	0.298	-.3856718	1.255335
clustering	-.2175841	.4693708	-0.46	0.643	-1.14086	.7056915
diversity	-2.809807	3.022705	-0.93	0.353	-8.755617	3.136004
proximity	.0153165	.0221047	0.69	0.489	-.0281645	.0587974
pct_d_developed	-.1141007	.0772405	-1.48	0.141	-.2660367	.0378353
pct_d_vege	-.027108	.0139853	-1.94	0.053	-.0546178	.0004019
pct_d_water	.0910947	.0773574	1.18	0.240	-.0610711	.2432605
d_popden_km	-.0000221	.0005846	-0.04	0.970	-.0011721	.0011279
mwcf	-2.581076	1.051203	-2.46	0.015	-4.648845	-.5133075
mc	-4.353643	1.229096	-3.54	0.000	-6.771336	-1.93595
nad	-2.231197	1.070254	-2.08	0.038	-4.336441	-.1259539
nf	-2.791735	.8223576	-3.39	0.001	-4.409354	-1.174117
gp	-2.723845	.7671363	-3.55	0.000	-4.23284	-1.21485
etf	-2.663383	.7387018	-3.61	0.000	-4.116446	-1.21032
twf	-4.587973	.9350086	-4.91	0.000	-6.427181	-2.748765
_cons	-38.17148	39.19352	-0.97	0.331	-115.2671	38.92411

Full model with new common ecoregions as dummies (base region = Day Ecoregion 3 (NFM))

```
Linear regression                               Number of obs =     353
                                                F( 11,   341) =    5.78
                                                Prob > F      =  0.0000
                                                R-squared     =  0.1999
                                                Root MSE      =   1.978
```

n_uhi	Coef.	Robust Std. Err.	t	P>|t|	[95% Conf.	Interval]
density	.1398568	.0843693	1.66	0.098	-.0260929	.3058065
continuity	.4453503	.39589	1.12	0.261	-.3333437	1.224044
clustering	-.2587165	.4370095	-0.59	0.554	-1.11829	.6008572
diversity	-2.944266	2.940739	-1.00	0.317	-8.728539	2.840007
proximity	.0105351	.0214465	0.49	0.624	-.0316491	.0527193
pct_d_developed	-.1064602	.0775482	-1.37	0.171	-.2589933	.046073
pct_d_vege	-.024871	.0137101	-1.81	0.071	-.0518381	.002096
pct_d_water	.0820639	.0754315	1.09	0.277	-.0663057	.2304334
d_popden_km	.0000842	.0005811	0.14	0.885	-.0010588	.0012272
night_eco1	-2.625848	.7341791	-3.58	0.000	-4.069938	-1.181758
night_eco2	-4.445666	1.13583	-3.91	0.000	-6.67978	-2.211551
_cons	-38.71684	37.16504	-1.04	0.298	-111.8184	34.38475